BRAIN ACTIVITY OF HUMAN MASTICATION.

by

Andres Alberto Quintero Valencia

A dissertation submitted in partial fulfillment
of the requirements for the degree of
Doctor of Philosophy
(Oral Health Sciences)
in The University of Michigan
2012

Doctoral Committee:

Associate Professor Geoffrey Gerstner, Chair
Professor Robert Bradley
Professor Edward Rothman
Associate Professor Catherine Krull
Assistant Research Scientist Scott Peltier

DEDICATION

A Enrique, Maria del Socorro, Constanza y Carlos, por su amor y apoyo incondicional. “Mi Familia es mi Fortaleza”

ACKNOWLEDGMENTS

I am thankful with the following persons who in a direct or indirect way contributed to create and develop this project.

To Dr. Geoffrey Gerstner who more than an mentor is a friend, who guide me and advise me during this journey.

To Eric Ichesco, for his patience, desire to instruct, and the several number of hours spent at the MRI scanner and analyzing MRI data.

To Steve White, for all his help designing and constructing the oral dynamometer.

To Elizabeth Crane, for her help processing the oral dynamometer data.

To Chelsea Myers, Robert Schutt, Rebecca Baer, Randy Simon and Alysson Endycott for their help developing the project.

To my committee members, Dr. Robert Bradley, Dr. Katherine Krull, Dr. Scott Peltier and Dr. Edward Rothman, for their time invested reviewing this project and for their valuable advice and feedbacks.

To the Dean of the School of Dentistry, Directives and Staff of the Oral Health Science program for giving me this great opportunity in my life.

To all my friends, because after long days of work they were always there to remind me that I am still human.

To my classmates, because this trip would not be the same without you.

Finally, to all my family, because they were always there for me in the light and dark days.

TABLE OF CONTENTS.

Contents

LIST OF TABLES

LIST OF FIGURES.

LIST OF APPENDICES

Chapter I

Neural mechanisms of chewing.

Introduction.

Mastication is one of the most important mammalian oral functions, being absolutely essential for survival. Integrity of the masticatory system has been directly correlated with good health, nutrition [1] and quality of life [2] [3]. Mastication is the first step of digestion, consisting of breaking down the food into small particles to facilitate the swallowing process and to increase food surface area for better contact with digestive enzymes. During chewing there is an increase in saliva production, with the purpose of moistening the food to create a cohesive bolus to be swallowed [4]. Different factors such as bite force, number and condition of teeth, occlusion and malocclusion [5] will influence the chewing performance. Chewing is efficiently regulated by neural control, a mixed interaction between central motor systems and feedback and feed-forward from peripheral sensory systems.

Once ingestion has been performed, food is transported to the occlusal surfaces of posterior teeth; here the food will enter a processing stage where it will be broken down into small particles, moistened and flavors released. The number of required chewing cycles will depend on how difficult the food is to chew and process for safe swallowing [6]. The efficiency of the chewing cycle depends on the masticatory muscle activity, jaw movements, bite force [7], condition of the dentition, and the synchrony and coordination of tongue, cheek and lip muscles [8]. Factors such as bite force [9], muscle activity [10] and jaw movements can also be modified depending on food hardness [11] [12] [13].

Chewing is a cyclical and rhythmical process elicited by the central nervous system, and modified by the peripheral nervous system. A chewing cycle can be considered as the unit of the masticatory behavior. Typically, masticatory cycles can be composed of up to four different phases, which are defined by their position in the cycle and their relative velocity (slow opening, fast opening, fast closing and slow closing) [14].

Previous studies in small mammals and non-human primates have shown that the masticatory movements can be elicited by stimulation of a motor cortex zone called the cortical masticatory area (CMA) [15] [16] [17]. When the CMA is obliterated there are changes in the animal's behavior and chewing dynamics such as decrease of food intake, abnormal tongue movements, wider jaw

opening and difficulty in starting the closing movement; however the chewing rhythm remains unaltered[18].

Several animal studies have demonstrated that chewing rhythm is very stable and that the masticatory rhythm is generated in central pattern generator (CPG) circuits in the brainstem [19] [20]. Also it has been reported that stimulation of the CPG induces rhythmical fictive chewing cycles in animals, even when the animals have been decerebrated [21]. Peripheral changes in the masticatory system, such as artificially increasing the weight of the jaw, do not induce changes in the chewing rhythm. This is because sensory inputs provide feedback that modulates bite force through varying muscle recruitment levels with the net effect being a relative invariant chewing frequency.

There are different types of reflexes [22] coming from the muscles' spindles, the periodontal ligament [23], the muscular tendons [24] and oral mucosa that provide a fast and accurate sensory feedback during chewing. When these reflexes are eliminated by damage of the sensory nerves, changes in the length of the chewing cycle are observed [25].

Although brain activity related to mastication has been widely studied in small mammals and non-human primates, our knowledge about brain activity during human chewing is very limited. Most of the techniques used in animal studies, such as decerebration, electrical or pharmaceutical stimulation, are extremely

invasive and cannot be performed in humans. In the last decade some positron emission tomography (PET) and functional magnetic resonance imaging studies have given some insights into the brain activity related with oral function [26] [27] and parafunction [28] [29] [30] in humans. Similar to the results found in previous animal models, these human studies have shown that the motor cortex and sensory-motor cortex demonstrate increased activity associated with oral function [26] [31] [32] [16]. However the experimental designs used in the studies present some limitations, such as small sample sizes, absence of control of chewing side, and manipulation of the chewing rhythm using a metronome. I decided to develop a new set of experiments using MRI technology, with the purpose being to understand the neural mechanisms associated with human chewing.

Virtually everything that is known about chewing is based on work performed in animal models. Also numerous brain regions, e.g., cerebellum, precuneus, basal ganglia, supplementary motor cortex, known to be involved in movement production and motor coordination have not been studied in terms of their potential roles in chewing. In addition, knowledge of brain mechanisms involved in human chewing rely on very few imaging studies or on inferences from human movement disorders involving the oral structures. This study was design to rectify this dearth in knowledge.

BOLD. Blood Oxygen Level Dependent.

Cerebral blood flow and brain activity.

Functional Magnetic Resonance Imaging (fMRI) is a technique used in neuroscience, which allows human in vivo brain activity related to a determined task to be evaluated. Generally speaking BOLD is a method that measures blood flow changes in the brain, and uses these changes to determine which brain areas are more or less active during a specific task. To explain the BOLD concept, there is a direct correlation between neuronal activity, energy demand and cerebral blood flow (the latter of which is the variable assessed during fMRI). 50% to 60% of the energy consumed by the brain is used to maintain the electrophysiological function (i.e. maintain membrane gradients, synthesis and reuptake of neurotransmitters), and the 40% remaining is used to maintain cell homeostasis [33]. Glucose and oxygen supply energy to the brain. It has been established that there are regional increases in blood flow associated with increases in brain activity [34]. This concept of increased blood flow during brain activity is the basis for fMRI studies.

In nature, atomic nuclei with an odd number of protons or neutrons have a property called spin, which creates an angular momentum. Under a strong magnetic field, these spinning nuclei become aligned with the magnetic field. In the presence of a second magnetic coil that is used to energize the spinning nuclei, changes in energy of the spinning nuclei can be registered. Two different

types of resulting energy signals can be recorded, depending on the proton relaxation process. These two signals are known as the T1 and T2 signals, and images created from them are known as T1 and T2-weighted images, respectively. In T1 weighted images the strength of the relaxation is dependent on the concentration of protons. Since each water molecule is made up of two protons, T1-weighted images match a gray scale depending on the quantity of water in the tissue. The greater the concentration of water, the darker the image. These T1 images are typically high contrast and provide detailed anatomical data about the imaged brain. In MRI studies, these images are used to provide detailed maps of a given subject's brain; however, they provide no information about function. The T2 weighted image, is used in fMRI studies to identify areas of brain activity [35]. Deoxy-hemoglobin due to its Fe2+ nuclei, is paramagnetic, i.e., magnetic in the presence of a magnetic field [36], and it is the key feature exploited to generate the BOLD contrast in fMRI images. When deoxy-hemoglobin becomes oxygenated, it enters a low spin state, and this difference will allow fields having a higher concentration of deoxy-hemoglobin to be differentiated from those having a higher concentration of oxy-hemoglobin. As described before there is a direct relation between brain activity and cerebral blood flow; hence, while the brain is coordinating a specific experimental task, there is an increase in blood flow, what will result in changes in deoxy-hemoglobin levels between the resting state and the task state [37]. The difference between the resting and task states is used in BOLD studies to identify regions that are involved in a task. Because it is the difference between the

resting and task states that is necessary to identify, statistical contrasts (subtraction of the data obtained during rest from data obtained during the task) are performed on data to identify brain activations. However since BOLD contrasts measure the dynamic changes in the cerebral blood response, a hemodynamic response function, which is a statistical “template” defining how blood flow changes occur through time, is used as a predictor in fMRI analysis to identify blood flow changes that are task related. This is done by convolving the hemodynamic response function on the contrasted images in order to identify “real”, i.e., task-related” changes in brain activation and differentiate such changes from statistical noise.

General hypothesis

All the central nervous system areas known to participate in motor control will be involved in human chewing production.

Specific aims

Aim 1. To use functional MRI to describe brain activity associated with human chewing.

Hypothesis: Chewing will produce activations patterns in the orofacial primary, secondary and supplementary motor and sensory cortices, pontine brainstem, precuneus and cerebellum.

Aim 2. To determine the central connectivity patterns associated with human chewing using fcMRI.

Hypothesis: Chewing will produce functional connectivity maps integrating the orofacial primary, secondary and supplementary motor and sensory cortices, pontine brainstem, precuneus and cerebellum.

Aim 3. To develop a new mechanism to evaluate dynamic changes in chewing work.

Purpose: Design, test and validate a new technology that will allow the assessment of human chewing under controlled conditions for long time periods.

References.

1. Dion, N., J.L. Cotart, and M. Rabilloud, *Correction of nutrition test errors for more accurate quantification of the link between dental health and malnutrition.* Nutrition, 2007. **23**(4): p. 301-7.
2. Chavers, L.S., G.H. Gilbert, and B.J. Shelton, *Two-year incidence of oral disadvantage, a measure of oral health-related quality of life.* Community Dent Oral Epidemiol, 2003. **31**(1): p. 21-9.
3. Miura, H., et al., *Chewing ability and quality of life among the elderly residing in a rural community in Japan.* J Oral Rehabil, 2000. **27**(8): p. 731-4.
4. Pedersen, A.M., et al., *Saliva and gastrointestinal functions of taste, mastication, swallowing and digestion.* Oral Dis, 2002. **8**(3): p. 117-29.
5. Magalhaes, I.B., et al., *The influence of malocclusion on masticatory performance. A systematic review.* Angle Orthod, 2010. **80**(5): p. 981-7.
6. Fontijn-Tekamp, F.A., et al., *Swallowing threshold and masticatory performance in dentate adults.* Physiol Behav, 2004. **83**(3): p. 431-6.
7. Okiyama, S., K. Ikebe, and T. Nokubi, *Association between masticatory performance and maximal occlusal force in young men.* J Oral Rehabil, 2003. **30**(3): p. 278-82.
8. Mazari, A., M.R. Heath, and J.F. Prinz, *Contribution of the cheeks to the intraoral manipulation of food.* Dysphagia, 2007. **22**(2): p. 117-21.
9. Kohyama, K., et al., *Effects of sample hardness on human chewing force: a model study using silicone rubber.* Arch Oral Biol, 2004. **49**(10): p. 805-16.
10. Mioche, L., et al., *Variations in human masseter and temporalis muscle activity related to food texture during free and side-imposed mastication.* Arch Oral Biol, 1999. **44**(12): p. 1005-12.
11. van der Bilt, A., et al., *Oral physiology and mastication.* Physiol Behav, 2006. **89**(1): p. 22-7.
12. Yamashita, S., J.P. Hatch, and J.D. Rugh, *Does chewing performance depend upon a specific masticatory pattern?* J Oral Rehabil, 1999. **26**(7): p. 547-53.
13. Horio, T. and Y. Kawamura, *Effects of texture of food on chewing patterns in the human subject.* J Oral Rehabil, 1989. **16**(2): p. 177-83.

14. Thexton, A.J., K.M. Hiiemae, and A.W. Crompton, *Food consistency and bite size as regulators of jaw movement during feeding in the cat.* J Neurophysiol, 1980. **44**(3): p. 456-74.
15. Lund, J.P. and Y. Lamarre, *Activity of neurons in the lower precentral cortex during voluntary and rhythmical jaw movements in the monkey.* Exp Brain Res, 1974. **19**(3): p. 282-99.
16. Sessle, B.J., et al., *Neuroplasticity of face primary motor cortex control of orofacial movements.* Arch Oral Biol, 2007. **52**(4): p. 334-7.
17. Yamamura, K., et al., *Effects of reversible bilateral inactivation of face primary motor cortex on mastication and swallowing.* Brain Res, 2002. **944**(1-2): p. 40-55.
18. Hiraba, H. and T. Sato, *Cortical control of mastication in cats. 2. Deficits of masticatory movements following a lesion in the motor cortex.* Somatosens Mot Res, 2005. **22**(3): p. 183-92.
19. Dellow, P.G. and J.P. Lund, *Evidence for central timing of rhythmical mastication.* J Physiol, 1971. **215**(1): p. 1-13.
20. Nozaki, S., A. Iriki, and Y. Nakamura, *Localization of central rhythm generator involved in cortically induced rhythmical masticatory jaw-opening movement in the guinea pig.* J Neurophysiol, 1986. **55**(4): p. 806-25.
21. Nakamura, Y., et al., *Rhythm generation for food-ingestive movements.* Prog Brain Res, 2004. **143**: p. 97-103.
22. Lund, J.P., S. Rossignol, and T. Murakami, *Interactions between the jaw-opening reflex and mastication.* Can J Physiol Pharmacol, 1981. **59**(7): p. 683-90.
23. Appenteng, K., J.P. Lund, and J.J. Seguin, *Intraoral mechanoreceptor activity during jaw movement in the anesthetized rabbit.* J Neurophysiol, 1982. **48**(1): p. 27-37.
24. Komuro, A., et al., *Putative feed-forward control of jaw-closing muscle activity during rhythmic jaw movements in the anesthetized rabbit.* J Neurophysiol, 2001. **86**(6): p. 2834-44.
25. Lavigne, G., et al., *Evidence that periodontal pressoreceptors provide positive feedback to jaw closing muscles during mastication.* J Neurophysiol, 1987. **58**(2): p. 342-58.
26. Bracco, P., et al., *Hemispheric prevalence during chewing in normal right-handed and left-handed subjects: a functional magnetic resonance imaging preliminary study.* Cranio, 2010. **28**(2): p. 114-21.
27. Kimoto, K., et al., *Chewing-induced regional brain activity in edentulous patients who received mandibular implant-supported overdentures: a preliminary report.* J Prosthodont Res, 2011. **55**(2): p. 89-97.
28. Byrd, K.E., et al., *fMRI study of brain activity elicited by oral parafunctional movements.* J Oral Rehabil, 2009. **36**(5): p. 346-61.
29. Jiang, H., et al., *The effects of chewing-side preference on human brain activity during tooth clenching: an fMRI study.* J Oral Rehabil, 2010. **37**(12): p. 877-83.

30. Tamura, T., et al., *Functional magnetic resonance imaging of human jaw movements.* J Oral Rehabil, 2003. **30**(6): p. 614-22.
31. Lund, J.P. and B.J. Sessle, *Oral-facial and jaw muscle afferent projections to neurons in cat frontal cortex.* Exp Neurol, 1974. **45**(2): p. 314-31.
32. Lund, J.P., et al., *Analysis of rhythmical jaw movements produced by electrical stimulation of motor-sensory cortex of rabbits.* J Neurophysiol, 1984. **52**(6): p. 1014-29.
33. Ames, A., 3rd, *CNS energy metabolism as related to function.* Brain Res Brain Res Rev, 2000. **34**(1-2): p. 42-68.
34. Sokoloff, L., *Relation between physiological function and energy metabolism in the central nervous system.* J Neurochem, 1977. **29**(1): p. 13-26.
35. Logothetis, N.K., *The neural basis of the blood-oxygen-level-dependent functional magnetic resonance imaging signal.* Philos Trans R Soc Lond B Biol Sci, 2002. **357**(1424): p. 1003-37.
36. Pauling, L. and C.D. Coryell, *The Magnetic Properties and Structure of Hemoglobin, Oxyhemoglobin and Carbonmonoxyhemoglobin.* Proc Natl Acad Sci U S A, 1936. **22**(4): p. 210-6.
37. Bandettini, P.A., et al., *Characterization of cerebral blood oxygenation and flow changes during prolonged brain activation.* Hum Brain Mapp, 1997. **5**(2): p. 93-109.

Chapter II

Functional magnetic resonance imaging (fMRI) of human chewing.

Introduction.

The purpose of the orofacial sciences is to preserve and restore the structural and functional integrity of the masticatory system. Although large efforts have been made to find different ways to reestablish the function of the masticatory system, the brain mechanisms that underlie human chewing remain poorly studied. Animal studies have shown that the brainstem is responsible for the generation of the masticatory rhythm, and it is also responsible for coordination of masticatory, jaw, facial and tongue muscles activity [1] [2] . Animal studies have also shown that the masticatory rhythm is evocable with stimulation of the cerebral cortex [3]. The degree to which human neural mechanisms of oral motor control compare with or are similar to non-human mammalian neural mechanisms of oral motor control is unclear.

Most of the studies concerning brain activity related to chewing have been performed in animals, using different invasive techniques such as neural ensemble recording, electromyography, electrical stimulation, brain slice preparations, obliteration of cortical areas and complete decerebration among others [4]. Since none of these protocols can be used in humans, we have used functional magnetic resonance imaging (fMRI) technology as a non-invasive method to understand the cortical and subcortical brain structures related to human chewing.

Positron emission tomography (PET) has been used to assess blood flow while humans chewed gum. The contrast between chewing and rest showed increased blood flow in the precentral gyrus, insula, supplementary motor cortex, thalamus, stratium, cerebellum and prefontral areas [5]. Similar results were found in edentulous patients, who underwent an fMRI scan performing a chewing task using complete dentures and later an implant overdenture [6]. Blood oxygen level dependent (BOLD) studies, where left and right handed patients were clenching and resting for periods of 30 seconds, showed that there were bilateral activations in the motor and premotor areas, and unilateral activation in the prefrontal and parietal cortex [7]. These few PET and fMRI studies have provided some understandings of brain activity related to oral function [8] [6] and parafunction [9] [7] [10]. However the experimental designs used in the studies present some limitations, such as small sample sizes, absence of control of chewing side, and manipulation of the chewing rhythm using a metronome. The

purpose of this investigation was to develop an appropriately controlled paradigm to study the brain mechanisms associated with relatively naturalistic chewing in human subjects.

Material and Methods.

Subjects.

This study was evaluated and approved by the medical institutional review board (IRB-Med) of the University of Michigan. Subjects read and signed an informed consent before starting any procedure.

Twenty nine healthy right handed subjects (15 males and 14 females), with class I occlusion and fully dentate, pain-free and with an average age of 24 years (SD+/-3.5), were selected for the study. The research diagnosis criteria for temporomandibular disorders (RDC-TMD) [11] was used to exclude any subject that had any myogenic or extreme arthrogenic alteration in the masticatory system. All subjects selected were medication-free, without diagnoses of systemic, vascular and central nervous diseases. A safety fMRI questionnaire was performed before the subjects went into the scanner; this questionnaire was used to exclude subjects with devices and conditions that otherwise would be dangerous for the subjects, or would not be compatible with the fMRI environment.

Functional MRI protocol.

A 3 Tesla GE scanner at the Functional MRI laboratory at the University of Michigan was used to perform the magnetic resonance scanning. Subjects were placed in the scanner and their heads were securely fastened in order to decrease movement artifacts. T1 images were recorded under the following parameters TR = 12.3, TE = 5.2, flip angle = 15 degrees, bandwidth = 15.63, field of view = 26cm, number of slices = 144 and slice thickness = 1mm, and used during the analysis for preprocessing of the anatomic and functional data. Subjects used mirror glasses to watch a visual projection that guided the subjects to chew gum on the right side for 25 seconds and then to stop chewing, stay still and rest for 25 seconds (Figure 1); this sequence was repeated 10 times. fMRI images were recorded using a TR=2500 ms, TE = 30, flip angle = 90 degrees, field of view = 22, slice thickness = 3.0mm, number of scans = 200, number of slices = 53 and voxel size = 3.44x3.44x3. For each run, the first 5 images were discarded to allow signal stabilization.

Functional MRI data analysis.

The functional data were analyzed using SPM 5 (http://www.fil.ion.ucl.ac.uk/spm/software/spm5/) executed under Matlab 7.1. The images were preprocessed using a time correction and a motion correction realigning all the images with the first image. Then the anatomical images were normalized following a standard Montreal Neurological Institute (MNI) template.

Thereafter, all images were smoothed using a 6mm Gaussian kernel. Fitting the data with hemodynamic response functions (HRF) a first level analysis was performed for each set of data for each subject, contrasting the chew task blocks with the resting period blocks. A second level analysis was performed to compare group differences between the chew task and rest. A corrected p-value< 0.001 was used to establish brain responses associated with chewing.

Animal studies have described that the brain activity responsible for chewing initiation (beginning of the chewing movement) is different from the brain activity related to the sustained chewing action (continued chewing after initiation) [4]. Based on this concept, a second analysis was performed. This unique analysis involved dividing the chewing block into five segments of 5 seconds each (Figure 1). To evaluate the differences in brain activity between segments of the chewing block, a first level analysis for each subject and a second level analysis for the group of subjects, was performed where each chewing segment was contrasted versus the rest block, viz., rest vs. 1/5, rest vs. 2/5, rest vs. 3/5, rest vs. 4/5, and rest vs. 5/5, and also versus successive segments, viz., 1/5 vs. 2/5; 2/5 vs. 3/5; 3/5 vs. 4/5; 4/5 vs. 5/5.

Results.

Contrast between chew and rest blocks.

The fMRI analysis demonstrated that the head translational movement artifact in the x, y and z axes was < 1 mm and that rotational head movement artifact was < 1^{o}. Table 1 and Figure 2 show the results associated with the chewing versus rest contrast. The contrast of chew versus rest revealed a bilateral activation in the posterior lobes of the cerebellum ($p<0.001$). This activation was relatively large involving clusters of 1734 voxels (left) and 383 voxels (right).

Also, there were activations in the left and right precentral gyrus extending over the primary motor cortex, Brodmann areas 3, 4 and 6 and the postcentral gyrus, (464 and 390 voxels in the left and right cortices respectively, $p<0.001$). In addition, there were activations in the rostrum of the corpus callosum, and in the head of the caudate nucleus (92 voxels $p<0.01$).

On the other hand, the contrast between rest versus chewing (Table 1), which represent areas that were more active during rest than chewing, showed extremely large clusters of activity in the right frontal lobe with peak values at the level of the inferior frontal gyrus (23897 voxels, $p<0.001$) and the inferior operculum (259 voxels, $p<0.001$).

Contrast between chewing block segments and rest.

The results of the contrast between each chewing block segment versus rest are shown in Table 2 and Figure 3. Activations in the posterior lobe of the left cerebellum were present among the contrasts between all five chewing segments and rest. On the other hand, the same contrast showed that activations in the posterior lobe of the right cerebellum were only present in the first three segments. There were bilateral activations in the right and left precentral gyrus for all five contrasts as well.

Contrast between successive chewing segments.

The results of the contrasts between successive chewing segments are shown in Table 3 and Figure 4.

Contrast of the first segment versus second segment.

The contrast between the first and second segment showed an activation in the left superior frontal gyrus that extended to the supplementary motor cortex, the Brodmann area 6 and middle frontal cortex. This contrast means that the brain was more active in these areas during the first segment compared with the second segment. In addition an activation at the level of the precentral gyrus extended to the Brodmann area 4 and 6. Also increased activity was present in the caudate and putamen nuclei.

Contrast of the second segment versus third segment.

The contrast between the second and third segment showed no significant results. This result indicates that brain activity remained unchanged during these two segments. After brain activity necessary for initiation of the chewing movements (showed in the first segment), the brain regions involved with sustained chewing appear to have arrived at constant activation levels.

Contrast of the third segment versus fourth segment.

The contrast between the third and fourth segment showed activity in the anterior lobe of the right cerebellum, temporal gyrus and cuneus.

Fourth segment minus fifth segment contrast.

Lastly the contrast between the fourth and the last fifth showed activity increased in the right anterior and posterior cingulate cortex. These results demonstrated that brain activity associated with chewing evolved through time.

Discussion.

The results of contrasts between chew block versus rest block in this study are similar to the results of brain activity observed in animal experiments; activity in the primary motor cortex and supplementary motor cortex is seen in both human and animal chewing [4]. Figure 2 shows the bilateral activations in the middle section of the precentral gyrus, corresponding to the mouth and face in the motor

homunculus. Increased activity has been described in Brodmann's areas 4 and 6 in patients chewing two gums of different consistencies [8]. It has been proposed that these cortical areas can evoke masticatory movements, and have thus been named the cortical masticatory areas (CMA) [1]. Animal experiments where the CMA was obliterated revealed that this area is responsible for initiating the contraction of digastric, masseter and pterygoid muscles [12] [13]. In non-human primates, chewing, swallowing and ingestion can be altered when the CMA is anesthetized; these studies demonstrated that CMA extended from the motor areas in the precentral gyrus to the sensory cortex in the postcentral gyrus [14] [15]. Lund, et al. support the idea that chewing rhythm can be activated by the cortex or by inputs from the peripheral sensory system from the oral cavity [16]. Even though our subjects were chewing on the right side, there were no differences between left- and right-sided results (Table 1), suggesting an interhemispheric interaction and that chewing is associated with right and left cortical activity. In addition, other fMRI studies have reported increased activity in the somatosensory cortex in subjects performing oral parafunctional tasks such as clenching and grinding teeth [9].

Apart from the CMA, brain activations have been reported also in the supplementary motor area (SMA), dorsolateral frontal cortex and posterior parietal cortex during teeth clenching [17]. The SMA [18] is involved with the modulation of chewing movements depending on the hardness of the bolus. Since the shape of a food bolus varies and the amount of force necessary to

chew on the bolus varies as well, the SMA is likely an important area to complement the action of the primary motor cortex. The SMA is an association area that regulates the different type of muscular contractions. Because gum stiffness remains relatively stable over time, the role of the SMA in this study is unclear. However we can speculate that the SMA modulates the shaping, folding and repositioning of the gum bolus.

We have described bilateral activations in the posterior lobe of the cerebellum close to the midline; similar to results reported by Onozuka and colleagues [19]; however, these investigations only found activation in the posterior lobe of the left cerebellum. In our experiment, subjects were allowed to chew at their own paces, without a metronome. Hence, the differences in the cerebellum activation between the two studies could be related to the differences in study designs vis-à-vis control of the masticatory rhythm. According to animal studies, the cerebellum controls voluntary muscle movements, the muscle tonus, balance and coordination of the movement (i.e. hand and eye movement coordination) [20]. Although chewing studies in animals do not focus on the cerebellum, studies from other systems (i.e. eye movements) have suggested the importance of the cerebellum in motor coordination [21]. Also it has been reported that circuits formed by the motor cortex, pons and cerebellum will be involved in motor coordination [22]. FMRI studies which evaluate eye movement have shown bilateral activation in the cerebellum [23]. In addition it has been

demonstrated that the cerebellum is involved in the coordination and rhythmicity of oral function such as licking [24].

In addition the present study reported an activation that ran from the midbrain to the pons. Previous studies performed in small mammals showed that the superior portion of the motor nuclei of the trigeminal nerve, as well as the motor nuclei of the facial nerve are responsible for the generation of the masticatory rhythm; in fact, these nuclei can maintain the rhythm in absence of sensory feedback or inputs from suprabulbar or spinal systems [16] [25] [26] [27]. Thus, our results of brainstem activations suggest that these regions are involved in similar ways as they are in other mammals.

Also the stimulation of the sensory cortex has been shown to induce jaw movements with different features than when the motor cortex and the cortical masticatory area are stimulated [28]. It has been suggested that the posterolateral somatosensory cortex is related to lateral movements rather than opening and closing movements [3]. We hypothesize, therefore that this area is probably involved with modifying the basic chewing pattern, and that chewing pattern modification was a minor requisite in our study where subjects chewed an even-consistency gum on the right side.

In the second analysis we divided the chewing block into five segments. The contrast between the first segment and the second segment showed a large number of activations (Table 3). In particular there was increased activity in the left motor cortex. There is evidence from small animal studies that the CMA is responsible for the initiation of the chewing movement [29]. Our results suggest that the motor cortex plays a similar initiatory role in humans. These results indicate that activity in the motor cortex or other brain areas is not constant during a chewing sequence, rather activations can change dynamically over time.

Also, we described an activation cluster at the level of the brainstem; however, the fMRI technique does not provide adequate spatial resolution to determine the specific area in the brainstem. Due to the position of the cluster in the pons, we can infer that it is including the pontine section of the trigeminal motor nuclei; this is consistent with findings in animal experiments, where the motor nuclei of the trigeminal nerve, as well as other nuclei in the brainstem are involved with the masticatory rhythm and pattern generation [30].

In addition the analysis contrasting the segments of the chewing block versus the rest block showed activations at the level of the head of the caudate nucleus and in the body of the putamen nucleus; both nuclei have been described to be associated with movement control [31]. Although little evidence exists about the role of the basal ganglia in mastication, an fMRI study showed increased activity

in the putamen and caudate while subjects were clenching their teeth [7]. These results show how both nuclei are related to oral parafunction and our findings suggest that they are associated with oral function as well; since both tasks (chewing and clenching) are similar it was expected for them to have similar brain activity patterns.

It is noted that the contrast between each segment of the chewing block and the rest block showed a consistent activity in the motor and supplementary motor cortex and the cerebellum; however the contrast between successive segments of the chewing block showed different sizes (number of voxels) of activation in these brain regions, suggesting dynamic changes over time in the brain activity while the subjects were chewing. Since chewing is a rhythmical sequence of movements, without presenting large kinetic changes, we were expecting that the brain activity in the chewing block would be stable; however we showed how brain activity evolves over time during the chewing cycle.

Information about the role of the cerebellum in mastication is very limited; however, based on what it is known from other studies the cerebellum plays a major role in movement [32] [33]. Results from this study and results that will be discussed in the next chapter suggest that the cerebellum is playing a major role in mastication. Further experiments will be necessary to elucidate its role.

Previous studies of small mammals and non-human primates have shown that the brainstem generates the masticatory rhythm. There are difficulties with high-resolution imaging of the brainstem using MRI methods. The brainstem has a high concentration of small nuclei and these nuclei are involved in different systems (motor, sensory, autonomic). Images generated by fMRI do not have the resolution necessary to differentiate these nuclei. Therefore when activity changes were observed in the brainstem, we assumed that these changes were associated with chewing, and would thus represent activations of the masticatory CPG in the pons. In addition, there can be large anatomical variations in the brainstem considering that it is a small structure. Although all the images were normalized to a brain template, the areas of activation between subjects can differ. Also the vertebral arteries can provoke movement artifacts that can affect the image resolution.

In conclusion, the contrast between the chewing block and the rest block showed activations in the motor cortex, and these activations were constant when the five segments of the chewing block were contrasted with the rest block. However when the segments of the chewing block were contrasted between successive segments, there were differences in activation patterns. This showed that brain activity related to chewing has dynamic changes. Also there were activations in the supplementary motor cortex, basal ganglia and brainstem associated with human chewing. One of our most important descriptions was the activations in the cerebellum. These activations remained present during the contrast of the

chewing block versus the rest block, and the contrasts of the five segments of the chewing block and the rest block. Finally our analysis of the chewing block by segments showed how there were dynamic changes in brain activity patterns over time.

Block	Anatomical Structure	Cluster size	T	Z	Coordinates x	y	z
Chew-Rest	Left cerebellum posterior lobe***	1734	10.08	6.50	-18	-72	-18
	Right Precentral gyrus***	390	9.72	6.38	48	-14	40
	Left Precentral gyrus***	464	9.54	6.32	-44	-14	34
	Right cerebellum posterior lobe***	383	9.31	6.24	10	-68	-48
	Corpus callosum and Caudate nuclei **	92	6.08	4.81	-2	20	2
	Right anterior cingulate cortex*	77	4.57	3.92	2	38	0
	Midbrain/Pons	83	4.36	3.55	-6	-22	-36
Rest-Chew	Right inferior frontal gyrus***	23897	9.87	6.43	32	30	-14
	Right frontal inferior operculum***	259	7.23	5.39	40	10	26
	Left cerebellum posterior lobe**	202	6.76	5.16	-34	-82	-46

Table 1. Results of the contrast between the chewing block versus the rest block. Table shows the peak corrected values for the cluster. *=p<0.05, **=p<0.01, ***=p<0.001. Cluster size is in total number of voxels. T = t-test score; Z = z score. Coordinates are anteroposterior (x), superior-inferior (y) and lateral (z).

Block	Anatomical Structure	Cluster size	T	Z	Coordinates x	y	Z
	Left cerebellum posterior lobe*	148	9.70	6.37	10	-68	-48
	Right precentral gyrus (6) (4)***	365	9.51	6.31	44	-16	40
1/5 - Rest	Left/right posterior cingulate cortex***	5521	9.21	6.23	-6	-44	4
	Left precentral gyrus (6)(4)***	310	7.94	5.70	-44	-16	34
	Right cerebellum posterior lobe**	203	6.88	5.22	-6	-68	-50
	Left cerebellum posterior lobe***	223	10.01	6.47	-16	-64	-18
	Left cerebellum inferior semilunar lobule***	242	9.56	6.32	-8	-70	-50
2/5 - Rest	Left precentral gyrus***	229	9.52	6.31	-44	-14	34
	Right cerebellum posterior lobe***	352	7.21	5.38	20	-58	-22
	Right precentral gyrus***	161	6.90	5.23	40	-12	34
	Right cerebellum posterior lobe***	1303	10.88	6.75	12	-60	-16
	Left cerebellum posterior lobe***	231	7.98	5.72	-10	-68	-46
	Right cerebellum inferior semi-lunar lobule**	182	6.92	5.24	12	-68	-46
3/5 - Rest	Left precentral gyrus**	165	6.89	5.23	-46	-14	36
	Right precentral gyrus**	169	6.61	5.09	42	-10	34
	Left cerebellum posterior lobe***	234	8.91	6.08	-6	-68	-50
	Left precentral gyrus***	281	8.56	5.95	-42	-16	32
4/5 - Rest	Right precentral gyrus***	199	8.02	5.73	46	-14	40
	Right anterior cingulate cortex***	307	5.48	4.48	6	22	2
	Right precentral gyrus***	1535	13.50	7.46	46	-10	34
	Left precentral gyrus***	2184	12.26	7.15	-50	-12	44
	Left cerebellum posterior lobe***	1364	10.09	6.50	-24	-60	-20
5/5 - Rest	Right inferior parietal lobe**	354	6.26	4.91	60	-38	26
	Right occipital pole*	109	5.90	4.72	12	-102	-2
	Right middle cingulate*	110	5.80	4.66	8	10	44

Table 2. Results of the contrasts between each segment of the chewing block and the rest block. The first column shows the specific contrast. The table shows peak corrected values for the cluster were a positive contrast was found. *=p<0.05, **=p<0.01, ***=p<0.001. Brodmann areas are shown in parentheses. Cluster size is in total number of voxels. T = t-test score; Z = z score. Coordinates are anteroposterior (x), superior-inferior (y) and lateral (z).

Block	Anatomical Structure	Cluster size	T	Z	Coordinates x	y	Z
	Occipital lobe/temporal lobe/precuneus***	12436	9.87	6.43	-4	-42	4
	Left superior temporal gyrus***	964	8.75	6.02	-40	-34	16
	Superior frontal gyrus (6)	314	8.72	6.01	0	-6	76
	Right superior temporal gyrus**	161	8.17	5.79	48	12	-8
	Right superior temporal gyrus (8)***	264	6.96	5.26	36	4	-14
	Left posterior insula*	96	6.78	5.17	-36	-22	-2
	Left caudate nuclei	249	6.76	5.16	-14	22	0
	Left superior temporal gyrus***	274	6.56	5.07	-56	16	-6
1/5 – 2/5	Right amygdala**	137	6.52	5.05	20	0	-12
	Left putamen nuclei*	98	6.10	4.83	32	-18	-2
	Left Cerebellum posterior lobe/Tonsil*	126	5.80	4.66	-18	-52	-50
	Left precentral gyrus**	186	5.68	4.60	-44	-16	40
	Brainstem**	147	5.61	4.55	-6	-26	-6
	Right cingulate gyrus***	227	5.38	4342	2	8	44
	Right cuneus*	132	5.50	4.49	18	-90	10
2/5 -3/5	No significant results						
3/5 – 4/5	Right cerebellum anterior lobe***	254	6.79	5.18	28	-50	-22
	Right superior temporal gyrus***	248	6.71	5.14	50	-56	12
	Right occipital lobe*	97	6.46	5.01	16	-88	10
	Right cerebellum anterior lobe***	279	5.39	4.43	12	-62	-14
	Left posterior cingulate cortex	178	5.10	4.25	-14	-62	6
	Right cuneus**	146	5.01	4.20	2	-78	30
4/5 – 5/5	Right posterior cingulate***	445	7.70	5.60	4	-54	12
	Right anterior cingulate***	814	7.08	5.32	4	44	0

Table 3. Results of the contrasts between the successive segments of the chewing cycle. Table shows peak corrected values for the cluster. *=p<0.05, **=p<0.01, ***=p<0.001. Brodmann areas are shown in parentheses. Cluster size is in total number of voxels. T = t-test score; Z = z score. Coordinates are anteroposterior (x), superior-inferior (y) and lateral (z).

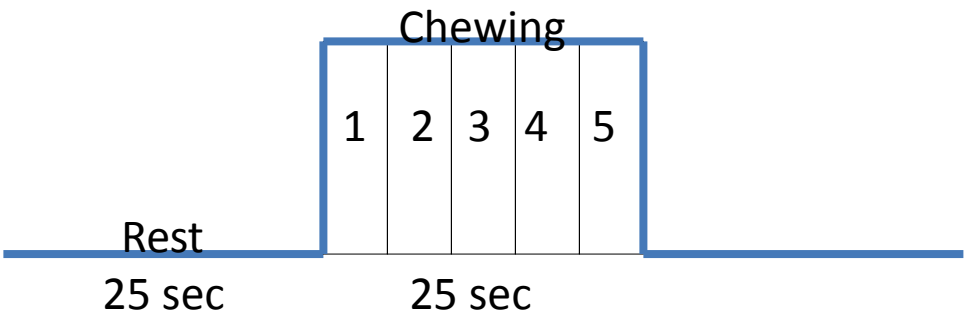

Figure 1. Block design used during the scanning sessions at the MRI laboratory. Subjects were lying in the MRI scanner and asked to stay at rest for 25 seconds and to chew on the right side for 25 seconds; this sequence was repeated ten times. The chewing block was divided in five segments for analysis purposes.

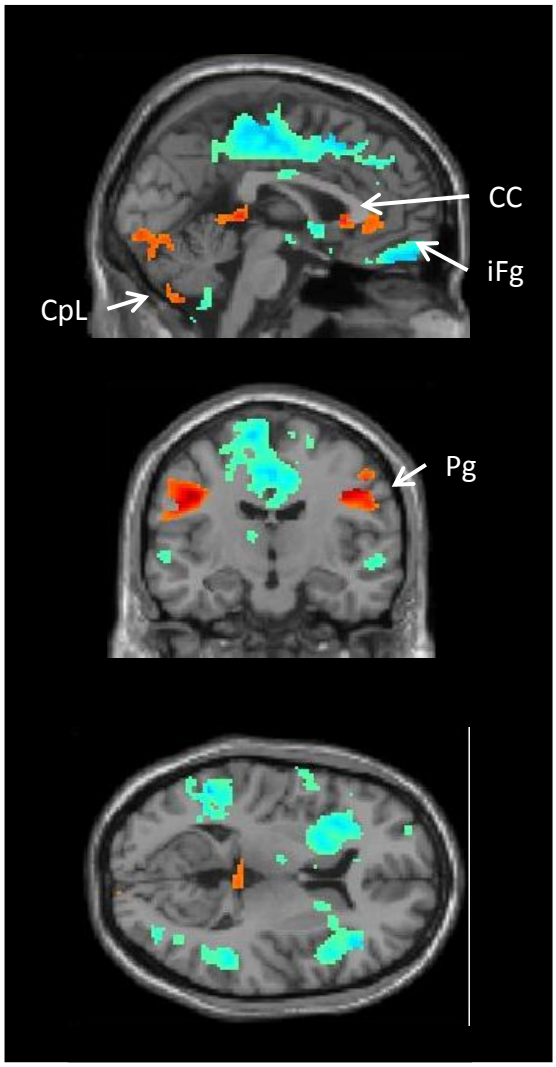

Figure 2. fMRI results of the contrast between chewing blocks minus rest blocks. Red/yellow areas show activations during chewing blocks compared to successive rest blocks and blue/green areas show deactivations during chewing blocks compared with successive rest blocks. Pg= Precentral Gyrus. CC= Corpus callosum. CpL=Cerebellum posterior lobe. iFg= inferior frontal gyrus.

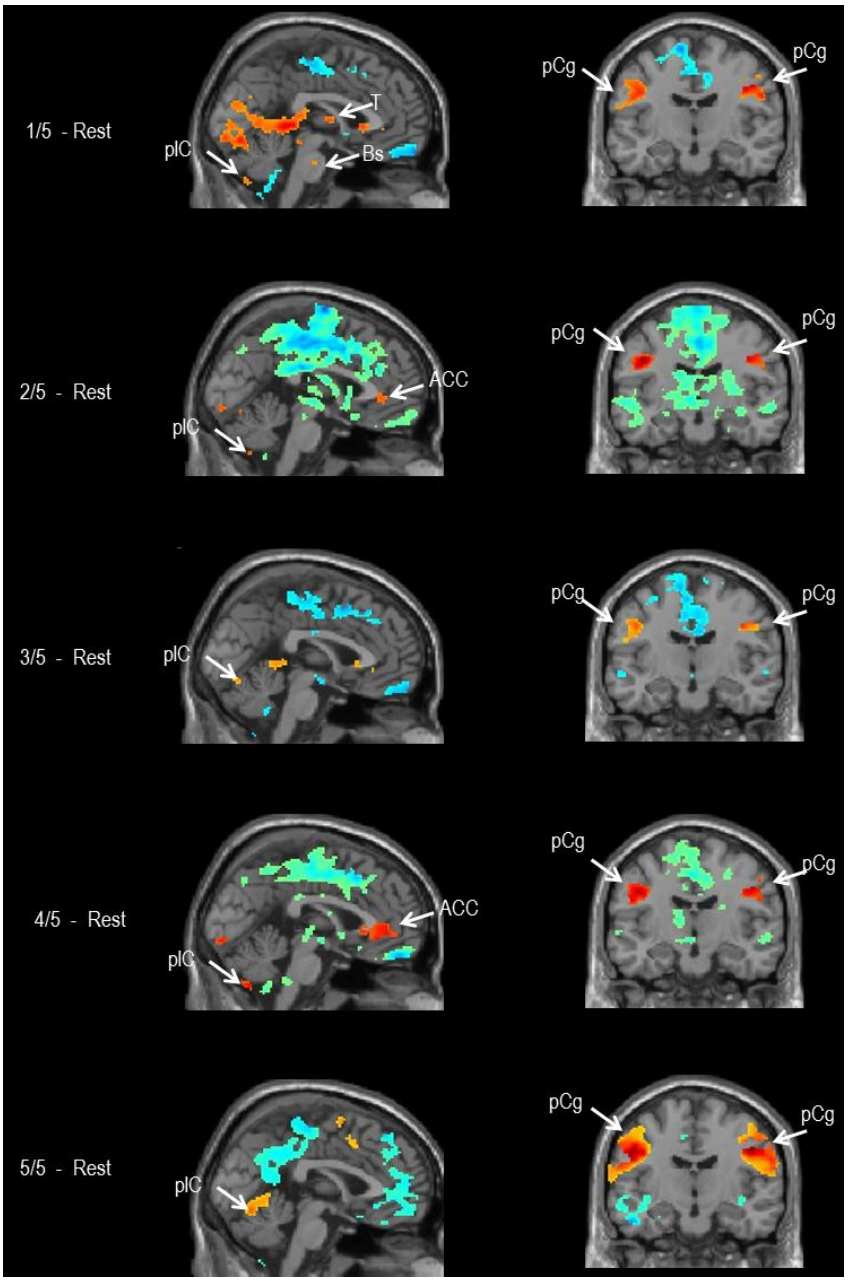

Figure 3. Images of the contrast between the five segments of the chewing block and rest block. Red/yellow areas show activations (increased brain activity during the respective chewing segments compared to subsequent rest) and blue/green areas show deactivations (decreased brain activity during the respective chewing segments compared to subsequent rest) in the contrast. Sagittal images show activation in the cerebellum in all five contrasts. Coronal images show activations in the left and right precentral gyrus in all five contrasts. pCg=Precentral gyrus; plC=Posterior lobe of the cerebellum; Bs=Brainstem; ACC=Anterior cingulate cortex.

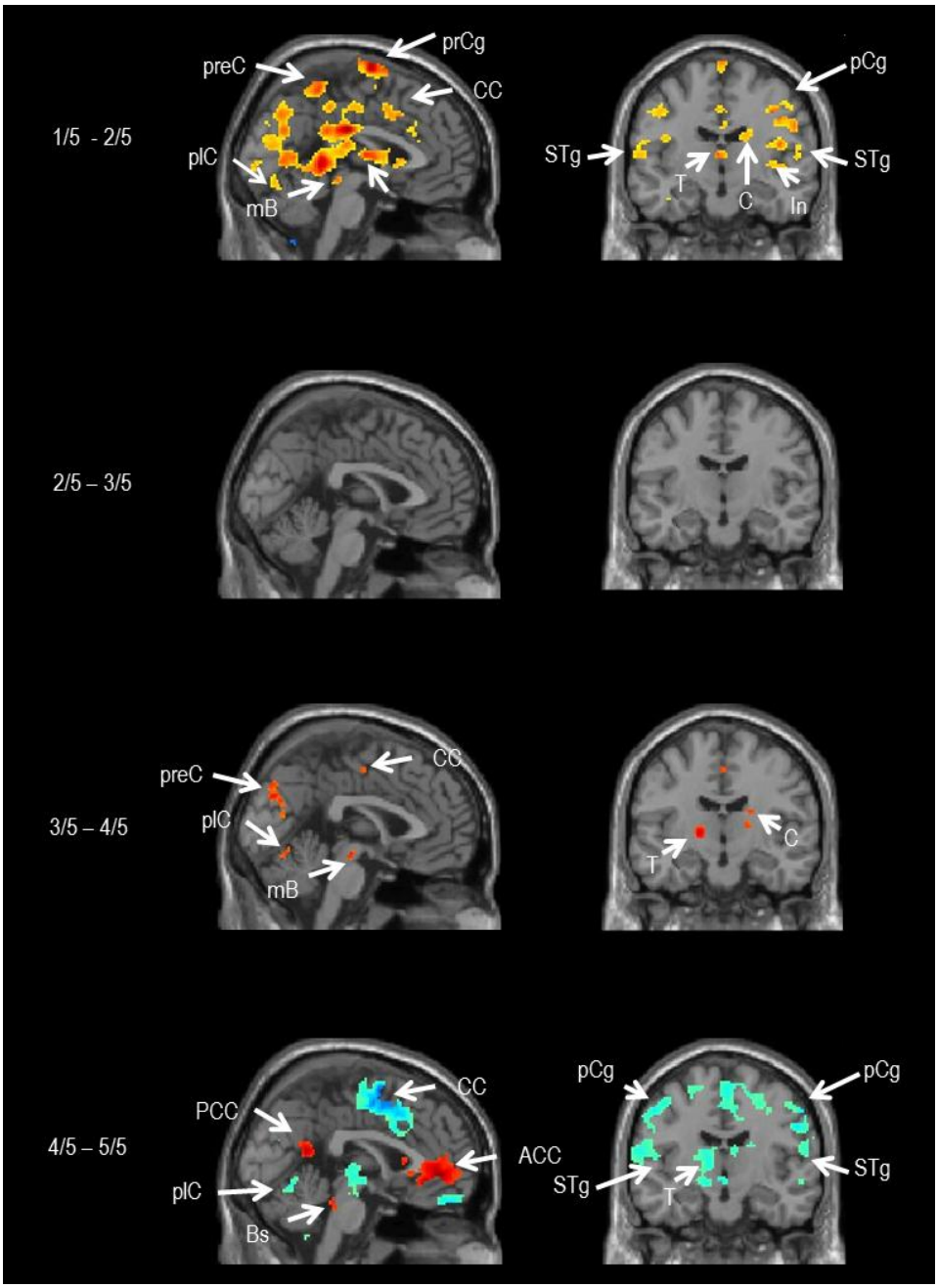

Figure 4. Images of the contrasts between successive segments of the chewing block. Red/yellow areas show activations (where brain activity increased in the time between one segment and the next) and blue/green areas show deactivations (where brain activity decreased in the time between one segment and the next). The first contrast (1/5 – 2/5) shows the brain activations during the initiation of the chewing movement. The other contrasts show brain activity during sustained chewing. Note that brain activity dynamically evolves over the duration of the chewing block. pCg=precentral gyrus; prCg=paracentral gyrus; preC=Precuneus; CC=Cingulate Cortex; ACC= Anterior cingulate cortex; PCC= Posterior Cingulate cortex; plC=Cerebellum posterior lobe; T=Thalamus; C=Caudate nucleus; In=Insula; mB=Midbrain; Bs=Brainstem; STg=Superior Temporal gyrus.

References

1. Nakamura, Y. and N. Katakura, *Generation of masticatory rhythm in the brainstem.* Neurosci Res, 1995. **23**(1): p. 1-19.
2. Lund, J.P., *Chapter 15--chew before you swallow.* Prog Brain Res, 2011. **188**: p. 219-28.
3. Lund, J.P., et al., *Analysis of rhythmical jaw movements produced by electrical stimulation of motor-sensory cortex of rabbits.* J Neurophysiol, 1984. **52**(6): p. 1014-29.
4. Lund, J.P. and A. Kolta, *Generation of the central masticatory pattern and its modification by sensory feedback.* Dysphagia, 2006. **21**(3): p. 167-74.
5. Momose, T., et al., *Effect of mastication on regional cerebral blood flow in humans examined by positron-emission tomography with (1)O-labelled water and magnetic resonance imaging.* Arch Oral Biol, 1997. **42**(1): p. 57-61.
6. Kimoto, K., et al., *Chewing-induced regional brain activity in edentulous patients who received mandibular implant-supported overdentures: a preliminary report.* J Prosthodont Res, 2011. **55**(2): p. 89-97.
7. Jiang, H., et al., *The effects of chewing-side preference on human brain activity during tooth clenching: an fMRI study.* J Oral Rehabil, 2010. **37**(12): p. 877-83.
8. Bracco, P., et al., *Hemispheric prevalence during chewing in normal right-handed and left-handed subjects: a functional magnetic resonance imaging preliminary study.* Cranio, 2010. **28**(2): p. 114-21.
9. Byrd, K.E., et al., *fMRI study of brain activity elicited by oral parafunctional movements.* J Oral Rehabil, 2009. **36**(5): p. 346-61.
10. Tamura, T., et al., *Functional magnetic resonance imaging of human jaw movements.* J Oral Rehabil, 2003. **30**(6): p. 614-22.
11. Dworkin, S.F. and L. LeResche, *Research diagnostic criteria for temporomandibular disorders: review, criteria, examinations and specifications, critique.* J Craniomandib Disord, 1992. **6**(4): p. 301-55.
12. Enomoto, S., G. Schwartz, and J.P. Lund, *The effects of cortical ablation on mastication in the rabbit.* Neurosci Lett, 1987. **82**(2): p. 162-6.
13. Nakamura, Y. and Y. Kubo, *Masticatory rhythm in intracellular potential of trigeminal motoneurons induced by stimulation of orbital cortex and amygdala in cats.* Brain Res, 1978. **148**(2): p. 504-9.

14. Lund, J.P. and Y. Lamarre, *Activity of neurons in the lower precentral cortex during voluntary and rhythmical jaw movements in the monkey.* Exp Brain Res, 1974. **19**(3): p. 282-99.
15. Sessle, B.J., et al., *Properties and plasticity of the primate somatosensory and motor cortex related to orofacial sensorimotor function.* Clin Exp Pharmacol Physiol, 2005. **32**(1-2): p. 109-14.
16. Dellow, P.G. and J.P. Lund, *Evidence for central timing of rhythmical mastication.* J Physiol, 1971. **215**(1): p. 1-13.
17. Iida, T., et al., *Comparison of cerebral activity during teeth clenching and fist clenching: a functional magnetic resonance imaging study.* Eur J Oral Sci, 2010. **118**(6): p. 635-41.
18. Takahashi, T., et al., *Cerebral activation related to the control of mastication during changes in food hardness.* Neuroscience, 2007. **145**(3): p. 791-4.
19. Onozuka, M., et al., *Mapping brain region activity during chewing: a functional magnetic resonance imaging study.* J Dent Res, 2002. **81**(11): p. 743-6.
20. Shik, M.L. and G.N. Orlovsky, *Neurophysiology of locomotor automatism.* Physiol Rev, 1976. **56**(3): p. 465-501.
21. Ilg, U.J. and P. Thier, *The neural basis of smooth pursuit eye movements in the rhesus monkey brain.* Brain Cogn, 2008. **68**(3): p. 229-40.
22. Glickstein, M. and K. Doron, *Cerebellum: connections and functions.* Cerebellum, 2008. **7**(4): p. 589-94.
23. Alvarez, T.L., et al., *Vision therapy in adults with convergence insufficiency: clinical and functional magnetic resonance imaging measures.* Optom Vis Sci, 2010. **87**(12): p. E985-1002.
24. Bryant, J.L., et al., *Cerebellar cortical output encodes temporal aspects of rhythmic licking movements and is necessary for normal licking frequency.* Eur J Neurosci, 2010. **32**(1): p. 41-52.
25. Nakamura, Y., et al., *Rhythm generation for food-ingestive movements.* Prog Brain Res, 2004. **143**: p. 97-103.
26. Nozaki, S., A. Iriki, and Y. Nakamura, *Localization of central rhythm generator involved in cortically induced rhythmical masticatory jaw-opening movement in the guinea pig.* J Neurophysiol, 1986. **55**(4): p. 806-25.
27. Lund, J.P. and A. Kolta, *Brainstem circuits that control mastication: do they have anything to say during speech?* J Commun Disord, 2006. **39**(5): p. 381-90.
28. Huang, C.S., et al., *Topographical distribution and functional properties of cortically induced rhythmical jaw movements in the monkey (Macaca fascicularis).* J Neurophysiol, 1989. **61**(3): p. 635-50.
29. Sessle, B.J., *Chapter 5--face sensorimotor cortex: its role and neuroplasticity in the control of orofacial movements.* Prog Brain Res, 2011. **188**: p. 71-82.

30. Kolta, A., et al., *Modulation of rhythmogenic properties of trigeminal neurons contributing to the masticatory CPG.* Prog Brain Res, 2010. **187**: p. 137-48.
31. Afifi, A.K., *Basal ganglia: functional anatomy and physiology. Part 1.* J Child Neurol, 1994. **9**(3): p. 249-60.
32. Miall, R.C., G.Z. Reckess, and H. Imamizu, *The cerebellum coordinates eye and hand tracking movements.* Nat Neurosci, 2001. **4**(6): p. 638-44.
33. Keele, S.W. and R. Ivry, *Does the cerebellum provide a common computation for diverse tasks? A timing hypothesis.* Ann N Y Acad Sci, 1990. **608**: p. 179-207; discussion 207-11.

Chapter III

Functional connectivity of human chewing.

Introduction.

Chewing can be described as one of the main functions of the orofacial system that is important in survival. Previous animal studies have described brain areas and their axonal connections related to chewing. Motor areas in the cortex, e.g., the cortical masticatory area in M1 and motor nuclei in the brainstem, e.g., nucleus paragigantocellularis, nucleus gigantocellularis pars oralis, and the parvocellular reticular formation are involved in the generation, rhythmicity and coordination of the masticatory, facial and tongue muscles [1] . Also, sensory trigeminal nuclei and sensory cortical areas play a role providing feedback from the masticatory activity. Studies in cats have shown connections between motor cortex and the orbital gyrus with motoneurons of the trigeminal system related to jaw closing movements [2] [3] [4]. Other studies have demonstrated a relation between stimulation of the oral mucosa [5], periodontal ligament [6] and muscle spindles [7] and changes in neuron firing at the brainstem level.

In our previous chapter in the fMRI study we showed that motor cortex, brainstem and cerebellum were active during chewing in humans; however, how these structures interact with each other and with other areas of the central nervous system remains unclear. As far as we are aware, no other research team has evaluated brain activity associated with chewing using functional connectivity MRI (fcMRI). fcMRI is a novel methodology which allows investigators to select a specific region of the brain (seed region) and find which other areas are highly correlated with the seed region. However fcMRI does not provide direct information about anatomical connectivity between two areas; rather, this method gives information about areas that are highly correlated among themselves during a specific task or at resting state. Although correlation does not mean causation, the design of fcMRI studies demonstrates functional associations between brain regions. The aim of this study was to use fcMRI as a noninvasive method to evaluate the connectivity of different areas of the central nervous system related to chewing.

Methods.

Subjects.

This study was evaluated and approved by the medical institutional review board (IRB-Med) of the University of Michigan. Subjects read and signed an informed consent before starting any procedure.

Twenty nine healthy right-handed subjects (15 males and 14 females), with class I occlusion and fully dentate, pain-free and with an average age of 24 years (SD+/-3.5), were selected for the study. The research diagnosis criteria for temporomandibular disorders (RDC-TMD) [8] was used to exclude any subject that had any myogenic or extreme arthrogenic alteration in the masticatory system. All subjects selected were medication-free, without diagnoses of systemic, vascular and central nervous diseases. A safety fMRI questionnaire was performed before the subjects went into the scanner; this questionnaire was used to exclude subjects with devices and conditions that otherwise would be dangerous for the subjects, or would not be compatible with the fMRI environment.

Functional MRI protocol.

A 3 Tesla GE scanner at the functional MRI laboratory at the University of Michigan was used to perform the magnetic resonance scanning. Subjects were placed in the scanner and their heads were securely fastened in order to decrease movement artifacts. T1 images were recorded under the following parameters TR = 12.3 ms, TE = 5.2 ms, flip angle = 15 degrees, bandwidth = 15.63 KHz, field of view = 26°, number of slices = 144 and slice thickness = 1mm, and used during the analysis for preprocessing of the anatomic and functional data. Subjects used mirror glasses to watch a visual projection that guided the subjects to chew gum on the right side for 25 seconds and then to stop chewing, stay still and rest for 25 seconds; this sequence was repeated 10

times. fMRI images were recorded using a TR=2500 ms, TE = 30 ms, flip angle = 90 degrees, field of view = 22mm, slice thickness = 3.0mm, number of scans = 200, number of slices = 53 and voxel size = 3.44 mm x 3.44 mm x 3 mm. For each run, the first 5 images were discarded to avoid magnetic field defects.

Functional connectivity pre-processing.

Version 8 of the Statistical Parametric Mapping (SPM) software from Functional Imaging Laboratories, London, UK and the functional connectivity toolbox Conn (http://www.nitrc.org/projects/conn) from the Cognitive and Affective Neuroscience Laboratory of the Massachusetts Institute of Technology, Cambridge, MA, USA, both running under Matlab 7.5b (Mathworks, Sherborn, MA, USA) were used to pre-process and analyze the data. Data preprocessing consisted of motion correction, normalization and smoothing. Functional and structural images were loaded for each subject. MarsBar software (http://marsbar.sourceforget.net) and coordinates from the Montreal Neurological Imaging were used to create 6mm spherical seeds in the right (x=42; y=-14; z=36) and left (x=-44; y=-12; z=34) motor cortex, right (x=10; y=-68; z=-48 and x=14; y=-58; z=-88) and left (x=-6; y=-68; z=-48 and x=-16; y=-62; z=-18) cerebellum and a 2mm spherical seed in the pons (x=0; y=-34; z=-34). Seeds were selected based on the results obtained in the previous chapter. Onset times and durations of the rest and chewing blocks were defined for each subject. High frequency noise was removed using a band pass filter of 0 to 0.03 Hz. The white matter, cerebral spinal fluid, motion parameters, the effect of rest and the

effect of chewing were used as confounds during the data preprocessing. Then a first level analysis to evaluate single subject differences was run using the seeds described above. Thereafter, a second level analysis was performed to determined group connectivity results.

Results.

Significant results for the fcMRI for chewing were determined using a corrected p-value<0.05 at cluster level.

Functional connectivity of the motor cortex seeds.

Table 1 and figure 1 show the results for the seeds in the right and left motor cortex. There was a functional connection of each motor cortex with the contralateral motor cortex. These were large clusters that had their peak values in the precentral gyri, but they extended over the postcentral gyrus, the parietal lobe, superior temporal gyrus, superior, middle, inferior and frontal gyrus, insula, putamen nucleus and thalamus. Also both cortices showed functional connections with clusters that had peak values in the posterior lobes of the cerebellum; this connectivity map extended to the inferior semi-lunar lobule and the vermis. Furthermore, the motor cortex seeds showed functional connections with the precuneus and the brainstem.

Functional connectivity of the pontine seed.

The seed in the pons showed functional connections with both parahippocampal cortices and also with the right cerebellum and the right inferior temporal cortex (Table 2; Figure 2).

Functional connectivity of the cerebellar seeds.

Both the right and left cerebellar hemispheres showed functional connections with the contralateral cerebellum. The cluster associated with the connectivity map in the contralateral cerebellum was vast, and included the anterior and posterior lobe of the cerebellum, the culmen, cerebellar tonsil, the inferior semilunar lobule and the occipital pole. The functional connectivity map with peak values in the contralateral motor cortex extended to superior parietal lobule, postcentral gyrus, paracentral lobule, superior and medial frontal gyrus and precuneus. Also the cerebellar seeds showed functional connections with the cingulate cortex (Table 3; Figure 3).

Discussion.

In our previous chapter, we showed how there were bilateral activations in the motor cortex during chewing on the right side. In this experiment the motor cortices showed contralateral functional connections (Table 1). Previous studies have shown connections between both sides of the cortex occur via the corpus callosum. Transcranial magnetic stimulation of the motor cortex has been shown

to elicit bilateral contraction of the masseter and digastric muscle in humans [9]. Studies in small mammals have shown the existence of the connection between the two motor cortices and how it is involved in mastication [10]. Also when one of the cortical sides is experimentally damaged, there are changes in jaw and tongue movements during chewing [11]. Similar results are found in patients suffering from stroke, where chewing efficiency is reduced [12]. These studies support our findings of bilateral connectivity between the motor cortices during chewing.

We also described that the motor cortex had a functional connection with the brainstem and the pons (Table 1). Animal studies have shown the existence of a corticobulbar tract between the cortex (cortical motor area) and the trigeminal motor nuclei in the pons and the reticular formation in the brainstem [13]. This tract modulates the brainstem central pattern generators responsible for the chewing movements [14]. The masticatory rhythm has been eliminated upon stimulation of the motor cortex in studies of small mammals where this tract has been obliterated [15]. It is, therefore possible that humans like animals possess these connections involved in the control of the masticatory movements.

Unique to this study, we found that the cerebellum played a role in chewing; however, what specific action the cerebellum performs during chewing still remains unclear. Pathways connecting the motor cortex and the cerebellum have been described previously. In animals, descending neurons from the cortex

synapse in the pons, and the postsynaptic neurons project to the cerebellum via the cerebellar peduncle [16] [17]. In addition, these projections to the cerebellum not only originate in the motor cortex but also in the cingulate cortex, somatosensory cortex and supplementary motor cortex [18]. An fcMRI study performed in humans has described functional connections between the motor cortex and the dorso-lateral prefrontal cortex with the cerebellum [19]; however, this previous experiment was performed at rest, and the connectivity map was not associated with any task. The present results support the idea of these regions being functionally connected during the chewing task. It is possible that the cerebellum is involved in the coordination of chewing movements. Also it is possible that the functional connections of the cerebellum are related to the coordination of the group of muscles involved in mastication (masticatory muscles, suprahyoid muscles, muscles of the tongue and facial muscles) and coordinating the chewing process with swallowing and breathing [20].

There were also connections between the motor cortex and both the precuneus and cuneus (Table 1). These areas have not been described before as being related to mastication. Other studies have shown that these areas increase in activity during other types of movements such as upper limb movements and eye movements [21] [22] [23] [24]. We hypothesize that the role of the precuneus during chewing could be that it is involved with the identification of shapes and textures of the bolus. It could also be involved with the association between movement and sensory inputs.

It was interesting that the main functional connections of the pons were with the left and right parahippocampal gyrus (Table 2). The parahippocampal gyrus traditionally is related to memory and not with movement tasks [25]. In addition, the importance of the pons in mastication has been described before; however it would require further MRI studies to understand how its relation with the parahippocampal gyrus will be involved with chewing. Since the pontine area contains multiple nuclei belonging to different motor and sensory systems, it is possible that the seed region in the pons reflects functional connections not related to trigeminal systems. In addition the axons of the trigeminal motor nucleus will project to the periphery, making it less probable to observe a connectivity map in the brain. These previous concepts could explain why the connectivity of the seed in the pons is not showing expected results.

The cerebellar seeds showed large connectivity maps (Table 3). It is interesting that the vast majority of the animal and human studies that assessed mastication have not described the importance of the cerebellum in oral function, and most of the mastication studies have focused on the CMA and the CPG. We described functional connections between the cerebellum and the precentral gyri (Brodmann areas 6 and 4); since this is the anatomical location of the cortical masticatory area [14], this result suggests the importance of this connection for the control of chewing movements. Also the cerebellar hemispheres were largely connected with the frontal cortex and the temporal cortex.

Chewing, swallowing, talking and breathing are functions that must be timed and coordinated. Furthermore there are common groups of muscles performing these functions, and many of the muscles and their neural circuitry will be involved in multiple tasks (i.e. there are specific tongue movements during chewing versus swallowing versus breathing). The extensive connectivity map of the cerebellum may be associated with the coordination of these oral functions (speech included) and breathing. Patients that suffered cerebellar stroke present speech difficulties [26], abnormalities in breathing [27] and swallowing complications [28].

In conclusion, fcMRI showed connectivity maps in humans related to chewing. We described that the motor cortices were functionally interconnected and connected to the brainstem (similar as in animals). In addition we showed a reciprocal functional connection during chewing between the motor cortices and the cerebellar hemispheres.

Seed region	Connectivity region	BA	Cluster size	Z score	Coordinates x	y	z
Right motor cortex	Left precentral gyrus***	6	14159	7.35	-46	-12	34
	Left cerebellum posterior lobe***	-	3314	7.28	-18	-64	-18
	Left cerebellum inferior semi lunar lobule***	-	394	5.33	-8	-72	-46
	Left cuneus***	-	827	4.99	-20	-90	22
	Right cerebellum posterior lobe ***		245	4.95	22	-86	-50
	Left superior parietal lobule*		145	4.93	-26	-50	64
	Posterior cingulate cortex***	30	254	4.73	-12	-66	8
	Left poscentral gyrus/inferior parietal lobule*		169	4.55	-32	-36	46
	Right cuneus/precuneus***		269	4.42	14	-82	40
	Left brainstem/Thalamus*	-	157	4.25	-12	-22	-4
Left motor cortex	Right precentral gyrus/ postcentral gyrus***	4/6	20719	6.98	50	-10	30
	Left cerebellum posterior lobe***	-	8867	6.68	-18	-60	-18
	- Right cerebellum posterior lobe***	-		6.39	16	-60	-18
	Left cerebellum inferior semi-lunar lobule***	-	278	5.58	-10	-70	-48
	Right cerebellum inferior semi-lunar lobule ***	-	308	4.93	14	-66	-52
	Right Middle/Superior frontal gyrus***	10/46	828	4.76	34	46	28
	Left Middle/Superior frontal gyrus ***	10/46	529	4.42	-44	42	20
	Right Precuneus*	19	133	4.26	34	-72	38
	Right Precuneus**	7	221	4.16	2	-52	56
	Pons/brainstem*	-	167	4.16	-2	-30	-34

Table 1. Results of the fcMRI for the motor cortex seeds. The table shows the connectivity map for the seeds in the right and left motor cortex. BA = Brodmann area. *=p<0.05, **=p<0.01, ***=p<0.001. Cluster size is in total number of voxels. T = t-test score; Z = z score. Coordinates are anteroposterior (x), superior-inferior (y) and lateral (z).

Seed region	Connectivity region	BA	Cluster size	Z score	Coordinates x	y	z
Pons	Right parahippocampal gyrus***	28	485	5.13	24	-10	-34
	Left parahippocampal gyrus***	20	492	4.88	-30	-10	-32
	Right cerebellar tonsil*		122	4.40	34	-46	-44
	Right inferior temporal gyrus*	20	130	4.05	42	-32	-12

Table 2. Results of the fcMRI for the seed in the pons. BA = Brodmann area. *=p<0.05, **=p<0.01, ***=p<0.001. Cluster size is in total number of voxels. T = t-test score; Z = z score. Coordinates are anteroposterior (x), superior-inferior (y) and lateral (z).

Seed region	Connectivity region	BA	Cluster size	Z score	Coordinates x	y	z
Right posterior cerebellum 10 -68 -48	Left Cerebellum Posterior lobe***	-	11385	6.18	-14	-64	-22
	Right Superior Temporal Gyrus/ Precentral gyrus/Postcentral gyrus***	22	523	4.92	62	-6	10
	Left precentral gyrus**	6/4	199	4.64	-44	-16	36
	Left Superior Pariental lobe***	7	264	4.55	-24	-62	58
	Left Superior Temporal Gyrus*	22	170	4.30	-58	-6	10
	Left Precentral Gyrus *	6/4	173	4.19	-34	-14	58
	Left Cingulate Gyrus/Supplementary Motor Area*	32	135	3.99	0	16	48
Right posterior cerebellum 14 -58 -18	Left Cerebellum Posterior Lobe***	-	43445	7.38	-24	-74	-22
	Right Inferior Frontal Gyrus**	10	215	4.52	48	50	4
	Left Middle Temporal Gyrus***	20	495	4.41	-42	2	-28
	Left Cingulate Gyrus***	24	303	4.24	-4	-22	36
	Left Inferior Parietal Lobule**	40	233	4.21	-32	-54	58
	Right Medial Frontal Gyrus/Frontal Orbital Gyrus*	11	139	4.11	4	50	-12
Left posterior cerebellum -16 -62 -18	Right superior parietal lobule ***	7	385	4.94	26	-58	62
	Left inferior temporal gyrus***	20	347	4.85	-40	2	-48
Left posterior cerebellum -6 -68 -48	Right cerebellum inferior semi lunar lobule***		14931	6.95	10	-64	-54
	Right medial frontal gyrus/paracentral gyrus***	6	2631	5.94	4	-24	80
	Left superior temporal gyrus***	22	650	5.16	-64	-6	4
	Right precentral/postcentral gyrus***	6	562	5.01	48	-12	34
	Right inferior temporal gyrus***	20	627	4.91	58	-8	-24
	Right precentral gyrus***	6	302	4.85	60	0	6
	Left precentral/postcentral gyrus ***	6	346	4.67	-46	-14	28
	Left insula**	13	237	4.45	-38	-10	16
	Left superior frontal gyrus **	10	235	4.39	-24	56	16
	Left posterior cingulate gyrus*	24	172	4.35	0	-26	28
	Left frontal orbital gyrus*	10	125	4.27	-10	70	-10
	Right superior frontal gyrus*	10	143	4.21	32	60	-4
	Left middle temporal gyrus **	21	208	4.17	-64	-12	-16
	Left superior frontal gyrus*	6	129	4.11	-28	-4	68

Table 3. Results of the fcMRI for the seeds in the cerebellum. BA = Brodmann area. The coordinates for each seed are shown under the name of the seed. The table shows the connectivity maps for each seed. *=p<0.05, **=p<0.01, ***=p<0.001. Cluster size is in total number of voxels. T = t-test score; Z = z score. Coordinates are anteroposterior (x), superior-inferior (y) and lateral (z).

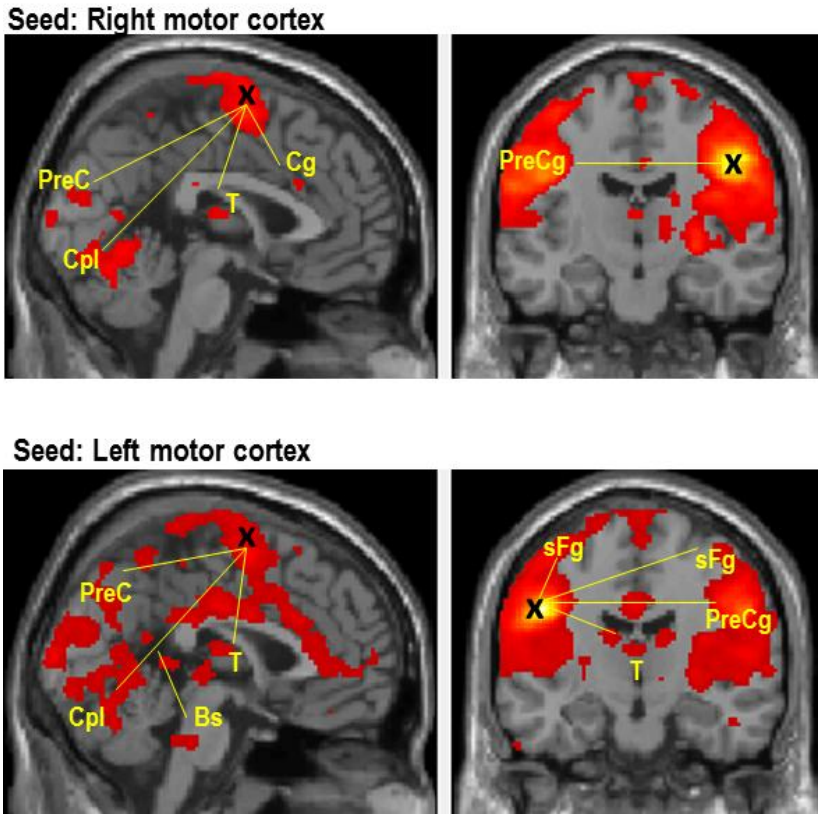

Figure 1. Images of the functional connectivity maps for the seeds in the motor cortices. Seed Region (X); Cingulate gyrus (Cg); Thalamus (T); Precuneus (PreC); Cerebellum posterior lobe (Cpl); precentral gyrus (PreCg); Brainstem (Bs); Pons (P); Cerebellum posterior lobe (Cpl); Superior frontal gyrus (sFg)

Seed: Pons

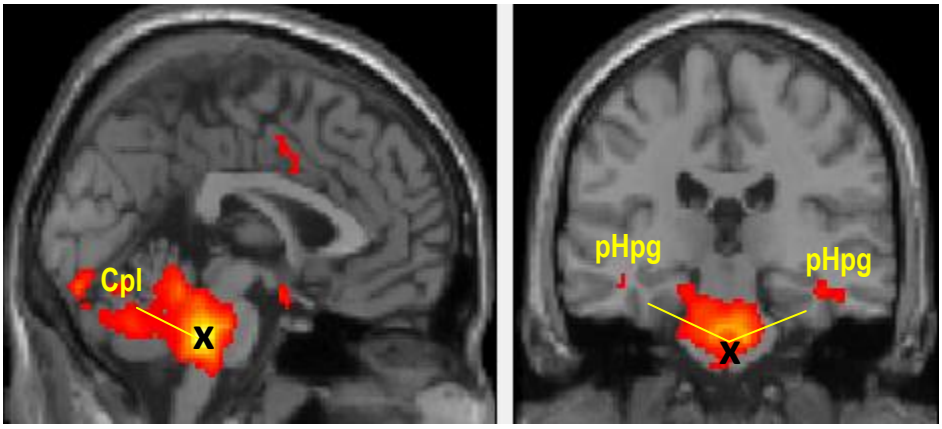

Figure 2. Images of the functional connectivity maps for the seed in the pons. Seed Region (X); Cerebellum posterior lobe (Cpl); Parahippocampal gyrus (pHpg)

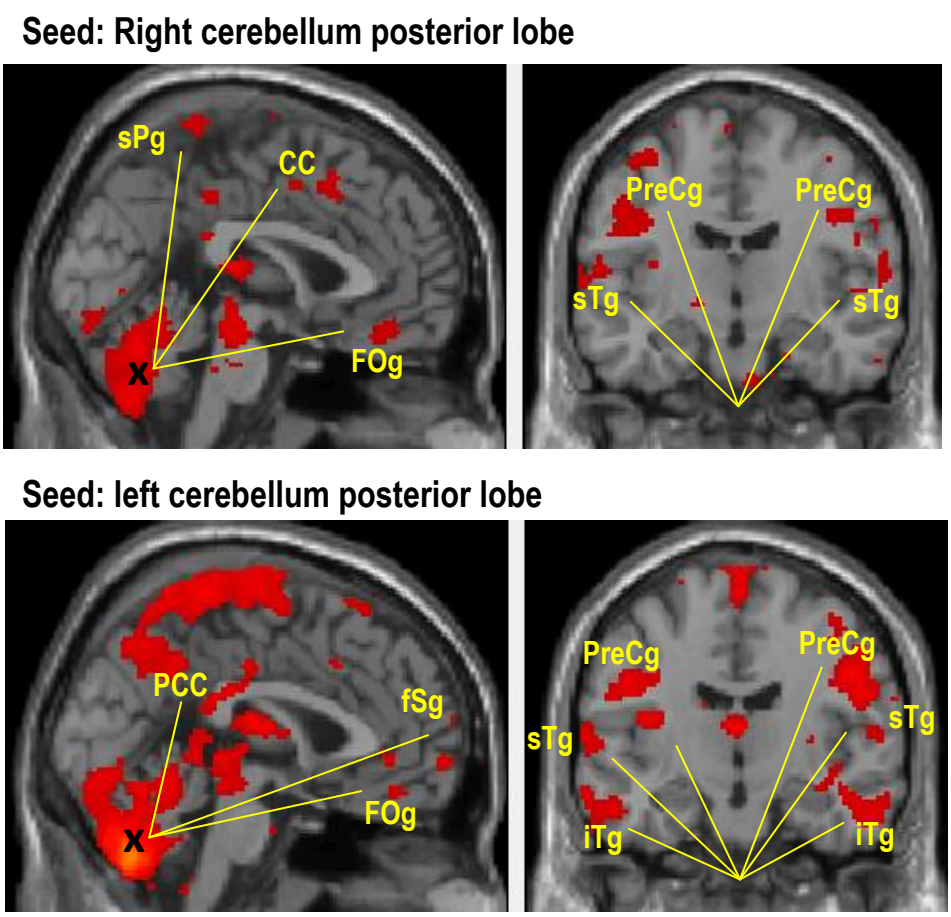

Figure 3. Images of the connectivity maps for the seeds in the cerebellum. Frontal orbital gyrus (FOg); Cingulate gyrus (CC); Superior Parietal gyrus (sPg); Precentral gyrus (preCg); Superior Temporal gyrus (STg); Superior Frontal gyrus (sFg); Posterior cingulate gyrus (PCC); Inferior temporal gyrus (iTg); Insula (In)

References

1. Borke, R.C., M.E. Nau, and R.L. Ringler, Jr., *Brain stem afferents of hypoglossal neurons in the rat.* Brain Res, 1983. **269**(1): p. 47-55.
2. Olsson, K.A., S. Landgren, and K.G. Westberg, *Location of, and peripheral convergence on, the interneuron in the disynaptic path from the coronal gyrus of the cerebral cortex to the trigeminal motoneurons in the cat.* Exp Brain Res, 1986. **65**(1): p. 83-97.
3. Sauerland, E.K., Y. Nakamura, and C.D. Clemente, *The role of the lower brain stem in cortically induced inhibition of somatic reflexes in the cat.* Brain Res, 1967. **6**(1): p. 164-80.
4. Nakamura, Y., L.J. Goldberg, and C.D. Clemente, *Nature of suppression of the masseteric monosynaptic reflex induced by stimulation of the orbital gyrus of the cat.* Brain Res, 1967. **6**(1): p. 184-98.
5. Chandler, S.H., L.J. Goldberg, and R.W. Lambert, *The effects of orofacial sensory input on spontaneously occurring and apomorphine-induced rhythmical jaw movements in the anesthetized guinea pig.* Neurosci Lett, 1985. **53**(1): p. 45-9.
6. Appenteng, K., J.P. Lund, and J.J. Seguin, *Intraoral mechanoreceptor activity during jaw movement in the anesthetized rabbit.* J Neurophysiol, 1982. **48**(1): p. 27-37.
7. Komuro, A., et al., *Putative feed-forward control of jaw-closing muscle activity during rhythmic jaw movements in the anesthetized rabbit.* J Neurophysiol, 2001. **86**(6): p. 2834-44.
8. Dworkin, S.F. and L. LeResche, *Research diagnostic criteria for temporomandibular disorders: review, criteria, examinations and specifications, critique.* J Craniomandib Disord, 1992. **6**(4): p. 301-55.
9. Nordstrom, M.A., *Insights into the bilateral cortical control of human masticatory muscles revealed by transcranial magnetic stimulation.* Arch Oral Biol, 2007. **52**(4): p. 338-42.
10. Hiraba, H. and T. Sato, *Cortical control of mastication in the cat: properties of mastication-related neurons in motor and masticatory cortices.* Somatosens Mot Res, 2004. **21**(3-4): p. 217-27.
11. Hiraba, H. and T. Sato, *Cortical control for mastication in cats: changes in masticatory movements following lesions in the masticatory cortex.* Somatosens Mot Res, 2005. **22**(3): p. 171-81.
12. Schimmel, M., et al., *Masticatory function and bite force in stroke patients.* J Dent Res, 2011. **90**(2): p. 230-4.

13. Kuypers, H.G., *Corticobular connexions to the pons and lower brain-stem in man: an anatomical study.* Brain, 1958. **81**(3): p. 364-88.
14. Nakamura, Y. and N. Katakura, *Generation of masticatory rhythm in the brainstem.* Neurosci Res, 1995. **23**(1): p. 1-19.
15. Hashimoto, N., et al., *Induction of rhythmic jaw movements by stimulation of the mesencephalic reticular formation in the guinea pig.* J Neurosci, 1989. **9**(8): p. 2887-901.
16. Brodal, P., *The corticopontine projection in the rhesus monkey. Origin and principles of organization.* Brain, 1978. **101**(2): p. 251-83.
17. Kelly, R.M. and P.L. Strick, *Cerebellar loops with motor cortex and prefrontal cortex of a nonhuman primate.* J Neurosci, 2003. **23**(23): p. 8432-44.
18. Glickstein, M., J.G. May, 3rd, and B.E. Mercier, *Corticopontine projection in the macaque: the distribution of labelled cortical cells after large injections of horseradish peroxidase in the pontine nuclei.* J Comp Neurol, 1985. **235**(3): p. 343-59.
19. Krienen, F.M. and R.L. Buckner, *Segregated fronto-cerebellar circuits revealed by intrinsic functional connectivity.* Cereb Cortex, 2009. **19**(10): p. 2485-97.
20. Matsuo, K. and J.B. Palmer, *Coordination of Mastication, Swallowing and Breathing.* Jpn Dent Sci Rev, 2009. **45**(1): p. 31-40.
21. Astafiev, S.V., et al., *Functional organization of human intraparietal and frontal cortex for attending, looking, and pointing.* J Neurosci, 2003. **23**(11): p. 4689-99.
22. Bedard, P. and J.N. Sanes, *Gaze and hand position effects on finger-movement-related human brain activation.* J Neurophysiol, 2009. **101**(2): p. 834-42.
23. Simon, O., et al., *Topographical layout of hand, eye, calculation, and language-related areas in the human parietal lobe.* Neuron, 2002. **33**(3): p. 475-87.
24. Wenderoth, N., et al., *The role of anterior cingulate cortex and precuneus in the coordination of motor behaviour.* Eur J Neurosci, 2005. **22**(1): p. 235-46.
25. Kohler, S., et al., *Memory impairments associated with hippocampal versus parahippocampal-gyrus atrophy: an MR volumetry study in Alzheimer's disease.* Neuropsychologia, 1998. **36**(9): p. 901-14.
26. Ogawa, K., et al., *Clinical study of the responsible lesion for dysarthria in the cerebellum.* Intern Med, 2010. **49**(9): p. 861-4.
27. Takashima, S. and L.E. Becker, *Relationship between abnormal respiratory control and perinatal brainstem and cerebellar infarctions.* Pediatr Neurol, 1989. **5**(4): p. 211-5.
28. Perie, S., et al., *Swallowing difficulties for cerebellar stroke may recover beyond three years.* Am J Otolaryngol, 1999. **20**(5): p. 314-7.

Chapter IV.

The oral dynamometer: a new technology to evaluate human chewing.

Introduction.

Chewing is the first step of the digestion process, where the food is ground into small pieces to increase the surface area for a better interaction with saliva and gastrointestinal digestive enzymes and to moisturize the food for adequate swallowing. Different technologies have been used to investigate human chewing. Gum base and commercially available gum have been used in conjunction with a recording systems (i.e. videos, electromyography) to analyze chewing [1] [2] [3] [4]. However chewing gum does not represent the same task as chewing food, because gum is not ingested one bite at a time, transported to the molar region for reduction and then swallowed. From a research perspective, gum also has some limitations. For instance, gum loses its consistency with time and there are no direct methods to assess how much pressure is being applied to the gum during each chewing cycle.

Food such as bread, peanuts [5], carrots [6], beef, salmon among others [7] and artificial foods such as Optocal ATF [8], CutterSil [9] and silicone [10] have been

used to evaluate chewing performance. Real and artificial foods have the same disadvantages. They can provide data for only around 30 chewing cycles, and bite pressure and physical parameters of the chewing function cannot be recorded.

Electromyography (EMG) has been used to evaluate the activity of the muscles of mastication (masseter, temporalis and digastric muscles) during chewing [11] [12] [13]. Although this technique allows the researcher to assess directly the muscle activity, variables such as food used in the experiment, electrode placement, tissue impedance and electrical activity from distant muscles can influence the outcome. In addition, the EMG gives the information about individual muscle contractions and relaxations, but the overall pressure required to grind the food remains undetermined.

Chewing has been evaluated using digital tracking systems [3] [14], where reflective or light generating markers are placed on the subjects face and jaw, and then their movement is used to track jaw and head movements via video recording while subjects chewed. This method is able to evaluate chewing kinematics (movements); however, similar to the other methods, chewing pressure is a variable that remains unmeasured.

The aim of this project was to create an oral dynamometer, a new device where the subjects can perform a chewing like task, at a constant pressure, for a long

period of time, and where pressures and pressure changes during chewing can be recorded.

Material and Methods

Oral dynamometer.

The oral dynamometer consisted of two unilateral plastic trays (superior and inferior) (Figure 1A). Both trays were attached via their handles to a 40 psi 1 inch long piston. The piston (Norgreen® RLA01ADAPNA00) was connected through a hose to an air-regulated source (Figure 1B). A pressure sensor in the air regulator was used to send a voltage signal to a data acquisition system (National Instruments® NI USB-6009). The trays were stabilized on the posterior teeth from the second premolar to the second molars using Blue Bite®. Once the trays were in place, air was delivered to the piston, which created a positive pressure inside the piston, inducing an opening movement in the jaw. When the subject started chewing on the trays, there were recordable changes in the pressure in the piston, which decreased and increased when the subject opened and closed during chewing, respectively. These changes of pressure were recorded and stored in a computer for further analysis.

Subjects.

This study was evaluated and approved by the medical institutional review board (IRB-Med) of the University of Michigan. Subjects read and signed an informed consent before starting any procedure.

Forty subjects (22 men and 18 women) with an age average of 24 years (SD±3.7), fully dentate, with Class I occlusion were selected for the project.

Chewing protocol.

The trays of the oral dynamometer, already adapted to the piston, were secured on the right (superior and inferior) premolars and molars using Blue Bite®. An air pressure of 8 psi was applied to the piston, and the subjects were asked to start chewing at their own preferred chewing rate. Pressure in the piston was recorded at a frequency of 10Hz. All the subjects chewed on the oral dynamometer for 10 minutes. After the 10 minutes, the air pressure was suspended and the trays were removed from the mouth.

Data preprocessing.

Data obtained with the oral dynamometer were preprocessed using the software R version 2.12.1 (R Development Core Team, 2010). Single chewing cycle durations were determined by calculating the time frame between maximum opening values. The number of chewing cycles per minute was determined for each subject. Chewing pressure was calculated for each chewing cycle by

measuring the difference between the first maximum (cycle onset) and minimum values in each cycle.

Results.

Figure 2 shows an example of the pressure recorded on the oral dynamometer while a subject was chewing. The pressure inside the piston increased and decreased from a baseline value of 8 psi as the subjects opened and closed their jaws. The spikes in the graph (Figure 2) where the pressures are at a maximum represent the points of the chewing cycles when the jaw was closed and the lower minimum points in the curve represent the instances when the mouth was open. A complete chewing cycle can be defined either from a maximum point pressure to another one or from a minimum point of pressure to the next minimum. Either way represents an effective method whereby the number of chews per minute can be determined for each subject. For purposes of this project, chewing cycles were defined from maximum to maximum pressure values.

Work associated with chewing.

An index of the amount of work performed for each chewing cycle was determined by calculating the product of the duration of the cycle by the corresponding pressure of that cycle, with the latter being defined as the difference between the first maximum and minimum pressures occurring during the given cycle. The chewing work per minute was determined by summing all

chewing cycle work values for each minute of the 10-min trial during which the subjects were performing the task. A principal component analysis was performed using the ten 1-min values for each subject as variables. The coefficients for each of the ten minutes ranged from 0.946 to 0.978, indicating that each minute contributed approximately equally to the first principal component (Table 1). Furthermore, virtually all the variation in the data set was captured in a single principal component. These results show that chewing work was stable through time in healthy subjects. Figure 3 shows that chewing work was normally distributed, and the Q-Q plot (Figure 4) also supports the hypothesis that chewing work in healthy subjects follows a normal distribution. A t-test was performed to identify differences between men and women (Figure 5). There were no significant differences between genders with respect to chewing work.

In Figure 6 the numbers of chewing cycles per minute for each subject are represented. To assess the stability of chewing rate over time, subjects were divided into quartiles based on their mean chewing rates for the first minute of chewing, and these means were compared with the means obtained from the tenth minute of chewing. A Chi-square test with a McNamara posttest was then performed to determine whether subjects grouped into fast, average or slow chewers based on the initial minute of chewing maintained this group membership at minute ten. Results presented in Table 2A and 2B show that there were no statistically significant differences in group memberships from

minute one to minute ten, indicating that the subjects kept their chewing frequency stable.

Discussion.

The aim of this chapter was to introduce the oral dynamometer as a new technology to assess human mastication. We have shown how the oral dynamometer allows subjects to perform a chewing like task at a constant pressure for a long period of time. Other devices to register bite pressure have been developed before, but they are only able to measure single bite pressures [15] [16], some of them with the limitation that they only record pressures when the teeth crowns are in contact. The advantage of the oral dynamometer is that it allowed us to differentiate subjects according to their chewing frequency, and we observed that the frequency remained stable over time. We will be interested in further studies to evaluate if increasing the pressure resistance in the oral dynamometer's piston will induce a change of chewing frequency over time and how it affects chewing performance.

In addition the new device permitted us to record pressures for every chewing cycle. We estimated the masticatory work per subject for each minute that they performed the task, and we were able to establish that in healthy subjects chewing work was normally distributed. Both of these findings indicate that mastication is a task that has high efficacy, which showed no statistically significant differences between men and women (Figure 5). Also chewing rate

was stable for both genders, with minor variation among each gender. Due to these stable results, the oral dynamometer promises to be a useful tool to evaluate chewing in subjects that may have alteration in their masticatory system such as TMD pain [17].

Minute	Work per minute	Component
1	894	.946
2	1219	.959
3	1447	.972
4	1570	.963
5	1400	.978
6	1212	.978
7	1300	.973
8	1367	.957
9	1519	.958
10	1573	.969

Table 1. A principal component was assigned to chewing work (for each minute). The results of the principal component analysis demonstrate that chewing work in healthy subjects is stable over time.

A.

Chewing frequency		Minute 10			
		Slow	Average	Fast	Total
Minute 1	Slow	6	2	0	8
	Average	3	10	5	18
	Fast	0	3	5	8
Total		9	15	10	34

B.

Chi-Square Tests

	P Value	df	Asymp. Sig. (2-sided)
McNemar-Bowker Test	.700	2	.705
N of Valid Cases	34		

Table 2. A. Crosstabulation between minute one and minute 10 for chewing frequency. Subjects have been assigned to Slow (lower quartile), Average (middle quartiles) or Fast (upper quartile) groups for minute 1 and for minute 10 separately. B. Chi-Square test with McNamara posttest results for subject groupings shown in A. This table showed that the variation in chewing frequency over time is not statistical significant, indicating that subjects' chewing frequencies remained stable from minute 1 to minute 10.

A

B

Figure 1A. Trays used on the oral dynamometer.

Figure 1B. Oral dynamometer's air regulator.

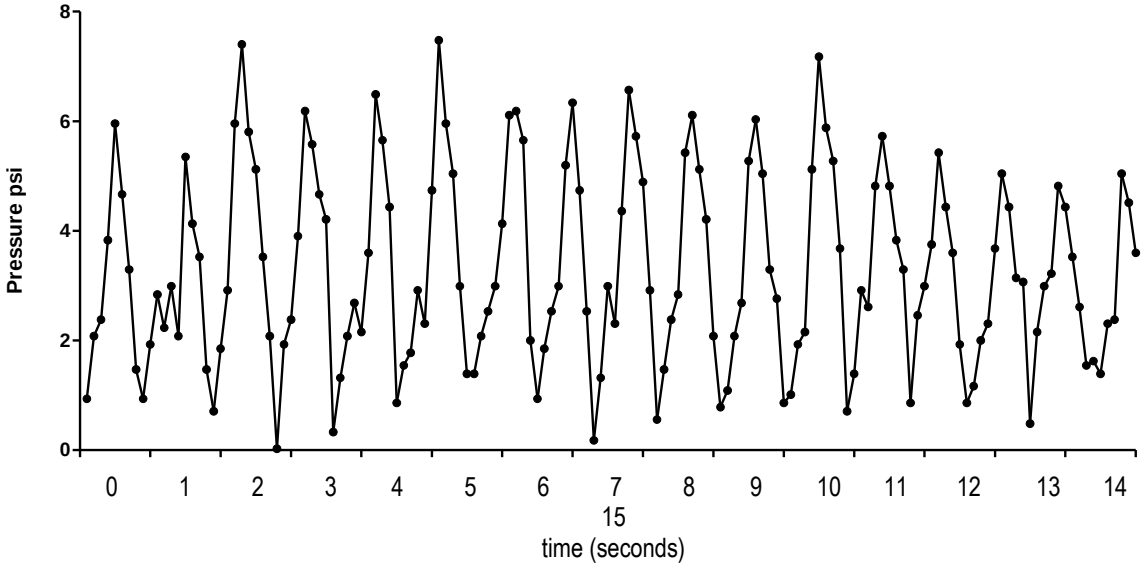

Figure 2. Example of changes in pressure while one subject was chewing on the oral dynamometer (only 15 seconds of the total 10 minutes are displayed in this graph). A chewing cycle was defined as the length of time between two successive maximum values. The pressure for each chewing cycle was determined as the difference between the maximum value and the minimum value of each chewing cycle.

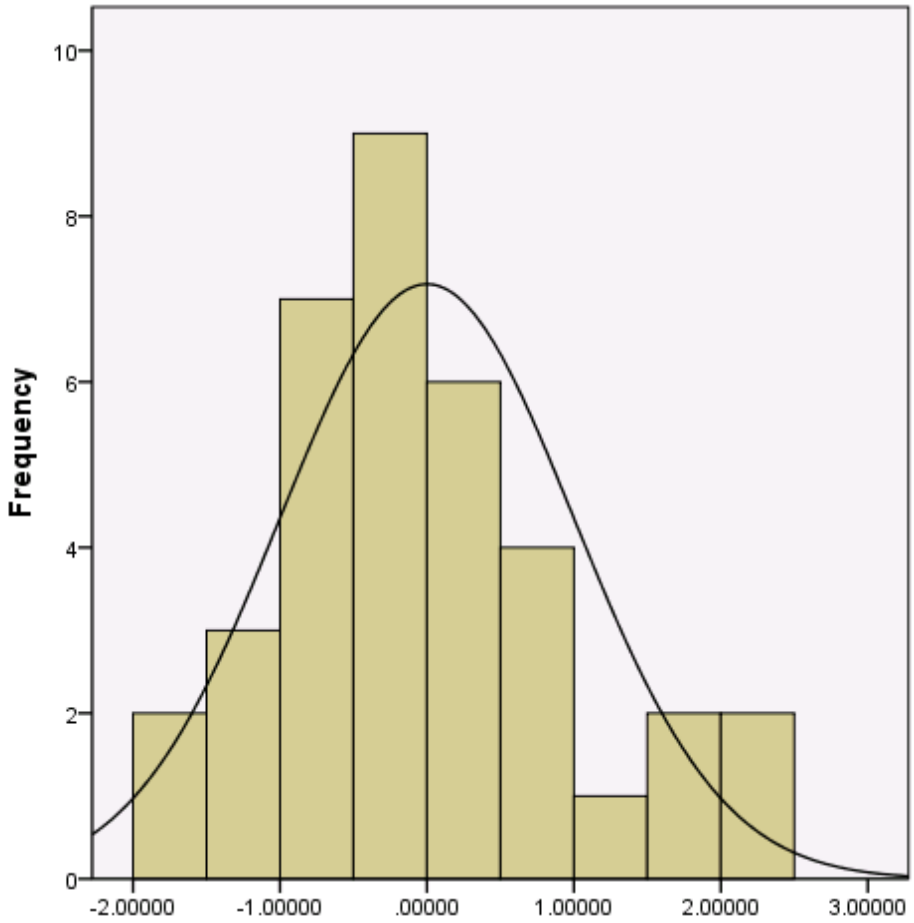

Figure 3. Chewing work.

Work distribution over 10 minutes of chewing on the oral dynamometer. Zero (0) is the mean value, 1 and -1 are the value of one standard deviation.

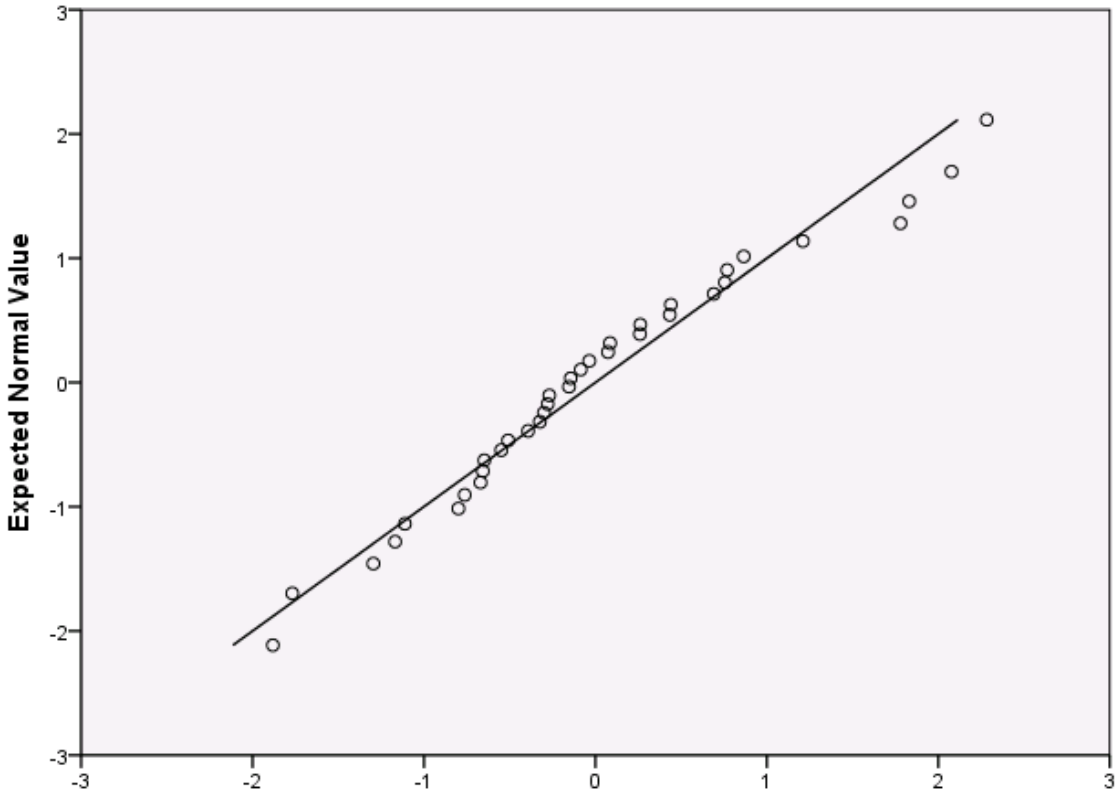

Figure 4. Q-Q plot for chewing work. Theoretical quantiles are plotted against the expected normal values.

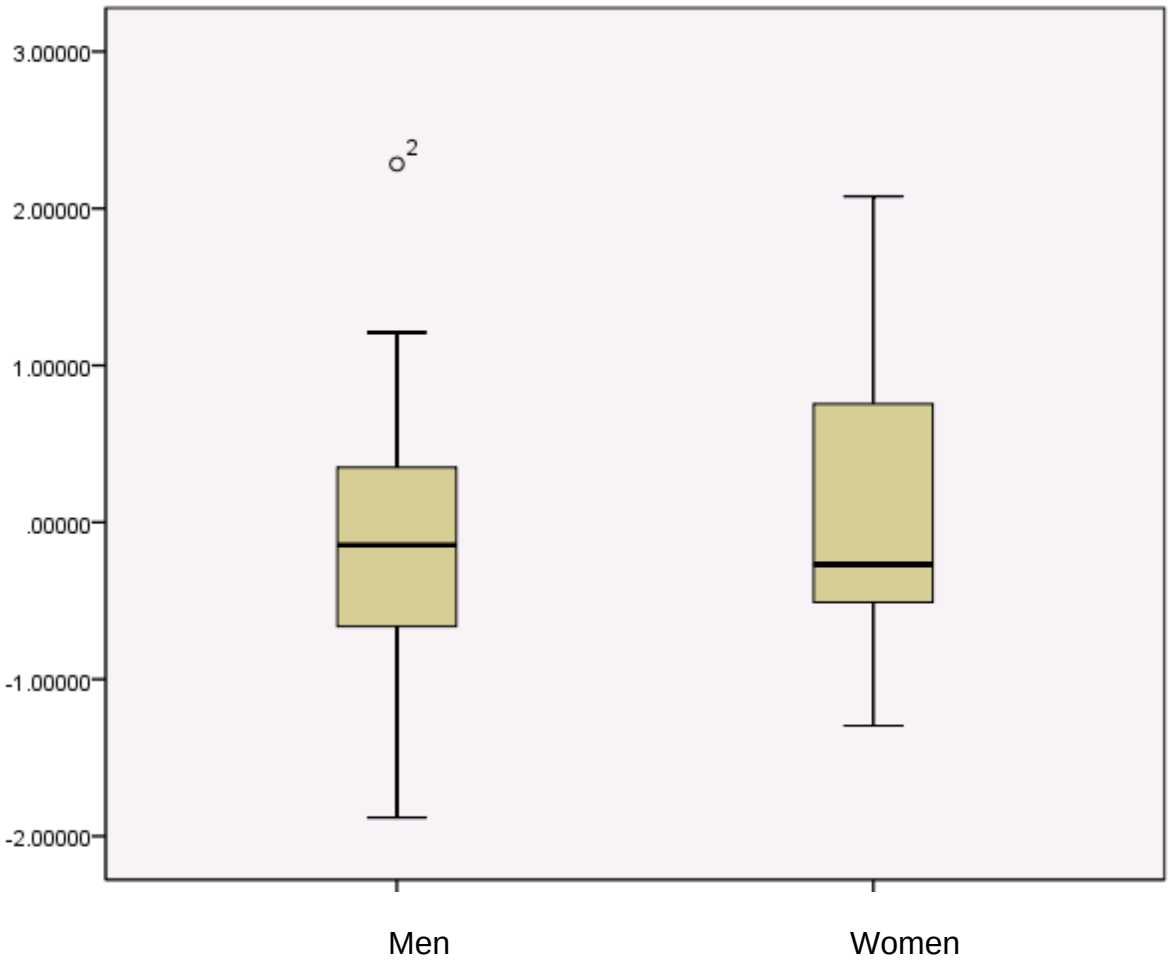

Figure 5. Comparison of chewing work between men and women.
Zero (0) is the mean, 1 and -1 are one standard deviation.

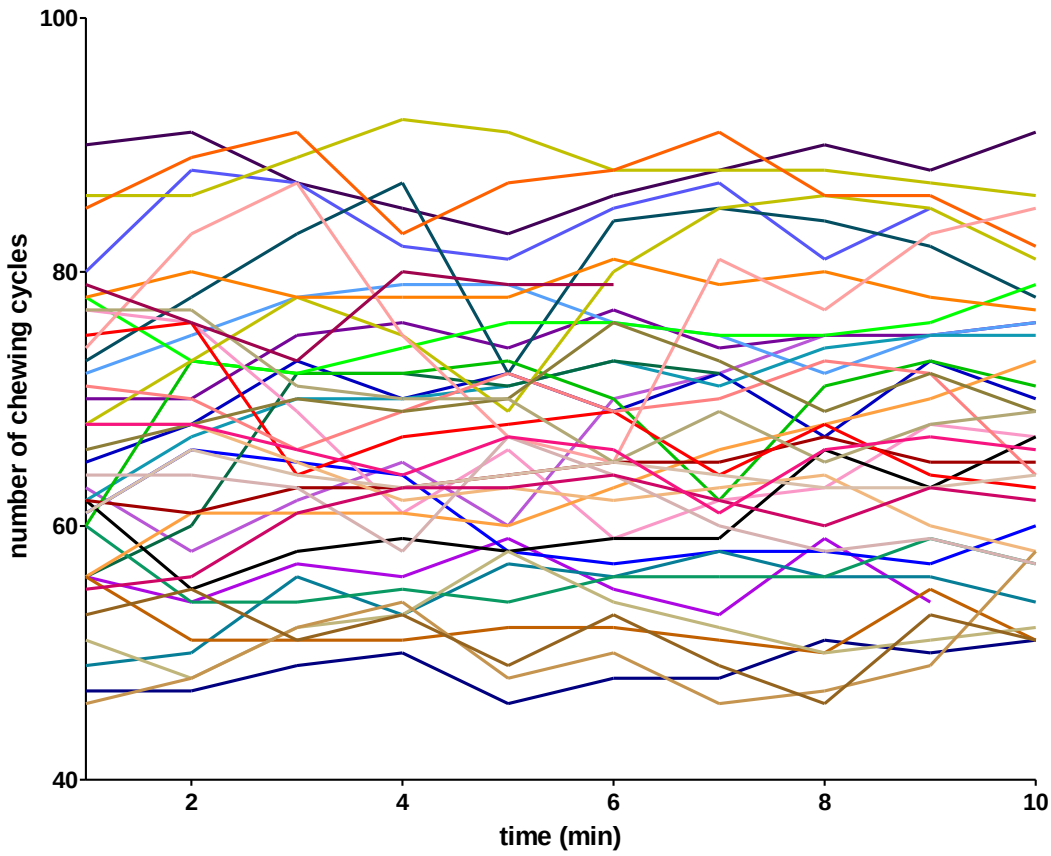

Figure 6. Chewing frequency. Number of chewing cycles per minute for all the subjects over ten minutes of chewing on the oral dynamometer.

References.

1. Ferrario, V.F., et al., *Neuromuscular coordination of masticatory muscles in subjects with two types of implant-supported prostheses.* Clin Oral Implants Res, 2004. **15**(2): p. 219-25.
2. Shiga, H., et al., *Influence of two masticating conditions on assessment of movement path stability.* J Prosthodont Res, 2011.
3. Crane, E.A., et al., *Effect of registration on cyclical kinematic data.* J Biomech, 2010. **43**(12): p. 2444-7.
4. Kubota, N., et al., *Jaw motion during gum-chewing in children with primary dentition.* Cranio, 2010. **28**(1): p. 19-29.
5. Rilo, B., et al., *Distance of the contact glide in the closing masticatory stroke during mastication of three types of food.* J Oral Rehabil, 2009. **36**(8): p. 571-6.
6. Woda, A., et al., *The masticatory normative indicator.* J Dent Res, 2010. **89**(3): p. 281-5.
7. KRISHAN KAPUR, S.S., ALIGARDAS YURKSTAS, *TEST FOODS FOR MEASURING MASTICATORY PERFORMANCE OF DENTURE WEARERS* J. PROSTHET. DENT, 1964. **14**: p. 483-491.
8. Goiato, M.C., et al., *Analysis of masticatory cycle efficiency in complete denture wearers.* J Prosthodont, 2010. **19**(1): p. 10-3.
9. Owens, S., et al., *Masticatory performance and areas of occlusal contact and near contact in subjects with normal occlusion and malocclusion.* Am J Orthod Dentofacial Orthop, 2002. **121**(6): p. 602-9.
10. Gomes, S.G., et al., *Masticatory features, EMG activity and muscle effort of subjects with different facial patterns.* J Oral Rehabil, 2010. **37**(11): p. 813-9.
11. Pereira, L.J., et al., *Masticatory function in subacute TMD patients before and after treatment.* J Oral Rehabil, 2009. **36**(6): p. 391-402.
12. Paphangkorakit, J., et al., *Determination of chewing efficiency using muscle work.* Arch Oral Biol, 2008. **53**(6): p. 533-7.
13. Wilding, R.J. and M. Shaikh, *Muscle activity and jaw movements as predictors of chewing performance.* J Orofac Pain, 1997. **11**(1): p. 24-36.
14. Lepley, C., et al., *Masticatory performance and chewing cycle kinematics-are they related?* Angle Orthod, 2010. **80**(2): p. 295-301.

15. Lin, K.R., et al., *Experimental and numerical estimations into the force distribution on an occlusal surface utilizing a flexible force sensor array.* J Biomech, 2011. **44**(10): p. 1879-84.
16. Komagamine, Y., et al., *Association between masticatory performance using a colour-changeable chewing gum and jaw movement.* J Oral Rehabil, 2011. **38**(8): p. 555-63.
17. Conti, P.C., et al., *Effect of experimental chewing on masticatory muscle pain onset.* J Appl Oral Sci, 2011. **19**(1): p. 34-40.

Chapter V.

Conclusions.

Outgoing contributions.

In summary our studies helped to generate a better understanding about brain mechanisms associated with chewing in healthy humans. In addition through this research we created a new device to evaluate human chewing, giving us the opportunity to study and understand chewing kinematics and chewing work in healthy patients.

fMRI contributions.

Although there are other fMRI and PET studies that have assessed brain activity during chewing, our fMRI study had advantages that the other studies did not consider. First, when the patients were in the MRI scanner, they received instructions to chew exclusively on the right side; chewing side has not been controlled in other studies. Our fMRI study showed brain activity related to unilateral chewing in healthy subjects. Given this design it is informative that our

results show symmetrical brain activity in the motor cortices during unilateral chewing. However, during chewing both sides of the jaw move at the same time albeit asymmetrically. This is, perhaps, a reason for bilateral brain activity, when the chewing block and the rest block were contrasted. In addition unique from our study, we divided the chewing block in five segments of 5 seconds each, and we contrasted each of these segments versus the rest block. The results from this analysis showed that brain activity related to chewing remained constant in the motor cortex and in the cerebellum; however, the size and precise positions of these activations changed over the segments. After that we contrasted successive segments of the chewing block, we were expecting to observe constant patterns of brain activity in all the contrasts; however, what we described was completely different. The brain activity associated with the initiation of the chewing movement was unique, and the pattern of brain activity evolved and changed over the duration of the chewing block. In summary this study showed that there was a specific brain activity pattern related to chewing in healthy subjects, and that this pattern had dynamic changes over time.

fcMRI contributions.

In chapter III we described brain activations related to chewing. Our second interest was to describe how the main areas that have been described to be involved in chewing such as the motor cortex and the brainstem and new areas that we described in our previous chapter that have a substantial role in chewing such as the cerebellum are connected among themselves and to others areas in

the brain. Unique to this research, we showed that both sensorimotor cortices were reciprocally connected. Also our findings demonstrated that the right and left motor cortices were functionally connected with the left and right cerebellar hemispheres, and these connections were reciprocal between the cerebellum and motor cortex. In addition we revealed the connections between the motor cortex and the precuneus, brainstem and thalamus. Moreover the cerebellum was shown to be functionally connected to both superior temporal gyri, inferior temporal gyri, insula, orbital gyrus and precuneus.

Oral dynamometer contributions.

In the fourth chapter we described the oral dynamometer as a new device to evaluate human chewing. The purpose was to create a device that could overcome the disadvantages of other methods used to evaluate chewing. We demonstrated that the oral dynamometer is biocompatible, safe to use, and that it will be an excellent method to record chewing pressure data, chewing frequency and chewing kinematics. We tested the oral dynamometer in a group of 40 healthy subjects, and we concluded that chewing frequency remains constant; we calculated the work output of the chewing task, and we determined that it was normally distributed. Since both variables (frequency and work) were shown to be stable, they can be used in further studies using traditional parametric tests to evaluate chewing function in other cohorts of patients.

Limitations.

During our study we found some limitations during the development of the experimental protocols.

First, during the fMRI and fcMRI study we analyzed the images at the level of the brainstem. The brainstem is an area that has a high concentration of small nuclei and both imaging techniques do not provide a sufficiently high resolution of the brainstem, making it difficult to identify specific nuclei.

Second, in the MRI scanner, subjects were chewing gum, which is similar to chewing food, with the difference being that gum is not converted into small pieces and that it is not swallowed after being chewed. Even though both actions are similar, we have to take into account that it is possible that the brain activity associated with chewing gum and chewing food might be different.

Third, while in the scanner the subjects were asked to chew on their right side; however it is known that during spontaneous chewing, the bolus changes from one side to the other in the mouth. We have to consider the possibility that maybe the brain activity and the connectivity maps could be different while the patients are chewing on just one side, compared with if they had been chewing on the contralateral side or chewing in a normal manner.

Also there were some difficulties with the experimental protocols of the oral dynamometer. First, normal chewing allows the temporomandibular joint to move in three directions, however the oral dynamometer allowed movements mainly in two directions (in the vertical plane and the horizontal plane). One of our purposes was to use the oral dynamometer in the MRI scanner, but since the piston is cast in magnetic metals, it was impossible to use it in scanner-based research.

A second difficulty was that the material for the trays started breaking after applying more than eight psi of pressure to the piston. This disadvantage made it impossible to test how chewing frequency or chewing work could vary when the pressure in the piston was increased.

Ideas for further studies.

In further studies we will develop new fMRI paradigms get a better understanding of the role of the cerebellum and the precuneus during chewing. Also we will use DTI to determine the pathways that are connecting the different areas that we described in chapters two and three. In addition we will research if there are differences in brain activity depending on the chewing side (left or right) or following a normal pattern of chewing. Also we will develop an MRI compatible oral dynamometer, to be able to compare our results from the MRI scanner with the chewing activity.

In addition, we will build high pressure resistant trays, that will allow us to evaluate chewing variables (frequency, work and kinematics) when subjects are chewing at high pressures. Also we would like to introduce a new variable which is chewing evoked pain; the aim will be to induce pain by eliciting extreme muscular activity as a result of chewing against high pressures. This will allow studies of function-evoked pain, fatigue and exercise to be implemented.

APPENDICES

Appendix A. Individual fMRI results for the brainstem. Images are the contrast between the chewing and rest blocks for each subject. They show the p-values where activations were detected in the brainstem.

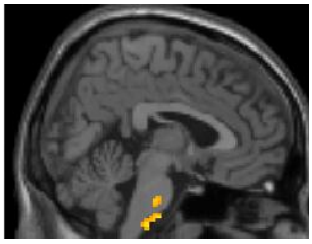

P<0.005-482voxels

P<0.001-662voxels

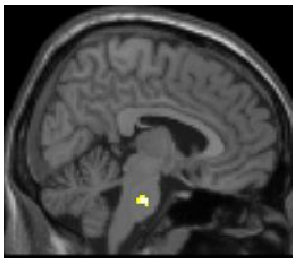

P<0.001-36voxels

P<0.05-791voxels

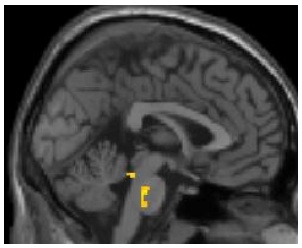

P<0.001-654voxels

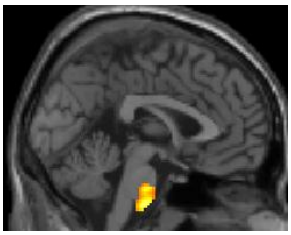

P<0.001-3110voxels

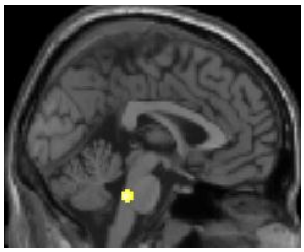

P<0.001-137voxels

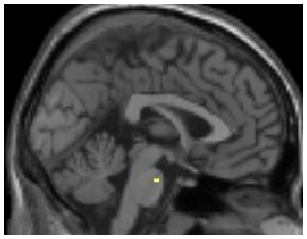

P<0.05-17voxels

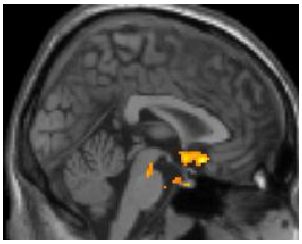

P<0.05-645voxels

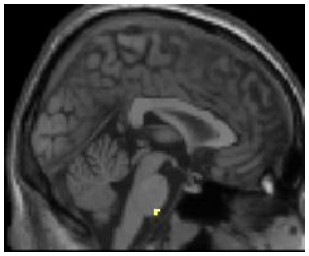

P<0.001-21voxels

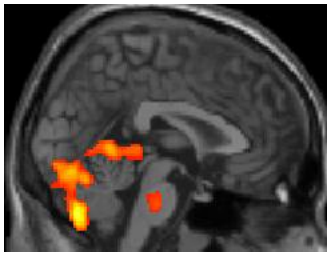

P<0.001-10254voxels

P<0.005-47voxels

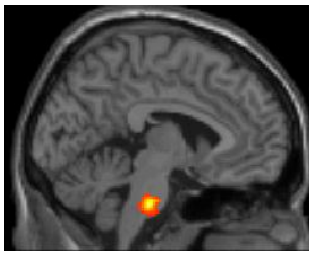

P<0.001-N/A voxels

P<0.1-5voxels

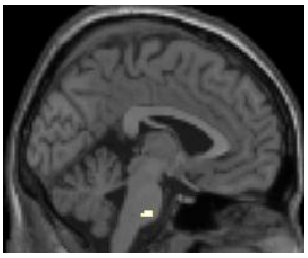

P<0.001-22voxels

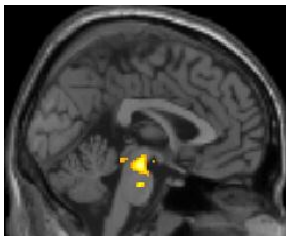

P<0.001-831voxels

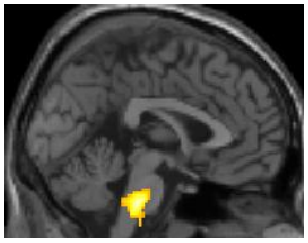

P<0.001-714voxels

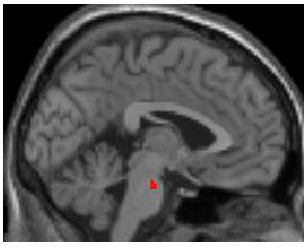

P<0.005-N/A voxels

P<0.001-499voxels

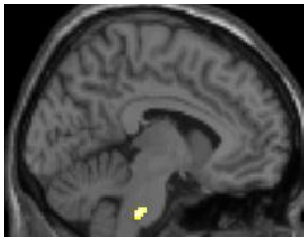

P<0.01-42voxels

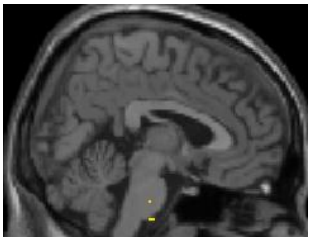

P<0.001-216voxels

P<0.001-390voxels

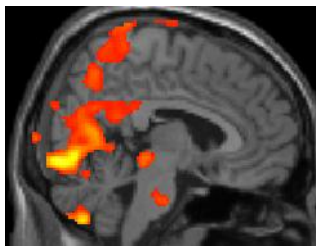

P<0.001-19072voxels

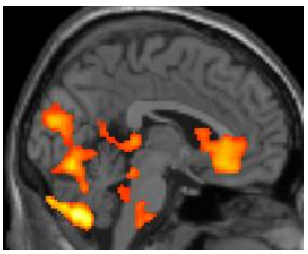

P<0.001-14566voxels

Appendix B. Brodmann's areas.

In our experiments we described patterns of activity and connectivity in the cerebral cortex. One of the most frequent maps used to identify functional zones in the cerebral cortex is the map of Brodmann's areas. (image obtained from: http://www.mrc-cbu.cam.ac.uk/people/jessica.grahn/neuroanatomy.html).

Primary motor cortex, supplementary motor cortex, premotor cortex are located in areas 4 and 6.

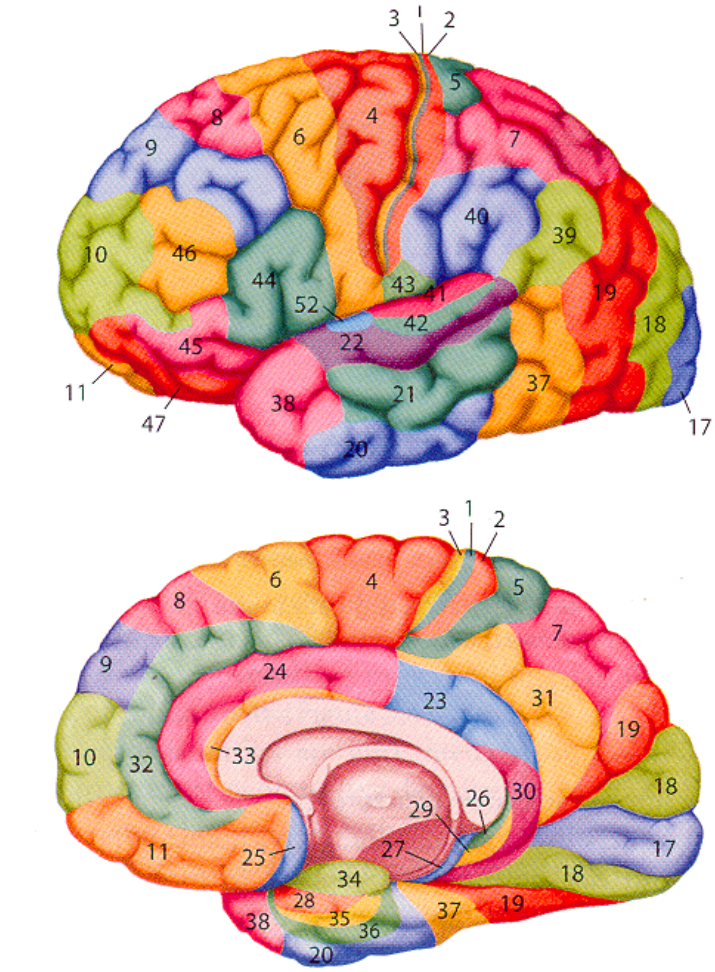

Appendix C. MRI Glossary

Voxel: Is a three dimensional volume (cuboidal shape), that represents a single data point in the three dimensional data set. In MRI all three dimensional images are formed by a group of voxels.

Cluster: Is a group of voxels that defines a volume in the data set. In MRI, clusters are the volumes that represent the zones with activations or deactivations.

Activations (opposite deactivation): In fMRI, when performing a contrast between two blocks (i.e. chewing and rest) the positive results of such a contrast are referred to as activations, and the negative results are referred to as deactivations.

Seed Region: In fcMRI, the area that is selected as the starting point for the connectivity map is named the seed region.

TE (Echo time). Time between middle of exciting radiofrequency pulse and middle of spin echo production.

TR (Repetition time): The period of time between the beginning of a pulse sequence and the beginning of the succeeding pulse sequence.

Field of view (FOV): The rectangular region superimposed over the human body over which MRI data are acquired. Its dimensions are specified in length in each in-plane direction.

Appendix D. Changes in regional gray and white matter volume in patients with myofascial-type temporomandibular disorders: a voxel-based morphometry study. Gerstner G, Ichesco E, Quintero A, Schmidt-Wilcke T. J Orofac Pain. 2011 Spring;25(2):99-106

Changes in Regional Gray and White Matter Volume in Patients with Myofascial-type Temporomandibular Disorders: A Voxel-based Morphometry Study

Geoffrey Gerstner, DDS, MS, PhD
Associate Professor
Department of Biologic and Materials Sciences
School of Dentistry and
Department of Psychology
University of Michigan
Ann Arbor, Michigan

Eric Ichesco, BS
Research Associate
Department of Biologic and Materials Sciences
School of Dentistry and
Chronic Pain and Fatigue Research Center
School of Medicine
University of Michigan
Ann Arbor, Michigan

Andres Quintero, BDS
Doctoral Candidate
Department of Biologic and Materials Sciences
School of Dentistry
University of Michigan
Ann Arbor, Michigan

Tobias Schmidt-Wilcke, MD
Research Fellow
Chronic Pain and Fatigue Research Center
Department of Anesthesiology
School of Medicine
University of Michigan
Ann Arbor, Michigan

Correspondence to:
Dr Geoffrey Gerstner
Department of Biologic and Materials Sciences
School of Dentistry
1011 North University
Ann Arbor, MI 48109-1078
Fax: (734) 763-3453
Email: geger@umich.edu

Aims: *To use magnetic resonance imaging (MRI) and voxel-based morphometry (VBM) to search for evidence of altered brain morphology in patients with temporomandibular disorders (TMD).* ***Methods:*** *Using VBM, regional gray and white matter volume was investigated in nine TMD patients and nine carefully matched healthy controls.* ***Results:*** *A decrease in gray matter volume occurred in the left anterior cingulate gyrus, in the right posterior cingulate gyrus, the right anterior insular cortex, left inferior frontal gyrus, as well as the superior temporal gyrus bilaterally in the TMD patients. Also, white matter analyses revealed decreases in regional white matter volume in the medial prefrontal cortex bilaterally in TMD patients.* ***Conclusion:*** *These data support previous findings by showing that TMD, like other chronic pain states, is associated with changes in brain morphology in brain regions known to be part of the central pain system.* J OROFAC PAIN 2011;25:99–106

Key words: anterior cingulate gyrus, central sensitization, chronic pain, neuroimaging, voxel-based morphometry

Temporomandibular disorders (TMD) are defined on the basis of clinical signs and symptoms, including temporomandibular joint (TMJ) sounds, impaired mandibular movement or limitation of mouth opening, and pain located in preauricular, facial, and masticatory muscle regions. Patients with TMD often describe symptoms of pain and dysfunction that also affect the ears, eyes, or throat, and headaches that involve virtually any cranial region and often cervical regions as well.[1] Most recently, there has been growing international agreement to classify TMD into three categories: *(1)* myofascial pain, manifesting as pain primarily in masticatory muscles, *(2)* TMJ disc-condyle discoordination, involving irregularities of joint mechanics, and *(3)* arthritides of the TMJ, eg, rheumatoid or osteoarthritis.[2-4]

According to US National Institutes of Health statistics, TMD represent the most common chronic orofacial pain, and they are the second-most common chronic pain condition behind lower back pain.[5] Historically, TMD pain was believed to be caused by peripheral mechanisms such as acute or chronic inflammation of the joint, tenderness of the masticatory musculature due to microtrauma, oromotor dysfunction, or "imbalance" of the dentoskeletal and neuromuscular systems. However, recent attention has been turned toward genetic predispositions[6] and the concept of central sensitization.[7] From a neurobiological perspective, the mechanisms contributing to pain amplification and chronicity are heterogeneous and are thought to occur at various levels of the peripheral and central nervous system (CNS). It is increasingly recognized that the role of the brain in

chronic pain states is not purely receptive but can be viewed as amplifying or possibly even constitutive. In such cases, studies of brain anatomy, function, and physiology are critical to understanding the root etiologies and pathophysiologies of chronic pain conditions such as TMD.

To date, numerous human neuroimaging studies have provided insights into brain activation associated with pain perception.[8,9] Recent findings provide promising results regarding aberrant activation patterns in response to painful stimuli in chronic pain states, such as fibromyalgia (FM),[10–12] a chronic pain condition often associated with TMD.[13] Furthermore, changes in brain morphology have been described in various chronic pain conditions affecting the head and face, including chronic tension-type headache,[14] migraine,[15,16] chronic trigeminal neuropathic pain,[17] persistent idiopathic facial pain,[18] and, very recently, also TMD.[19] The most reproducible finding across pain syndromes is a decrease in gray matter (GM) density/volume in the anterior cingulate gyrus (ACC) and insular cortex (IC).[20] It has been suggested that changes in regional brain morphology not only contribute to the evolution of chronic pain but might also contribute to other clinical traits frequently found in chronic pain patients, such as increased levels of anxiety and depression, as well as cognitive impairment.[21] However, little research has been done in this regard on TMD patients.

Therefore, the aim of this study was to use magnetic resonance imaging (MRI) and voxel-based morphometry (VBM) to search for evidence of altered brain morphology in patients with TMD.

Materials and Methods

Subjects

Nine female patients with myofascial-type TMD and nine age-, gender-, ethnicity-, weight-, and height-matched healthy controls were recruited for the study. All subjects with TMD were carefully examined and screened by an experienced orofacial pain investigator who applied the Research Diagnostic Criteria (RDC) for the diagnosis of myofascial-type TMD (Group Ia,b).[4] Only those subjects who fulfilled the Group I myofascial pain criteria were included. All subjects were right-handed. Because pain symptoms can be coupled to menstrual cycle phase in premenopausal women and women on oral contraceptives,[22] all subjects participated in pain and imaging studies within 3 days of menstrual onset.

Inclusion and exclusion criteria consisted of the following. Inclusion criteria included: *(1)* presence of ongoing pain in the face, jaws, or temples > 1 time per week, *(2)* presence of pain symptoms for > 3 months, and *(3)* meeting the RDC/TMD criteria for myofascial pain Group Ia,b. The main inclusion criterion for healthy controls was absence of TMD pain, or facial pain < 1 time per week. Exclusion criteria for all subjects included physical impairment, any outstanding history of systemic or medical conditions, psychiatric illnesses, substance abuse within 2 years, and presence of head or neck pain other than masticatory myalgia. Nonsteroidal anti-inflammatory drugs were allowed until 3 days before the pain and scanning trials. All participants signed an informed consent that detailed the procedures of the study. The study had been approved by the Institutional Review Board at the University of Michigan.

Clinical Pain

The clinical pain experience of patients with TMD and healthy controls was assessed using the visual analog scale (VAS) and the pain rating index (PRI) from the Short Form McGill Pain Questionnaire (SF-MPQ).[23] The VAS consisted of a 10-cm line anchored on the left with "no pain" and on the right with "worst possible pain." Participants in the study were asked to rate their present orofacial pain by placing a tick along this line. The PRI component of the SF-MPQ consisted of 15 word descriptors (11 sensory and 4 affective). Participants rated these descriptors as either "none," "mild," "moderate," or "severe," giving a score of 0, 1, 2, or 3, respectively, for each descriptor. The measures were added to yield sensory, affective, and total scores. Another questionnaire used to evaluate clinical pain was the Brief Pain Inventory (BPI).[24] Information from this measure was used to determine both severity of pain and the degree of pain interference. Questions for these measures were answered using a 0 to 10 numeric rating scale for each item.

Depression and Anxiety

The State-Trait Personality Inventory (STPI) is a self-report tool designed to measure anxiety and depression. The STPI consists of eight 10-item subscales. The trait depression and anxiety scales were used to assess each subject's emotional disposition, and both scales were rated on a four-point intensity scale.[25]

Due to the relatively small sample size, the Mann-Whitney *U* test was applied to assess significant differences in age, height, and behavioral scores (pain, depression, and anxiety) between groups. Differences were deemed significant at $P < .05$ (corrected for multiple comparisons). Table 1 provides detailed information on patients and healthy controls. The Spearman

Table 1 Behavioral Data of Individual Subjects

	Age (y)	Gender	Pain duration (y)	BPI SEV	BPI INT	MPQ Tot	MPQ Sens	MPQ Aff	MPQ-VAS	STPIDA Ax	STPIDA D
TMD patients											
t01	23	F	1.5	0.25	0.43	3	2	1	0.6	16	13
t02	26	F	1.75	2.75	0	6	6	0	1.9	12	13
t03	23	F	3	2	0.14	5	5	0	1.7	12	11
t04	27	F	0.5	3.75	8.29	3	3	0	1.5	25	25
t05	25	F	4	2.5	6.71	16	14	2	5	22	18
t06	24	F	1	3	0.71	14	12	2	3.8	12	10
t07	24	F	0.75	3	1.43	3	3	0	2.6	19	18
t08	31	F	7	0.75	0	3	3	0	2	11	10
t09	26	F	3	0	0	2	2	0	1	26	27
Controls											
c01	25	F	0	2	0	0	0	0	0.1	17	15
c02	25	F	0	NA	NA	0	0	0	0	17	11
c03	22	F	0	0	0	0	0	0	0	10	10
c04	24	F	0	0	0	0	0	0	0	10	10
c05	25	F	0	0.75	0	4	4	0	1.7	14	10
c06	26	F	0	0	0	0	0	0	0	12	10
c07	24	F	0	0.75	0	0	0	0	0	11	10
c08	25	F	0	0.25	0	0	0	0	0.2	13	10
c09	27	F	0	0.75	0.71	0	0	0	0	12	14
Mann-Whitney	0.796			0.136	0.190	0.001*	0.001*	0.258	< 0.001*	0.136	0.050

BPI INT = Brief Pain Inventory pain interference; BPI SEV = Brief Pain Inventory pain severity; MPQ Tot = Short Form McGill Pain Questionnaire Pain Rating Index – Total Score; MPQ Sens = Short Form McGill Pain Questionnaire Pain Rating Index – Sensory Score; MPQ Aff = Short Form McGill Pain Questionnaire Pain Rating Index – Affective Score; MPQ-VAS = Short Form McGill Pain Questionnaire Visual Analog Scale; NA = not available, missing data; STPIDA Ax = State-Trait Personality Inventory trait anxiety; STPIDA D = State-Trait Personality Inventory trait depression. Mann-Whitney *U* test was used for group comparison. *P* values were deemed significant at $P < .05$ after correction for multiple comparisons (*significant differences).

rank correlation analysis was also used to test for significant correlations between pain measures (pain duration, BPI scores, MPQ scores), depression, and anxiety measures. Correlations were deemed significant at $P < .05$ (corrected for multiple comparisons).

Scanning Protocol

Magnetic resonance imaging (MRI) was performed on a 3.0 Tesla GE Signa scanner (LX [VH3] release, neuro-optimized gradients). For each subject, a T-1 weighted gradient echo data set (TR 1400 ms, TE 5.5 ms, flip angle 20 degrees, FOV 256 x 256, yielding 124 sagittal slices with a defined voxel size of 1 × 1 × 1.2 mm) was acquired. Inspection of individual T1 MRI scans revealed no gross morphological abnormalities for any patient or subject.

Preprocessing and Statistical Analysis

The SPM5 software package (Functional Imaging Laboratories) running under Matlab 7b was used to preprocess and analyze structural data.[26] Estimation of total gray matter volume (GMV), white matter volume (WMV), and cerebrospinal fluid (CSF) was performed by segmenting the original image, using the Ibaspm toolbox (toolbox for automatic parcellation of brain structures), provided by the Cuban Neuroscience Center.[27] Groups were then compared using a Mann-Whitney *U* test.

Preprocessing of structural images was performed using the VBM toolbox (VBM 5.1, provided by C Gaser, default settings), which involved spatial normalization, segmentation, and spatial smoothing (Gaussian kernel of 8 mm full-width at half maximum for

Table 2 Behavioral Data of the Two Groups

	TMD	Controls	P
Age	25.4 ± 2.5	24.8 ± 1.4	.796
Pain duration	2.5 ± 2.1	0 ± 0	
BPI SEV	2.0 ± 1.3	0.6 ± 0.7	.136
BPI INT	2.0 ± 3.2	0.1 ± 0.3	.190
MPQ Tot	6.1 ± 5.2	0.4 ± 1.3	.001*
MPQ Sens	5.6 ± 4.4	0.4 ± 1.3	.001*
MPQ Aff	0.6 ± 0.9	0 ± 0	.258
MPQ VAS	2.2 ± 1.4	0.2 ± 0.6	< .001*
STPIDA Ax	17.2 ± 6.0	12.9 ± 2.7	.136
STPIDA D	16.1 ± 6.4	11.1 ± 2.0	.050

Mann-Whitney *U* test was used for group comparison. *P* values were deemed significant at $P < .05$ after correction for multiple comparisons (*significant differences).

GM images). Normalized white matter (WM) images were smoothed with a kernel of 12 mm. Modulated images were used for statistical analyses; correspondingly, GM and WM values are referred to as regional GM or WM volume. Significant regional differences in GM and WM values between groups were identified by applying voxel-wise statistics using the SnPM (Statistical nonParametric Mapping) toolbox, which uses the general linear model to construct pseudo t-statistic images, and then assesses the data for significance by using a nonparametric multiple comparison procedure based on permutation testing. Permutation tests are recommended for designs with low degrees of freedom.[28] The following design module was applied: two groups; two sample *t* test; one scan per subject; with age as nuisance variable. To avoid possible edge effects around the border between gray and white matter and to include only relatively homogeneous voxels, all voxels were excluded with a matter value of < 0.1 (maximum value of 1). A total of 5,000 permutations were performed for GM and WM analyses. With respect to the brain regions shown to be activated by noxious stimuli, as well as the structural changes described in chronic pain patients,[20] which are most frequently found in the ACC and IC, the authors had a clearly defined a priori hypothesis. Therefore, a threshold of $P < .001$ (uncorrected for multiple comparisons, with a cluster extent of 200 contiguous voxels) was applied. For correlation analyses, the eigenvariate was extracted from a sphere of 4 mm around the peak coordinates of the GM clusters, yielding an average GM value for that region in each person; values were then transferred to SPSS version 17 (IBM) where correlation analyses (Spearman rank correlation) were performed, correlating extracted GM values with pain duration, pain intensity (VAS), STPI Trait-anxiety, and STPI Trait-Depression scores in the TMD group. Anatomical labeling of brain regions was performed using the SPM5 extension xjView.

Results

Subjects

Both groups did not differ significantly in age ($P = .48$), height ($P = .91$), or weight ($P = .76$). Furthermore, there were no significant differences in ethnicity (both groups consisted of one African American, three Asian, and five Caucasian participants).

Clinical Pain, Depressive, and Anxious Symptoms

After correcting for multiple comparisons, patients with TMD displayed significantly higher VAS scores ($P < .001$) than healthy controls (Table 2). TMD patients also showed higher scores than healthy controls for the measures of MPQ Tot ($P = .001$) and the MPQ Sens ($P = .001$), as shown in Table 2.

Within the TMD group, the STPI Trait-anxiety scores were significantly correlated with STPI Trait-depression scores ($\rho = 0.95$, $P < .001$). However, they were not significantly correlated with BPI pain scores or MPQ scores. Pain duration correlated with BPI severity ($r = -0.69$, $P = .04$), but this correlation did not survive correction for multiple comparisons.

Global GM and WM Volumes

There were no significant differences in GM or WM volumes between TMD patients (GM: 705.780 mm^3, SD = 60.174; WM: 419.005 mm^3, SD = 24.194) and healthy controls (GM: 699.154 mm^3, SD = 72.558; WM: 410.976 mm^3, SD = 37.692 mm^3; $P_{GM} = .83$, $P_{WM} = .60$).

VBM

A decrease occurred in regional GM volume among TMD patients compared with healthy controls at the following locations: the left ACC, the right posterior cingulate gyrus (PCC), the right IC, the left inferior frontal gyrus (IFG), as well as the superior temporal gyrus (STG) bilaterally, extending into the middle temporal gyrus (MTG) on the right-hand side. A decrease in regional WM volume was observed in the medial frontal (MFG) and superior frontal gyrus (SFG) bilaterally, left precuneus and left middle/inferior frontal gyrus. An increase in regional WM

Table 3 Results of Group Analyses–VBM

	Side	BA	Cluster size (no. of voxels)	Pseudo *t* values (peak voxel)	Coordinates X	Y	Z
GM group analysis*							
Decrease in regional GM in the TMD group							
IFG	L	45/46	676	4.86	–47	25	19
ACC/medial frontal gyrus	L	8/9/6/32	794	4.71	–7	21	45
PCC/Precuneus	R	31	339	4.21	11	–42	41
STG	L	22	322	4.03	–49	5	–3
Parahippocampal gyrus	R	36	394	3.88	32	–18	–25
STG/MTG	R	21	268	3.75	51	–7	–12
Anterior IC	R	47/13	320	3.47	29	23	–8
WM group analysis*							
Decrease in regional WM in the TMD group							
MFG/SFG/ACC	L		4133	4.79	–16	25	40
Precuneus	L		526	4.56	–17	–82	36
Inferior frontal/precentral gyrus	R		575	4.37	59	3	22
MFG/SFG/ACC	R		2007	4.26	18	25	43
Middle frontal gyrus	L		622	4.26	-35	26	29
Increase in regional WM in the TMD group							
STG/supramarginal gyrus	R		2887	5.07	43	–52	20
STG/MTG	L		1090	4.96	–35	–56	19

BA = Brodmann area; * = two sample *t* test with age as nuisance variable.

volume was found in the posterior parts of the STG bilaterally, reaching into the supramarginal gyrus on the right side. For details, see Table 3 and Fig 1. GM volume in the right STG/MTG correlated negatively with pain duration ($\rho = -0.78$, $P < .05$). The other clusters identified by the cohort analysis were not correlated with any pain, anxiety, and/or depression measures.

Discussion

A main finding in TMD patients was a decrease in GM volume in various parts of the central pain system, such as the left ACC, the right PCC, the right anterior IC, the left IFG, and STG bilaterally. WM analysis, on the other hand, revealed a decrease in WM volume in the medial prefrontal cortex, predominantly in the MFG and SFG bilaterally in TMD subjects. An increase in regional WM volume in TMD patients was found in the posterior STG bilaterally, reaching into the supramarginal gyrus on the right side. No differences in global GMV or WMV were detected.

The most reproducible finding across morphometric studies investigating chronic pain syndromes is a decrease in GM density/volume in the ACC and IC.[20] Interestingly, a regional atrophy in the ACC and IC has also been found in other headache[14,15,29] and facial pain syndromes.[18] Both structures are known to play a critical role in various aspects of pain experience and assessment, including anticipation of pain and antinociception. As such, the present findings could reflect either a local atrophy associated with hyperactivity in pain-perceptive brain structures, eg, a loss of inhibitory interneurons, or an impairment of antinociceptive structures, such as a loss of neurons contributing to descending inhibitory pathways.

On the other hand, it is conceivable that GM changes as delineated by VBM do not reflect neuronal damage, but rather changes in synaptic density or even altered regional blood flow, eg, microvascular volume changes.[30] However, in this study, GM atrophy in the ACC was accompanied by a neighboring atrophy of WM in the MFG and SFG (see below), and it has been suggested that shrinkage of local GM volume with evidence of concomitant loss of WM

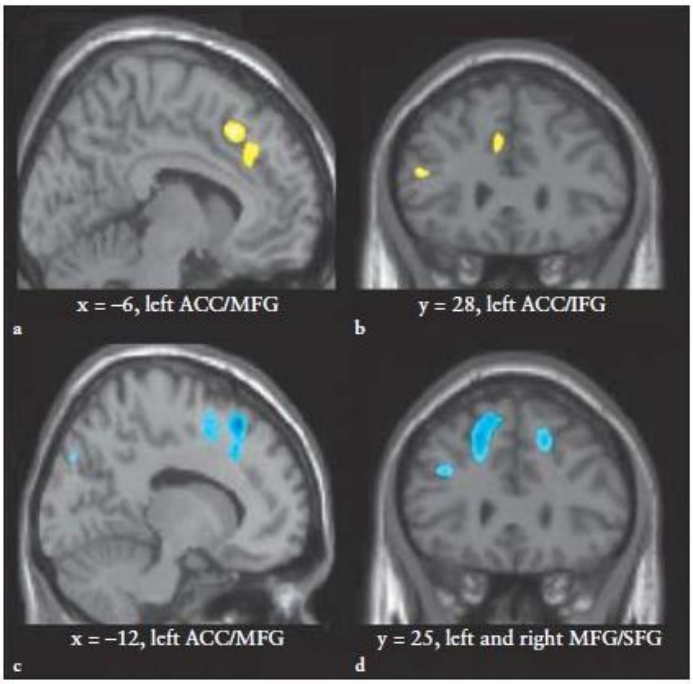

Fig 1 Regional changes in gray and white matter volume. *(a)* and *(b)* show statistical non-parametric maps (SnPM) demonstrating differences (decrease) in regional GM volume between TMD patients and healthy controls (significant findings are superimposed in yellow). *(c)* and *(d)* SnPM demonstrate differences (decrease) in regional WM volume between TMD patients and healthy controls (significant findings are superimposed in blue). *(a)* and *(c)* show left medial frontal cortex (sagittal view). *(b)* and *(d)* show coronal view. SnPMs were superimposed on a normalized high resolution image. The left sides of the pictures *(b)* and *(d)* are the left side of the brain. Significance threshold: $P < .001$ (uncorrected).

connectivity supports the neurodegeneration hypothesis.[31] It is tempting to hypothesize that these changes reflect a disconnection between the ACC and the superior/medial frontal gyrus. Interestingly, Geha et al reported a decrease in fractional anisotropy in the left cingulum-callosal bundle in patients with chronic regional pain syndrome (projecting close to the region where decreases in WM volume in TMD patients were found in this study), which they interpreted as an indication of a decreased structural connectivity between the ACC and supplementary motor cortex.[31] It has been demonstrated that the MFG and SFG play an important role in higher cognitive functions, such as working memory and decision making,[32] but also in cognitive evaluation of pain. Perhaps such a disconnection could either cause cognitive deficits, as they have been frequently described in chronic pain patients[33–35] (but not specifically investigated in this study), or aggravate the pain situation by further disabling cognitive modulation of pain.

Although not part of the classical pain system, the MTG and STG appear to be involved in the processing of trigeminal sensory input,[36] experimental dental pain,[37] and even virtual dental treatment,[38] suggesting that these regions may be noteworthy in chronic trigeminal pain conditions such as TMD. Interestingly, within the TMD group, GM volume in the right MTG/STG in this study was negatively correlated with pain duration. Other VBM studies investigating chronic pain states have also found an atrophy in the STG in FM patients[39] and chronic migraine patients.[16] Again, the present findings corroborate results from previous studies in these terms and suggest that the role of the MTG and STG in chronic pain may need to be more carefully studied.

Finally, an increase in WM volume was found in the posterior part of the STG and supramarginal gyrus. There had been no strong a priori hypothesis for this region, and to the authors' knowledge, such changes have not previously been reported in chronic pain syndromes. However, changes were rather pronounced, thus compelling an explanation. VBM does not allow an assessment of fiber orientation, enabling the allocation of the cluster to a specific fiber tract. However, the changes most likely map to the posterior thalamic radiation and/or the superior longitudinal fasciculus, which, in this location, connects the temporal lobe to the insular and frontal cortex. From this perspective, it is intriguing to hypothesize that the WM increase reflects a structural hyperconnectivity between the STG/MTG and the insular cortex and/or frontal lobe. However, at this

stage, findings should be viewed with caution, and assumptions are rather speculative.

In a recently published VBM study, Younger et al investigated 14 TMD patients and 14 healthy controls and reported decreased GM volume in the right somatosensory cortex, as well as increased GM volume in several brain areas, including the right IFG, right anterior IC, the right lentiform nucleus, and the thalamus bilaterally.[19] In addition, brainstem structures, including the trigeminal nucleus bilaterally and the middle cerebellar peduncle bilaterally, were shown to have an increase in GM volume. Both the study by Younger et al and the present study did not find any differences in global GMV between groups. Also, both studies identified the left ACC as an area that showed pain-related structural changes. On the other hand, both studies report opposite findings between the TMD and healthy control groups in the right anterior IC.

There are several reasons that could possibly account for the apparent differences in results between the two studies, both of which used the same methodological approach in the same pain condition. First, the study cohort investigated by Younger et al showed more diversity in age, and study participants were an average of 15-years older than those investigated in the present study. Secondly, the cohort investigated by Younger et al showed higher pain ratings as a group than those participating in the present study. Finally, nine out of 14 patients in the Younger et al study took centrally active drugs, mostly cyclobenzaprine, whereas, in the present study, all patients were drug naïve.

In most studies, chronic pain is associated with a decrease in regional GM volume, especially in the IC; however, there are several brain regions where an increase in GM volume and/or density has been described, eg, the thalamus [29,40] and the lentiform nucleus.[39,41] It is likely that the direction of change, whether it be an increase or a decrease, depends on the anatomical structures involved, the location of the nociceptive source, duration or chronicity of pain, and pain intensity. It is also important to acknowledge that centrally active drugs can have neuroplastic effects, eg, serotonin reuptake inhibitors,[42] neuroleptic drugs,[43] and opioids.[44] It will be critical for future studies to control for possible medication effects, by either including drug-naïve patients only or by applying a wash-out period prior to scanning.

Finally, several limitations inherent in the present study should be noted. Firstly, this study included a relatively small number of patients, and, as such, the study needs to be viewed as a pilot study. Secondly, from a methodological point of view, VBM cannot disclose the neurobiological basis of morphological differences found, and assumptions regarding the underlying cytoarchitecture, especially in a cross-sectional study, remain speculative for now. Thirdly, it is unclear whether GM volumetric reductions in the left ACC predispose someone to developing chronic TMD pain, or whether chronic TMD pain leads to GM volumetric reductions in the ACC. Future cross-sectional studies with larger sample sizes and longitudinal studies, including cross-correlation with functional imaging data, are required to confirm the present findings and to disclose the interaction between atrophy, pain, and brain plasticity. Finally, it needs to be pointed out that three out of nine TMD patients, although fulfilling the diagnostic criteria of TMD, had BPI severity scores and BPI interference scores < 1 at the time of the investigation. This might be a potential weakness in the sense that the TMD group investigated in the present study manifested relatively mild symptoms. On the other hand, the present results possibly reflect a snapshot of chronic pain in patients who are young and at the beginning of the chronification process. Such study samples might be interesting for future (longitudinal) studies that intend to unravel causes and consequences of chronic pain and to account for symptom heterogeneity among patients.

In conclusion, these data further support the idea that chronic pain is associated with structural changes of the CNS that are likely to contribute to pain chronification and the development of other core symptoms, such as anxiety and depression. Neuroimaging in TMD is just at its beginning, and further research is needed to uncover TMD-related changes in CNS function and structure.

Acknowledgments

This study was supported by an NIH Grant DE018528 to Geoffrey Gerstner. Tobias Schmidt-Wilcke is currently supported by a grant of the DFG (Deutsche Forschungsgemeinschaft, GZ: SchM 2665/1-1).

References

1. Suvinen TI, Reade PC, Kemppainen P, Kononen M, Dworkin SF. Review of aetiological concepts of temporomandibular pain disorders: Towards a biopsychosocial model for integration of physical disorder factors with psychological and psychosocial illness impact factors. Eur J Pain 2005;9:613–633.
2. Hasanain F, Durham J, Moufti A, Steen IN, Wassell RW. Adapting the diagnostic definitions of the RDC/TMD to routine clinical practice: A feasibility study. J Dent 2009; 37:955–962.
3. John MT, Hirsch C, Reiber T, Dworkin S. Translating the research diagnostic criteria for temporomandibular disorders into German: Evaluation of content and process. J Orofac Pain 2006;20:43–52.

4. Dworkin SF, LeResche L. Research diagnostic criteria for temporomandibular disorders: Review, criteria, examinations and specifications, critique. J Craniomandib Dis 1992;6:301–355.
5. Facial Pain. National Institute of Dental and Craniofacial Research website. http://www.nidcr.nih.gov/DataStatistics/FindDataByTopic/FacialPain/. Accessed 26 January 2011.
6. Diatchenko L, Slade GD, Nackley AG, et al. Genetic basis for individual variations in pain perception and the development of a chronic pain condition. Hum Mol Genet 2005;14:135–143.
7. Fernandez-de-las-Penas C, Galan-del-Rio F, Fernandez-Carnero J, Pesquera J, Arendt-Nielsen L, Svensson P. Bilateral widespread mechanical pain sensitivity in women with myofascial temporomandibular disorder: Evidence of impairment in central nociceptive processing. J Pain 2009;10:1170–1178.
8. Apkarian AV, Bushnell MC, Treede RD, Zubieta JK. Human brain mechanisms of pain perception and regulation in health and disease. Eur J Pain 2005;9:463–484.
9. Peyron R, Laurent B, Garcia-Larrea L. Functional imaging of brain responses to pain. A review and meta-analysis (2000). Neurophysiol Clin 2000;30:263–288.
10. Cook DB, Lange G, Ciccone DS, Liu WC, Steffener J, Natelson BH. Functional imaging of pain in patients with primary fibromyalgia. J Rheumatol 2004;31:364–378.
11. Gracely RH, Petzke F, Wolf JM, Clauw DJ. Functional magnetic resonance imaging evidence of augmented pain processing in fibromyalgia. Arthr Rheumatol 2002;46:1333–1343.
12. Pujol J, Lopez-Sola M, Ortiz H, et al. Mapping brain response to pain in fibromyalgia patients using temporal analysis of FMRI. PLoS One 2009;4:e5224.
13. Dadabhoy D, Clauw DJ. Therapy Insight: Fibromyalgia—A different type of pain needing a different type of treatment. Nat Clin Pract Rheumatol 2006;2:364–372.
14. Schmidt-Wilcke T, Leinisch E, Straube A, et al. Gray matter decrease in patients with chronic tension type headache. Neurology 2005;65:1483–1486.
15. Schmidt-Wilcke T, Ganssbauer S, Neuner T, Bogdahn U, May A. Subtle grey matter changes between migraine patients and healthy controls. Cephalalgia 2008;28:1–4.
16. Valfre W, Rainero I, Bergui M, Pinessi L. Voxel-based morphometry reveals gray matter abnormalities in migraine. Headache 2008;48:109–117.
17. DaSilva AF, Becerra L, Pendse G, Chizh B, Tully S, Borsook D. Colocalized structural and functional changes in the cortex of patients with trigeminal neuropathic pain. PLoS One 2008;3:e3396.
18. Schmidt-Wilcke T, Hierlmeier S, Leinisch E. Altered regional brain morphology in patients with chronic facial pain. Headache 2010;50:1278–1285.
19. Younger JW, Shen YF, Goddard G, Mackey SC. Chronic myofascial temporomandibular pain is associated with neural abnormalities in the trigeminal and limbic systems. Pain 2010;149:222–228.
20. May A. Chronic pain may change the structure of the brain. Pain 2008;137:7–15.
21. Schmidt-Wilcke T, Wood P, Lurding R. Cognitive impairment in patients suffering from fibromyalgia: An underestimated problem [in German]. Schmerz 2010;24:46–53.
22. LeResche L, Mancl L, Sherman JJ, Gandara B, Dworkin SF. Changes in temporomandibular pain and other symptoms across the menstrual cycle. Pain 2003;106:253–261.
23. Melzack R. The short-form McGill pain questionnaire. Pain 1987;30:191–197.
24. Daut RL, Cleeland CS, Flanery RC. Development of the Wisconsin brief pain questionnaire to assess pain in cancer and other diseases. Pain 1983;17:197–210.
25. Spielberger CD. Measure anxiety, anger, depression, and curiosity in one inventory. Mind Garden website. http://mindgarden.com/products/stpi.htm. Accessed 18 March 2010.
26. Ashburner J, Friston KJ. Unified segmentation. Neuroimage 2005;26:839–851.
27. Alemán-Gómez Y, Melie-García L, Valdés-Hernandez P. IBASPM: Toolbox for automatic parcellation of brain structures. Presented at the 12th Annual Meeting of the Organization for Human Brain Mapping, Florence, Italy, 11–15 June 2006.
28. Nichols TE, Holmes AP. Nonparametric permutation tests for functional neuroimaging: A primer with examples. Hum Brain Mapp 2002;15:1–25.
29. Obermann M, Nebel K, Schumann C, et al. Gray matter changes related to chronic posttraumatic headache. Neurology 2009;73:978–983.
30. Apkarian AV, Sosa Y, Sonty S, et al. Chronic back pain is associated with decreased prefrontal and thalamic gray matter density. J Neurosci 2004;24:10410–10415.
31. Geha PY, Baliki MN, Harden RN, Bauer WR, Parrish TB, Apkarian AV. The brain in chronic CRPS pain: Abnormal gray-white matter interactions in emotional and autonomic regions. Neuron 2008;60:570–581.
32. Cabeza R, Nyberg L. Imaging cognition II: An empirical review of 275 PET and fMRI studies. J Cogn Neurosci 2000;12:1–47.
33. Dick BD, Verrier MJ, Harker KT, Rashiq S. Disruption of cognitive function in fibromyalgia syndrome. Pain 2008;139:610–616
34. Glass JM, Park DC. Cognitive dysfunction in fibromyalgia. Curr Rheumatol Rep 2001;3:123–127.
35. Luerding R, Weigand T, Bogdahn U, Schmidt-Wilcke T. Working memory performance is correlated with local brain morphology in the medial frontal and anterior cingulate cortex in fibromyalgia patients: Structural correlates of pain-cognition interaction. Brain 2008;131:3222–3231.
36. Becerra L, Morris S, Bazes S, et al. Trigeminal neuropathic pain alters responses in CNS circuits to mechanical (brush) and thermal (cold and heat) stimuli. J Neurosci 2006;26:10646–10657.
37. Ettlin DA, Brugger M, Keller T, et al. Interindividual differences in the perception of dental stimulation and related brain activity. Eur J Oral Sci 2009;117:27–33.
38. Said Yekta S, Vohn R, Ellrich J. Cerebral activations resulting from virtual dental treatment. Eur J Oral Sci 2009;117:711–719.
39. Schmidt-Wilcke T, Luerding R, Weigand T, et al. Striatal grey matter increase in patients suffering from fibromyalgia: A voxel-based morphometry study. Pain 2007;132:S109–S116.
40. Schmidt-Wilcke T, Leinisch E, Ganssbauer S, et al. Affective components and intensity of pain correlate with structural differences in gray matter in chronic back pain patients. Pain 2006;125:89–97.
41. Schweinhardt P, Kuchinad A, Pukall CF, Bushnell MC. Increased gray matter density in young women with chronic vulvar pain. Pain 2008;140:411–419.
42. Bremner JD, Vermetten E. Neuroanatomical changes associated with pharmacotherapy in posttraumatic stress disorder. Ann N Y Acad Sci 2004;1032:154–157.
43. Tomelleri L, Jogia J, Perlini C, et al. Brain structural changes associated with chronicity and antipsychotic treatment in schizophrenia. Eur Neuropsychopharmacol 2009;19:835–840.
44. Kolb B, Pellis S, Robinson TE. Plasticity and functions of the orbital frontal cortex. Brain Cogn 2004;55:104–115.

Appendix E. Altered Functional Connectivity Between the Insula and the Cingulate Cortex in Patients With Temporomandibular Disorder: A Pilot Study. Ichesco E, Quintero A, Clauw DJ, Peltier S, Sundgren M, Gerstner GE, Schmidt-Wilcke T.

Headache
© 2011 American Headache Society

ISSN 0017-8748
doi: 10.1111/j.1526-4610.2011.01998.x
Published by Wiley Periodicals, Inc.

Research Submission

Altered Functional Connectivity Between the Insula and the Cingulate Cortex in Patients With Temporomandibular Disorder: A Pilot Study

Eric Ichesco, BS; Andres Quintero, BDS; Daniel J. Clauw, MD; Scott Peltier, PhD; Pia M. Sundgren, MD; Geoffrey E. Gerstner, DDS, MS, PhD; Tobias Schmidt-Wilcke, MD

Background.—Among the most common chronic pain conditions, yet poorly understood, are temporomandibular disorders (TMDs), with a prevalence estimate of 3-15% for Western populations. Although it is increasingly acknowledged that central nervous system mechanisms contribute to pain amplification and chronicity in TMDs, further research is needed to unravel neural correlates that might abet the development of chronic pain.

Objective.—The insular cortex (IC) and cingulate cortex (CC) are both critically involved in the experience of pain. The current study sought specifically to investigate IC–CC functional connectivity in TMD patients and healthy controls (HCs), both during resting state and during the application of a painful stimulus.

Methods.—Eight patients with TMD, and 8 age- and sex-matched HCs were enrolled in the present study. Functional magnetic resonance imaging data during resting state and during the performance of a pressure pain stimulus to the temple were acquired. Predefined seed regions were placed in the IC (anterior and posterior insular cortices) and the extracted signal was correlated with brain activity throughout the whole brain. Specifically, we were interested whether TMD patients and HCs would show differences in IC–CC connectivity, both during resting state and during the application of a painful stimulus to the face.

Results.—As a main finding, functional connectivity analyses revealed an increased functional connectivity between the left anterior IC and pregenual anterior cingulate cortex (ACC) in TMD patients, during both resting state and applied pressure pain. Within the patient group, there was a negative correlation between the anterior IC–ACC connectivity and clinical pain intensity as measured by a visual analog scale.

Conclusions.—Since the pregenual region of the ACC is critically involved in antinociception, we hypothesize that an increase in anterior IC–ACC connectivity is indicative of an adaptation of the pain modulatory system early in the chronification process.

Key words: chronic pain, temporomandibular disorder, functional connectivity, insular cortex, cingulate cortex

From Department of Biologic and Materials Sciences, School of Dentistry, University of Michigan, Ann Arbor, MI, USA (E. Ichesco, A. Quintero, and G.E. Gerstner); Chronic Pain and Fatigue Research Center, School of Medicine, University of Michigan, Ann Arbor, MI, USA (E. Ichesco); Chronic Pain and Fatigue Research Center, Department of Anesthesiology, School of Medicine, University of Michigan, Ann Arbor, MI, USA (D.J. Clauw and T. Schmidt-Wilcke); Functional MRI Laboratory, University of Michigan, Ann Arbor, MI, USA (S. Peltier); Department of Biomedical Engineering, University of Michigan, Ann Arbor, MI, USA (S. Peltier); Center for Medical Imaging and Physiology, Skåne University Hospital, Lund University, Lund, Sweden (P.M. Sundgren); Department of Psychology, University of Michigan, Ann Arbor, MI, USA (G.E. Gerstner).

Address all correspondence to T. Schmidt-Wilcke, Department of Anesthesiology, Chronic Pain and Fatigue Research Center, University of Michigan, 24 Frank Lloyd Wright Dr., P.O. Box 385 Lobby M, Ann Arbor, MI 48016, USA, email: tobiass@med.umich.edu

Accepted for publication July 27, 2011.

Geoffrey E. Gerstner and Tobias Schmidt-Wilcke contributed equally to the manuscript.

Conflict of Interest: None

Abbreviations: ACC anterior cingulate cortex, CNS central nervous system, GBS Gracely Box Scale, IC insular cortex, MCC mid cingulate cortex, NIH National Institutes of Health, PCC posterior cingulate cortex, SF-MPQ short form of McGill Pain Questionnaire, SMA supplementary motor area, STPI State-Trait Personality Inventory, TMD temporomandibular disorder

(*Headache* 2011;••:••-••)

Chronic non-malignant pain is a significant public health problem, thought to affect up to 40% of the general population at any single point in time.[1] Among the most common chronic pain conditions are temporomandibular disorders (TMDs), with a prevalence estimate of 3-15% for Western populations.[2] TMDs are partly defined on the basis of clinical signs such as temporomandibular joint sounds, impaired mandibular movement, or limitation of mouth opening. However, pain is in most cases the presenting and most problematic symptom and can affect various parts of the face and the head, such as preauricular, facial, and masticatory muscle regions.[3] Historically, pain in TMD was believed to be caused by peripheral mechanisms, such as acute or chronic inflammation of the joint, tenderness of the masticatory musculature resulting from microtrauma, oromotor dysfunction, or "imbalance" of the dentoskeletal and neuromuscular systems. However, in many TMD patients, no peripheral pain generator can be identified, which is especially true for the myofascial pain subgroup. On the other hand, the first brain imaging studies have begun to shed light on altered brain function and morphology in TMD patients,[4-7] giving evidence that in TMD, like in other chronic pain conditions, central nervous system mechanisms contribute to the process of pain amplification and chronification.

Two of the forebrain structures most consistently activated, when a subject experiences pain, are the insular cortex (IC) and the cingulate cortex (CC). Both structures have been reported to show structural and, in case of the IC, also neurochemical changes[8,9] in individuals with chronic pain. The structural connection between IC and CC has been extensively studied in primates, showing a connection between the anterior IC and the rostral extent of the anterior cingulate gyrus (rACC, BA 24); the mid and posterior primate IC on the other hand were shown to have connections with the dorsal CC (BA 23 and 24) and the upper banks of the cingulate sulcus and premotor cortex.[10] Only recently functional magnetic resonance imaging (fMRI) has been applied in humans to investigate functional connectivity between the IC and CC.[11] Functional connectivity has been operationally defined to refer to temporal correlations across cortical regions and can be assessed during the application of a pain stimulus, but also during resting state. The term "resting-state" functional connectivity refers to brain areas that have a strong temporally correlated activity in a non-task state. It is thought that these low-frequency (<0.1 Hz) fluctuations are functionally relevant indices of connectivity between brain regions subserving similar or related brain functions.[12]

With respect to functional connectivity, it has been suggested that the anterior and posterior IC, although part of the same anatomical structure and highly connected with each other, subserve different aspects of pain perception and are integrated into different neural networks. The anterior IC, functionally connected to the anterior cingulate cortex (ACC), has been suggested to integrate interoceptive input with its emotional salience, while the mid/posterior IC, functionally connected to the mid cingulate (MCC) and posterior cingulate cortex (PCC), is thought to be more related to environmental monitoring and response selection.[11] It is therefore not surprising that pain researchers try to explore IC connectivity, attempting to unravel neural correlates of chronic pain more thoroughly.

Given that the IC is critically involved in the experience of pain, but also in other functions, that are possibly relevant to chronic pain such as interoception and self-awareness, the current study sought specifically to investigate IC connectivity in TMD patients and healthy controls (HCs), both in the resting state and during the application of a painful stimulus. Following the approach of a recently published study by Taylor et al,[11] predefined seed regions

(SR) were placed in the IC (anterior and mid/posterior IC bilaterally totaling 4 regions overall). These predefined SR of interests' time series were used to perform a correlation with the time series of all the voxels in a whole-brain analysis. In a first step, we sought to replicate the findings of Taylor et al showing that the anterior IC is functionally connected with the posterior part of the ACC/MCC, whereas the mid/posterior IC is connected to the posterior MCC and supplementary motor area (SMA), demonstrating a segregated IC–CC connectivity along the anterior–posterior axis. We were then interested in whether TMD patients and HCs would show differences in IC–CC connectivity, both during resting state and during the application of a painful stimulus and whether IC–CC connectivity correlated with clinical pain measures and/or evoked pain ratings.

METHODS

Subjects and Behavioral Data.—Originally, 10 patients with myofascial-type TMD had initially been enrolled in the study. The structural images of 9 patients and 9 HCs were analyzed within a voxel-based morphometry study, and the results reported elsewhere.[6] The fMRI data of 8 patients (8 women; aged 23 to 31 years) and 8 HCs (8 women; aged 22 to 27 years) were available for functional connectivity analysis. Groups did not differ significantly in age ($P = .49$), or ethnicity (both groups consisted of 1 African American, 3 Asian, and 5 Caucasian participants).

All subjects with TMD had been carefully examined by a dentist with experience in orofacial pain applying the research diagnostic criteria (RDC) for the diagnosis of myofascial-type TMD (Group 1a, 1b).[13] Only those subjects that fulfilled the Group I myofascial pain criteria were included. Inclusion and exclusion criteria consisted of the following: (1) presence of pain in the face, jaws, or temples greater than 1× per week; (2) presence of pain symptoms for greater than 3 months; (3) meeting the RDC criteria for myofascial pain Group 1a, 1b; (4) no comorbidities of other chronic pain disorders (eg, fibromyalgia or irritable bowel syndrome). The main inclusion criterion for HCs was absence of TMD pain, or facial pain less than 1× per week. Exclusion criteria for all subjects included physical impairment (eg, complete blindness, deafness, paraplegia), or coexisting physical injury (eg, sprained ankle, neck injury, etc.), any outstanding history of systemic or medical conditions, psychiatric illnesses, substance abuse within 2 years, and presence of head or neck pain other than masticatory myalgia. Non-steroidal anti-inflammatory drugs and other over-the-counter analgesics were allowed until 3 days before the pain and scanning trials; medication overuse had been ruled out in all patients. All subjects were right-handed. Because pain symptoms can be coupled to menstrual cycle phase in premenopausal women and women on oral contraceptives,[14] the subjects (all female) participated in pain and imaging studies within 3 days of menstrual onset. The University of Michigan Medical School Institutional Review Board for Human Subject Research determined that project title entitled, Pain Mechanisms in Chronic Multisymptom Illnesses (CMI), conforms with applicable guidelines, state and federal regulations, and the University of Michigan's Federalwide Assurance (FWA) with the Department of Health and Human Services (HHS). All participants signed an informed consent that detailed the procedures of the study.

The clinical pain experience of patients with TMD and HCs was assessed using the visual analog scale (VAS) and the pain rating index (PRI) from the Short-Form McGill Pain Questionnaire (SF-MPQ).[15] The VAS consists of a 10-cm line anchored on the left with "No Pain" and on the right with "Worst Possible Pain." Participants in the study were asked to rate their present orofacial pain by placing a tick along this line. The PRI component of the SF-MPQ consisted of 15 word descriptors (11 sensory and 4 affective). Participants rated these descriptors as either "none," "mild," "moderate," or "severe," giving a score of 0, 1, 2, or 3, respectively, for each descriptor. The measures were added to yield sensory, affective, and total scores. Another questionnaire used to evaluate clinical pain was the Brief Pain Inventory (BPI).[16] Information from this measure was used to determine both severity of pain and the degree of pain interference. Questions for these measures were answered using a 0 to 10 numeric rating scale for each item. The State-Trait Personality Inventory (STPI) is a

self-report tool designed to measure anxiety and depression. The STPI consists of eight 10-item subscales. The trait depression scale and anxiety scale were used to assess each subject's emotional disposition, and both scales were rated on a 4-point intensity scale. Furthermore, the state anxiety scale was used to assess the current emotional state of each subject and was rated in standard fashion on a 4-point frequency scale.[17]

Prior to scanning, pressure pain values eliciting low pain (0.5 on the Gracely Box Scale [GBS], see below and Fig. S1), medium pain (7.5 on the GBS), and high pain (13.5 on GBS) were determined for every subject using the multiple random staircase (MRS) method. The GBS is a numerical scale that is used to evaluate present pain intensity. This scale is comprised of 21 boxes, sequentially numbered beginning with 0 and ending with 20. It is aligned vertically, with 0 as the lowest box. Descriptive words are arranged next to the numbers corresponding with varying levels of pain.[18] The corresponding pressures were determined for the left anterior temporalis region as follows. A form-fitting mask was created for each individual subject. The mask was molded to each subject's face using radiological thermoplastic mesh. Holes were placed for the subject's eyes and nose, and the mask was held in place using 2 Velcro straps (for an example, see Fig. 1). Once fit, a plunger with an area of ~1 cm^2 was attached to the mask located at the subject's left anterior temporalis region.

The following analyses were performed to describe and analyze clinical/behavioral data in both cohorts:

Analysis 1a: We looked for differences in age, pain scores, anxiety and depression levels between groups. Due to the relatively small sample size, we applied the Mann–Whitney *U*-test to test for significant differences in behavioral scores (pain, depression, and anxiety) between groups (Table 1). Differences were deemed significant at $P < .05$ (corrected for multiple comparisons using a Bonferroni correction).

Analysis 1b: We performed correlation analyses (Spearman rank correlation) looking for significant correlations between pain measures (pain duration, BPI scores, MPQ scores), depression and anxiety measures. Correlations were deemed significant at $P < .05$ (corrected for multiple comparisons using a Bonferroni correction). All statistical analyses investigating demographic and behavioral measures were assessed using SPSS, version 17.

Fig 1.—Mask used for the application of pressure pain. An example of the mask used to deliver pressure pain stimuli to each subject.

Neuroimaging – Data Acquisition.—*Resting State.*—Magnetic resonance imaging was performed on a 3.0 Tesla GE Signa scanner (LX [VH3] release, Neuro-optimized gradients). Resting-state fMRI data were acquired using a T2*-weighted spiral sequence (repetition time [TR] = 2.0 s, echo time [TE] = 30 ms, flip angle [FA] = 90°, matrix size 64 × 64 with 43 slices, field of view [FOV] = 20 cm and 3.12 × 3.12 × 3 mm voxels), using a General Electric Signa scanner 9.0, VH3 with 16 rod birdcage transmit-receive radio frequency coil. During the ~6-minute resting-state fMRI acquisition period (179 scans), the subjects were asked to remain awake with their eyes open. A motionless cross was presented on the screen. Minimal cognitive tasks such as staring at a cross are thought not to disrupt resting-state networks.[19] A T1-weighted gradient echo data set (TR 1400 ms, TE 1.8 ms, FA 15°, FOV 256 × 256, yielding 124 sagittal slices with a defined voxel size of 1 × 1 × 1.2 mm) was also acquired for each subject.

Table 1.—Behavioral Data

	TMD (Mean ± SD)	HC (Mean ± SD)	*P* Value
Age	25.4 ± 2.5	24.8 ± 1.4	.796
Pain duration	2.5 ± 2.1	–	NA
BPI Sev	2.0 ± 1.3	0.6 ± 0.7	.136
BPI Int	2.0 ± 3.2	0.1 ± 0.3	.190
MPQ Tot	6.1 ± 5.2	0.4 ± 1.3	**.001**
MPQ Sens	5.6 ± 4.4	0.4 ± 1.3	**.001**
MPQ Aff	0.6 ± 0.9	0 ± 0	.258
MPQ VAS	2.2 ± 1.4	0.2 ± 0.6	**<.001**
STPIA Ax	19.0 ± 6.9	13.1 ± 3.9	.031
STPIDA Ax	17.2 ± 6.0	12.9 ± 2.7	.136
STPIDA D	16.1 ± 6.4	11.1 ± 2.0	.050
Medium pressure—temple (kg/cm^2)	1.2 ± 0.7	1.0 ± 0.8	.654
High pressure—temple (kg/cm^2)	2.6 ± 1.5	2.4 ± 1.2	.840

Mann–Whitney *U*-test was used for group comparison. *P* values were deemed significant at $P < .05$ after correction for multiple comparisons (significant differences are indicated in bold type).
BPI Int = Brief Pain Inventory pain interference; BPI Sev = Brief Pain Inventory pain severity; HC = healthy control; MPQ Aff = Short-Form McGill Pain Questionnaire Pain Rating Index—Affective Score; MPQ Sens = Short-Form McGill Pain Questionnaire Pain Rating Index—Sensory Score; MPQ Tot = Short-Form McGill Pain Questionnaire Pain Rating Index—Total Score; MPQ VAS = Short-Form McGill Pain Questionnaire Visual Analog Scale; NA = not available, missing data; STPIA Ax = State-Trait Personality Inventory state anxiety; STPIDA Ax = State-Trait Personality Inventory trait anxiety; STPIDA D = State-Trait Personality Inventory trait depression; TMD = temporomandibular disorder; – = inconclusive results.

Pain Run.—Each participant was subjected to one 10-minute evoked pressure scan in the MRI scanner and images were collected using a T2*-weighted spiral sequence (TR = 2.5 s, TE = 30 ms, FA = 90°, matrix size 64×64 with 48 slices, FOV = 22 cm and $3.44 \times 3.44 \times 3$ mm voxels). Pressure pain was delivered with a pneumatic system. This system was comprised of medical grade tubing, several valves, an air supply containing medical grade air, and an analog air controller (used to regulate different pressures). Agilent VEE pro and E-prime software programs were used to coordinate pressure pain administration at the correct onsets. Further details of the pressure pain equipment setup are described in Gracely et al.[20] During the pain run, pressure pain was delivered to the left anterior temporalis region by a piston with a surface area of 1 cm^2. Pressures eliciting high and medium pain as previously determined (see *Subjects and behavioral data*) were applied in a pseudo random fashion and interleaved with an "off" condition (no pressure applied). A run contained a total of 12 pain blocks (6 medium, 6 high; each block 25 seconds in duration) and 12 off blocks (each block 25 seconds in duration).

Neuroimaging – Preprocessing and Statistical Analyses.—*Preprocessing and Analysis of Functional Connectivity – Resting State.*—The first 6 images were discarded from the data set and not analyzed in order to avoid equilibration effects. Data were preprocessed and analyzed using Statistical Parametric Mapping software packages (SPM, version 8; Functional Imaging Laboratories, London, UK), as well as the functional connectivity toolbox Conn (Cognitive and Affective Neuroscience Laboratory, Massachusetts Institute of Technology, Cambridge, MA, USA) running under Matlab 7.5b (Mathworks, Sherborn, MA, USA). Preprocessing steps included motion correction (realignment to the first image of the time series), normalization to the standard SPM–EPI template (generating $2 \times 2 \times 2$ mm resolution images) and smoothing (convolution with an 8-mm FWHM Gaussian Kernel).

Based on the approach by Taylor et al,[11] SR were defined within the anterior and posterior IC

bilaterally; SR were created as spheres (6-mm diameter) using MarsBaR software (http://marsbar.sourceforget.net). For details on center coordinates, presented in Montreal Neurological Imaging (MNI) space, see Figure 2 and Table S1. SR time series were extracted; white matter and cerebrospinal fluid signal, as well as realignment parameters were entered into the analysis as covariates of no interest, using *CompCor*, a principal component-based method for noise correction/reduction in BOLD and perfusion data.[21] A band pass filter (frequency window: 0.001-0.08 Hz) was applied, thus removing linear drift artifacts and high-frequency noise. First-level analyses were performed correlating SR signal with voxel signal throughout the whole brain, thereby creating SR-to-voxel connectivity maps (4 maps for each individual). Connectivity maps were then used for second-level (random effects) analyses.

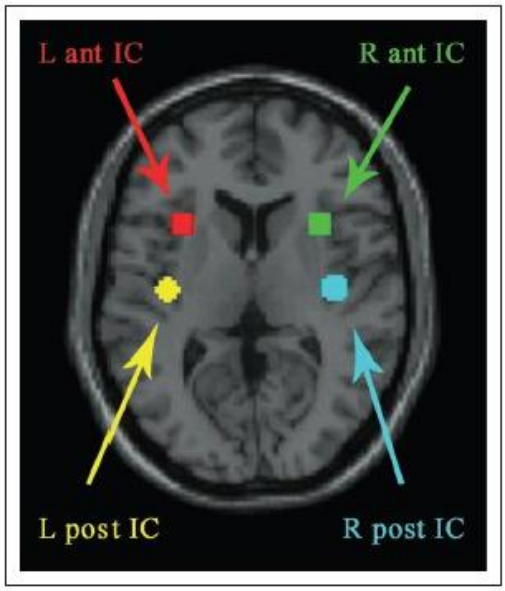

Fig 2.—Seed regions. This figure displays the 4 seed regions used for functional connectivity analyses. Seed regions were spheres of 6 mm surrounding a peak voxel. Montreal Neurological Imaging (MNI) coordinates for each voxel include: left (L) anterior (ant) insular cortex (IC): $x = -32$, $y = 16$, $z = 6$; left posterior (post) IC: $x = -39$, $y = -15$, $z = 1$; right (R) anterior IC: $x = 32$, $y = 16$, $z = 6$; right posterior IC: $x = 39$, $y = -15$, $z = 8$.

Analysis 2a: In a first step, IC connectivity was determined by performing a 1-sample *t*-test for each SR, including both TMD patients and HCs.

Analysis 2b: We were then interested in whether there were differences in functional connectivity between groups. To this end, 2-sample *t*-tests for each SR were performed. Age was added as nuisance variable.

Analysis 2c: To further evaluate behavioral/clinical relevance of the clusters found in Analysis 2b, correlations between functional connectivity and pain measures (eg, pain intensity, pain severity, pain duration) were assessed in a third step.

All statistical maps were corrected for multiple comparisons on the cluster level ($P < .05$), derived from an uncorrected $P < .001$ on the voxel level, with a cluster extent of 82 contiguous voxels, as estimated by the AlphaSim application (implemented in the Analysis of Functional NeuroImages [AFNI] software [http://afni.nimh.nih.gov/afni/doc/manual/AlphaSim]), based on a Monte Carlo simulation (5000 simulations) applied to a whole-brain mask. For explorative reasons, as we were specifically interested in IC–CC connectivity a second mask, just covering the cingulum (anterior, medial, and posterior, bilaterally) was created using the WFU_PickAtlas (http://www.nitrc.org/projects/wfu_pickatlas). Monte Carlo simulation using that mask resulted in a lower extent threshold: 28 contiguous voxels ($P < .001$, uncorrected, on the voxel level), yielding correction for multiple comparisons on the cluster level (within that mask). As these results could be interesting for future analyses, they are reported and briefly commented on; however, as they did not survive the correction for multiple comparisons throughout the whole brain, they should be viewed with caution. These results are specifically marked in *Result* and tables.

Anatomical regions were labeled following the nomenclature of the Automated Anatomical Labeling (AAL) atlas[22] and xjView viewing program for SPM (http://www.alivelearn.net/xjview8/).

Preprocessing and Analysis of Functional Connectivity – Pain Run.—Preprocessing steps were performed in a similar fashion to the resting-state analysis using the same SRs. A first-level model was implemented for each subject by compiling all of the

blocks for each condition respectively. Each pressure pain condition totaled six 25-s blocks and the off condition totaled twelve 25-s blocks. The block (off, medium, and high) were modeled as covariate of no interest (in addition to white matter signal, cerebrospinal fluid signal, and realignment parameters). First-level analyses were performed correlating SR signal with voxel signal throughout the whole brain for each condition, thereby creating SR-to-voxel connectivity maps (3 [conditions] × 4 [SR] maps for each individual). Connectivity maps were then used for second-level (random effects) analyses.

Analysis 2d: Using a flexible factorial design within the general linear model implemented in SPM, main effects across groups (medium/high pain vs off) were investigated.

Analysis 2e: We were then interested in whether there were differences in functional connectivity between groups (medium/high pain vs off). To this end interaction analyses were performed (group × stimulus [low pain vs off and high pain vs off]).

Statistical maps were corrected for multiple comparisons ($P < .001$, uncorrected on the voxel level, with a cluster extent of 82 contiguous voxels, as described above). Altered functional connectivity between the SR and a target region in the TMD group, as compared to the HC group, is referred to as a hyper-connection (increased functional connectivity), respectively hypo-connection (decreased functional connectivity), between the 2 regions. To further evaluate behavioral/clinical relevance of the clusters found in Analysis 2e, correlation analyses between contrast estimates (high pain) and pressure necessary to elicit high pain (determined outside the scanner, see *Subjects and behavioral data*) were performed in a third step. Parameter estimates were extracted from group-level results (clusters defined in Analysis 2e, interaction analysis), yielding 1 parameter estimate per subject, which were then transferred to SPSS, version 17, and further analyzed (using Spearman rank correlation).

RESULTS

Subjects and Behavioral Data.—*Analysis 1a:* As expected, patients with TMD displayed significantly higher clinical pain (VAS scores) than HCs (TMD: mean = 2.19, SD = 1.48; control: mean = 0.25, SD = 0.59; $P = .004$). TMD patients also showed higher scores than HCs for the MPQ Tot (TMD: mean = 6.50, SD = 5.42; control: mean = 0.50, SD = 1.41; $P = .009$) and the MPQ Sens (TMD: mean = 5.88, SD = 4.64; control: mean = 0.50, SD = 1.41; $P = .007$) measures (for details, see Table 1).

Analysis 1b: Within the TMD group, the STPI Trait-anxiety scores were significantly correlated with STPI Trait-depression scores ($\rho = 0.94$, $P = .001$). None of the anxiety and/or depression scores correlated significantly with BPI pain scores or MPQ scores. For details on the ρ values and P values, see Table S2.

Neuroimaging – Connectivity Analyses.—*Functional Connectivity – Resting State.*—Inspection of individual T1 MR-images revealed no gross morphological abnormalities for any participant. Functional connectivity analyses revealed functional connectivity between the chosen seeds and regions of the pain system. Results are summarized in Tables 1 and 2.

Analysis 2a: The anterior IC was functionally connected to the posterior ACC/MCC, and the posterior IC was functionally connected to the medial frontal gyrus/superior frontal gyrus/SMA (Fig. 3A).

Analysis 2b: For between-group comparisons, there were hyper-connections for the TMD patients compared to HCs. These occurred between the left anterior IC and the left rostral (pregenual) ACC (peak voxel: $x = 2$, $y = 38$, $z = 2$; Z value = 4.47), (Fig. S3) the left posterior IC and the left parahippocampal gyrus ($x = -14$, $y = -4$, $z = -26$; Z value = 5.07), and the right anterior IC with the right thalamus ($x = 8$, $y = -6$, $z = 6$; Z value = 4.35).

Analysis 2c: Within the TMD group, the functional connectivity of the left anterior IC and the rACC was negatively correlated with clinical pain ($\rho = -0.952$, $P < .001$, Figs. 3C and S2); that is, TMD patients with higher clinical pain had less anterior IC–rACC connectivity. The same association was found for MPQ total scores ($\rho = -0.830$, $P = .011$) in both analyses.

Functional Connectivity – Pain Runs.—Analysis 2d: For the main effect (high pain greater than off, across groups) an increase of functional connectivity between the left anterior IC and the left SII cortex, as well as the left cerebellum was observed (Table 2d).

Table 2a.—Results of 1-Sample *t*-Test – fcMRI Resting State

Seed Region	Connectivity Region	Brodmann Area	Cluster Size (# of Voxels)	Z Score (Peak Value)	Coordinates (MNI)		
					x	*y*	*z*
Left anterior IC	Right anterior insula cortex	13/47	2768	6.89	38	22	4
	Middle cingulate cortex	24	482	4.32	–4	0	40
	Left inferior parietal lobule*	40	256	3.85	–54	–40	44
	Right inferior parietal lobule	40	126	3.93	56	–44	40
Left posterior IC	Right posterior insula cortex	13	5007	6.63	38	–18	16
	Right SMA	6	881	4.78	2	–10	58
	Right SI	4/3	611	4.77	28	–34	66
	Left SI*	4/3	150	4.26	–22	–30	74
Right anterior IC	Left anterior insula cortex	13	2353	6.12	–34	16	0
	Middle cingulate cortex	32/6	1921	4.16	8	22	32
	Left inferior parietal lobule	40	312	4.29	–60	–36	34
	Right inferior parietal lobule	40	328	4.08	58	–40	28
	Left SI	2/3	115	3.56	–46	–22	50
Right posterior IC	Left posterior insula cortex	13	5175	6.17	–38	–28	14
	Middle cingulate cortex	24	51	3.98	–6	0	40
	Right SI**	3/4	203	4.78	42	–28	58

Table 2a describes the resting-state connectivity regions associated with the 4 seed regions (across groups, $P < .05$ corrected).
fcMRI = functional connectivity magnetic resonance imaging; IC = insula cortex; SI = primary somatosensory cortex; SMA = supplementary motor area.
*Voxel level uncorrected P value = .0005 was used to separate clusters. **Voxel level uncorrected P value < .0001 was used to separate clusters.

Analysis 2e: When groups were compared (interaction analysis), TMD patients displayed a hyper-connection between the left anterior IC and the rACC/medial frontal cortex (BA 32) compared to HCs for the high greater than off (peak voxel: $x = 4$, $y = 42$, $z = 16$; Z value = 3.92). Compared with HCs, TMD patients also displayed a hyper-connection between the right anterior IC and the ACC (peak voxel: $x = 18$,

Table 2b.—Results of Group Analyses – Resting-State Functional Connectivity

Seed Region	Connectivity Region	Brodmann Area	Cluster Size (# of Voxels)	Z Score (Peak Value)	Coordinates (MNI)		
					x	*y*	*z*
TMD > HC (2-sample *t*-test)							
Left anterior IC	Anterior cingulate cortex	24/32	101	4.47	2	38	2
Left posterior IC	Left parahippocampal gyrus	34	176	5.07	–14	–4	–26
Right anterior IC	Right thalamus	–	98	4.35	8	–6	6

Table 2b describes resting-state functional connectivity. Two-sample *t*-tests with a threshold of an uncorrected voxel level $P = .001$ (cluster extent of 82 contiguous voxels) were used to determine group differences among TMD patients and HCs.
DLPFC = dorsal lateral prefrontal cortex; HC = healthy control; IC = insula cortex; MNI = Montreal Neurological Imaging; TMD = temporomandibular disorder; – = inconclusive results.

Table 2c.—Results of TMD Behavioral Correlations With Functional Connectivity Resting State

Seed Region	Connectivity Region	Behavioral Correlate	BA	Cluster Size (# of Voxels)	ρ	Coordinates (MNI) x	y	z
Left anterior IC	Anterior cingulate cortex	VAS	32	29†	–0.952	2	42	6
	Anterior cingulate cortex	MPQ total	32	28†	–0.830	–4	48	10

Table 2c describes resting-state connectivity results correlated with behavioral data within TMD subjects. An uncorrected voxel level threshold value of $P = .001$ was used.
†Note that this cluster did not survive the a priori determined cluster extent of 82 contiguous voxels.
IC = insular cortex; MNI = Montreal Neurological Imaging; MPQ total = McGill Pain Questionnaire total score; TMD = temporomandibular disorder; VAS = visual analog scale.

$y = 32, z = 12$; Z value = 3.51). Functional connectivity for the pain run correlated with previously determined pressures used to elicit high pain ratings; that is, the more pressure required to elicit high pain (13.5 on the GBS), the more functional connectivity TMD patients showed between the aforementioned structures (left anterior IC and rACC/the medial frontal gyrus [peak voxel: $x = 0, y = 48, z = -6; \rho = 0.838, P = .009$]).

DISCUSSION

The current study sought to investigate functional connectivity of the IC in TMD patients and HCs. In a first step, we were able to demonstrate a segregated resting-state functional connectivity between subregions of the IC and the medial frontal wall. Within the medial frontal wall, the clusters showing connections with the anterior IC projected anterior to the clusters connected to the posterior IC. More specifically, we found that the anterior IC was functionally connected to the MCC (extending into the posterior ACC), whereas the posterior IC was functionally connected mainly to the SMA, extending into the MCC. A similar segregation has been described by Taylor et al.[11]

When comparing TMD patients and HCs, the left anterior IC was hyper-connected to the rostral

Table 2d.—Insular Connectivity in TMD Patients and HCs During Elicited Pain (High Pain vs Off)

Seed Region	Connectivity Region	Brodmann Area	Cluster Size (# of Voxels)	Z Score (Peak Value)	Coordinates (MNI) x	y	z
Main effect							
Left anterior IC	Left SII cortex	6	211	4.46	–56	–4	34
	Left cerebellum		82	4.10	–48	–70	–24
Left posterior IC	Right DLPFC	9	36	3.66	54	12	30
Interaction (pressure × group)							
Left anterior IC	Anterior cingulate cortex	32	590	3.92	4	42	16
	Right superior frontal gyrus	10/9	427	4.85	24	52	28
	Left medial frontal gyrus	9/10	176	4.70	–6	56	38
Right anterior IC	Right anterior cingulate cortex	32	24	3.51	18	38	12

Table 2d describes functional connectivity results within an evoked high pain vs off (no pain) block design. Shown are the main effect and the interaction (TMD patients > HCs), at an uncorrected threshold of $P < .001$.
IC = insular cortex; HCs = healthy controls; MNI = Montreal Neurological Imaging; SII cortex = secondary somatosensory cortex; DLPFC = dorsal lateral prefrontal cortex; TMD = temporomandibular disorder.

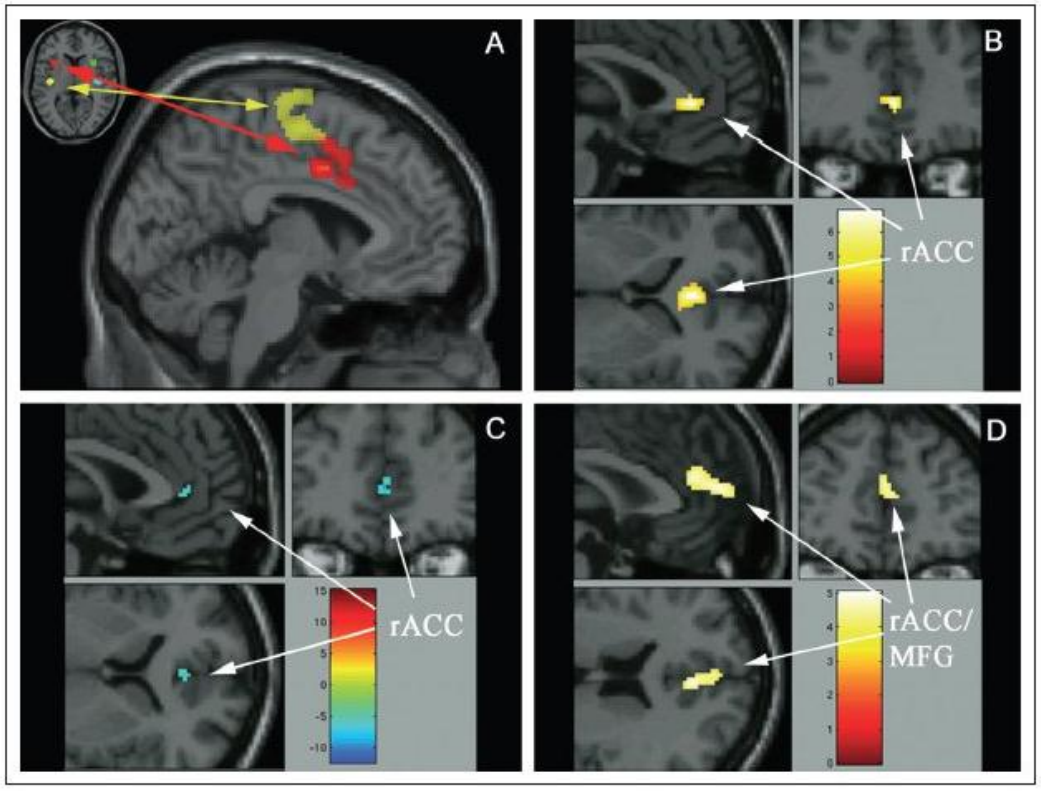

Fig 3.—Insular cortex connectivity maps during resting state and pain runs. (A) Functional connectivity between the anterior and posterior insular cortex and the cingulate cortex (Analysis 2a). (B) The resting-state hyper-connectivity in temporomandibular disorder (TMD) patients between the left anterior insular cortex and the rostral anterior cingulate cortex (rACC; Analysis 2b). (C) Negative correlation between visual analog scale scores (clinical pain) and the resting-state functional connectivity among TMD patients (Analysis 2c); color bar: red represents positive values (positive correlation) and blue represents negative values (negative correlation). (D) Hyper-connection in TMD patients compared to healthy controls between left anterior insular cortex and anterior cingulate cortex (ACC)/medial frontal gyrus (MFG) in evoked pain (high pain vs off condition, Analysis 2e). Clusters are displayed at a *P* value <.001, uncorrected.

(pregenual) ACC in the patients. At the same time there was a negative correlation between left IC–ACC connectivity and pain intensity within the TMD group; that is, those patients with decreased connectivity had relatively higher pain scores. Finally, we showed that TMD patients, compared to HCs, had an increased functional connectivity between the anterior IC and ACC when painful pressure stimuli were applied to the facial region.

Resting-state Connectivity.—It has been suggested that the anterior IC–ACC system integrates interoceptive input with its emotional salience, while the posterior IC–MCC system is thought to be more related to environmental monitoring and response selection.[11] On the other hand, with respect to pain perception, there is strong evidence that the anterior IC, as part of the medial pain system, together with the ACC, has a unique role in affective pain processing and learning, while the posterior IC, as part of the lateral pain matrix, together with regions such as the primary and secondary somatosensory cortices, encode pain intensity, laterality, and somatotopy.[23]

This is also supported by a recently published study by Peltz et al investigating IC connectivity during noxious and innocuous thermal stimulation, showing that the anterior IC is more strongly connected to the prefrontal cortex and ACC than is the posterior IC, and that the posterior IC is more strongly connected to the SI and MI cortex.[24] Although in the present study connectivity maps of the anterior and posterior IC were not directly (statistically) compared, we found a strong resting-state connectivity between the posterior IC and the primary somatosensory cortex (SI), supporting the idea of the posterior IC's integration in the lateral pain system.

Differences between groups were found between the left anterior IC–rACC connectivity (TMD patients greater than HCs). Furthermore, anterior IC–rACC connectivity was negatively associated with clinical pain; that is, TMD patients with less connectivity reported higher clinical pain, as assessed by the clinical pain and MPQ total. Just like the IC, the CC is functionally segregated with different parts being involved in different aspects of pain encoding[25] and pain anticipation,[26] but also involved in antinociception[27,28] and habituation.[29] Especially the rACC, as part of the medial prefrontal cortex, has repeatedly been shown to be critically involved in distraction, placebo, and opioid-associated analgesia,[28,30] as well as endogenous hyperalgesia-specific pain modulation.[31] As such, the rACC is strongly connected with the prefrontal cortex and periaqueductal gray, probably serving as a relay between prefrontal and brainstem structures involved in top–down antinociceptive mechanisms. Although there is an increasing body of evidence that suggests that the IC flexibly connects to attentional and emotional brain areas, and that these connections are in fact an important determinant of pain experience,[32] the literature on the capability of the ACC to modulate IC activity in pain conditions, or vice versa, is sparse. Interestingly, in a recently published study by Petrovic et al, the rACC displayed an increased functional connectivity with the orbitofrontal/ventrolateral cortex and anterior IC in the context of placebo analgesia.[33] Given that TMD patients have to deal with an increased nociceptive and/or proprioceptive input to the forebrain (without making any assumptions about the original pain generator), we hypothesize that an increase in anterior IC–rACC connectivity serves antinociception, ie, an adaptive process to down-regulate pain. This would explain the group difference between TMD patients and HCs, with TMD showing an increased functional connectivity. On the other hand, it would explain why those patients with less connectivity showed higher pain scores (clinical pain).

Pain Run Connectivity.—We also investigated IC connectivity for the pain runs. Analysis of the main effect showed that the left anterior IC was functionally more connected to the left SII during high pressure pain than during the off condition. This finding is again in line with the study by Peltz et al investigating IC connectivity during noxious and innocuous thermal stimulation, showing that the anterior IC connects more strongly to the SII cortex during pain. The interaction analysis revealed that TMD patients showed a higher connectivity than the HCs between the left anterior IC and the rACC in the high pain condition as compared to the off condition. Within the TMD group, those patients requiring higher pressures to elicit high pain (~13.5 on the GBS—same pain rating across subjects) showed an increased anterior IC–rACC connectivity, when these pressures were applied in the scanner (positive association).

Although experimental pain has been used as a surrogate marker for clinical pain, and frequently a decrease in pain thresholds has been found in chronic pain patients, in- and outside the region of clinical pain,[34-36] the broader concept that experimental pain and chronic pain rely on the same networks has been challenged.[37] To our knowledge, this is the first study to explore functional IC connectivity during resting state and a pain run in a cohort of pain patients and HCs. With respect to IC–CC connectivity, the increased functional connectivity seen during the pain run paralleled the findings during resting state. Again, our data suggest that IC–rACC connectivity subserves an antinociceptive process, especially since those patients with higher connectivity could take more pressure to elicit a certain amount of subjective pain. This in turn would suggest that the anterior IC–rACC system plays a role for both clinical and experimental antinociception. From this perspective,

it will be interesting to see whether a decrease in functional connectivity is actually associated with both worsening of clinical pain and a decrease of pain thresholds (increased pain ratings of a given stimulus) in- and outside the region of clinical pain.

Limitations.—There are several limitations to our study that need to be addressed. First of all, the study sample with 8 TMD patients and 8 HCs, although thoroughly investigated and carefully matched, is rather small and in these terms, this study needs to be considered a pilot study to be expanded upon.

The patients investigated in the current study are relatively young and only mildly affected. They are thus likely to be at the beginning of the chronification process and/or in a compensated stage. As such, they probably do not represent the clinical picture of "severely disabled" TMD. On the other hand, our results possibly reflect a snapshot of chronic pain in an early or compensated stage. Such study samples might be interesting for future (longitudinal) studies that intend to unravel causes and consequences of chronic pain and to account for symptom heterogeneity among patients. It will be interesting to see whether in some patients the hypothesized antinociceptive mechanism, ie, enhanced anterior IC–rACC connectivity, is "overstressed" with time, and whether this leads to further chronification in terms of more and/or increased clinical pain, as well as decreased reversibility.

A limitation inherent to the cross-sectional design is its inability to resolve conclusively the preexisting vs acquired nature of the observed alterations; that is, it is unclear whether chronic pain leads to the changes described or whether changes in IC connectivity predispose someone to developing TMD pain. Another potential weakness is that we used standardized SR. Subtle (natural) differences in functional anatomy across subjects and differences in brain size (and normalization) might have had an influence on connectivity maps. However, we would assume that variation in functional anatomy is equally distributed between groups and the fact that images had been smoothed prior to analysis helped to correct for such differences. The advantage of this approach lies in the ability to replicate the findings of Taylor et al.[11] Indeed, the fact that the study replicated the findings in previous work[11] provides support for the veracity of our findings, despite the small sample size.

Finally, functional connectivity as assessed by the approach chosen in this study (ie, correlation analyses) allows no assumptions on causality, or on directedness of influence. It is conceivable that functional connectivity between 2 regions is driven by a third region not identified in the analysis. More sophisticated approaches exploring effective connectivity and the relationship between functional and structural connectivity[38] in larger sample sizes will help to overcome such methodological shortcomings in future studies.

CONCLUSIONS AND OUTLOOK

The identification and investigation of resting-state networks is a promising approach and might in fact turn out to be a stronger tool than approaches using evoked pain paradigms, when it comes to the exploration of internal states, such as clinical pain and mood disturbances that are only insufficiently modeled by external stimuli. Our main goal was to investigate and compare IC connectivity in individuals with TMD and HCs. Our analyses revealed group differences in resting state and an evoked pain run-associated functional connectivity between the IC and the rACC, which we interpret as being indicative of an adaptation of the antinociceptive system early in the chronification process. This might help to further disentangle the neural correlates of chronic pain in TMDs.

Acknowledgments: This study was supported by an NIH Grant DE018528 to Geoffrey Gerstner. Tobias Schmidt-Wilcke is currently supported by a grant of the DFG (Deutsche Forschungsgemeinschaft, GZ: SchM 2665/1-1).

REFERENCES

1. Verhaak PF, Kerssens JJ, Dekker J, Sorbi MJ, Bensing JM. Prevalence of chronic benign pain disorder among adults: A review of the literature. *Pain*. 1998;77:231-239.
2. LeResche L. Epidemiology of temporomandibular disorders: Implications for the investigation of etiologic factors. *Crit Rev Oral Biol Med*. 1997;8:291-305.

3. Suvinen TI, Reade PC, Kemppainen P, Könönen M, Dworkin SF. Review of aetiological concepts of temporomandibular pain disorders: Towards a biopsychosocial model for integration of physical disorder factors with psychological and psychosocial illness impact factors. *Eur J Pain*. 2005;9:613-633.
4. Nebel MB, Folger S, Tommerdahl M, Hollins M, McGlone F, Essick G. Temporomandibular disorder modifies cortical response to tactile stimulation. *J Pain*. 2010;11:1083-1094.
5. Younger JW, Shen YF, Goddard G, Mackey SC. Chronic myofascial temporomandibular pain is associated with neural abnormalities in the trigeminal and limbic systems. *Pain*. 2010;149:222-228.
6. Gerstner G, Ichesco E, Quintero A, Schmidt-Wilcke T. Changes in regional gray and white matter volume in patients with myofascial-type temporomandibular disorders—a voxel based morphometry study. *J Orofac Pain*. 2011;25:99-106.
7. Weissman-Fogel I, Moayedi M, Tenenbaum HC, Goldberg MB, Freeman BV, Davis KD. Abnormal cortical activity in patients with temporomandibular disorder evoked by cognitive and emotional tasks. *Pain*. 2011;152:384-396.
8. Schmidt-Wilcke T, Leinisch E, Straube A, et al. Gray matter decrease in patients with chronic tension type headache. *Neurology*. 2005;65:1483-1486.
9. Harris RE, Sundgren PC, Pang Y, et al. Dynamic levels of glutamate within the insula are associated with improvements in multiple pain domains in fibromyalgia. *Arthritis Rheum*. 2008;58:903-907.
10. Mesulam MM, Mufson EJ. Insula of the old world monkey. III: Efferent cortical output and comments on function. *J Comp Neurol*. 1982;212:38-52.
11. Taylor KS, Seminowicz DA, Davis KD. Two systems of resting state connectivity between the insula and cingulate cortex. *Hum Brain Mapp*. 2009;30:2731-2745.
12. Birn RM. The behavioral significance of spontaneous fluctuations in brain activity. *Neuron*. 2007;56:8-9.
13. Dworkin SF, LeResche L. Research diagnostic criteria for temporomandibular disorders: Review, criteria, examinations and specifications, critique. *J Craniomandib Disord*. 1992;6:301-355.
14. LeResche L, Mancl L, Sherman JJ, Gandara B, Dworkin SF. Changes in temporomandibular pain and other symptoms across the menstrual cycle. *Pain*. 2003;106:253-261.
15. Melzack R. The short-form McGill Pain Questionnaire. *Pain*. 1987;30:191-197.
16. Daut RL, Cleeland CS, Flanery RC. Development of the Wisconsin Brief Pain Questionnaire to assess pain in cancer and other diseases. *Pain*. 1983;17:197-210.
17. Spielberger CD. State-Trait Personality Inventory: Measure Anxiety, Anger, Depression, & Curiosity in one Inventory. Available at: http://mindgarden.com/products/stpi.htm (accessed March 18, 2010).
18. Gracely RH, Kwilosz DM. The Descriptor Differential Scale: Applying psychophysical principles to clinical pain assessment. *Pain*. 1988;35:279-288.
19. Greicius MD, Krasnow B, Reiss AL, Menon V. Functional connectivity in the resting brain: A network analysis of the default mode hypothesis. *Proc Natl Acad Sci U S A*. 2003;100:253-258.
20. Gracely RH, Petzke F, Wolf JM, Clauw DJ. Functional magnetic resonance imaging evidence of augmented pain processing in fibromyalgia. *Arthritis Rheum*. 2002;46:1333-1343.
21. Behzadi Y, Restom K, Liau J, Liu TT. A component based noise correction method (CompCor) for BOLD and perfusion based fMRI. *NeuroImage*. 2007;37:90-101.
22. Tzourio-Mazoyer N, Landeau B, Papathanassiou D, et al. Automated anatomical labeling of activations in SPM using a macroscopic anatomical parcellation of the MNI MRI single-subject brain. *NeuroImage*. 2002;15:273-289.
23. Tracey I. Nociceptive processing in the human brain. *Curr Opin Neurobiol*. 2005;15:478-487.
24. Peltz E, Seifert F, DeCol R, Dörfler A, Schwab S, Maihöfner C. Functional connectivity of the human insular cortex during noxious and innocuous thermal stimulation. *NeuroImage*. 2010;54:1324-1335.
25. Büchel C, Bornhovd K, Quante M, Glauche V, Bromm B, Weiller C. Dissociable neural responses related to pain intensity, stimulus intensity, and stimulus awareness within the anterior cingulate cortex: A parametric single-trial laser functional magnetic resonance imaging study. *J Neurosci*. 2002;22:970-976.
26. Berman SM, Naliboff BD, Suyenobu B, et al. Reduced brainstem inhibition during anticipated pelvic visceral pain correlates with enhanced brain response to the visceral stimulus in women with irritable bowel syndrome. *J Neurosci*. 2008;28:349-359.

27. Bingel U, Lorenz J, Schoell E, Weiller C, Büchel C. Mechanisms of placebo analgesia: RACC recruitment of a subcortical antinociceptive network. *Pain*. 2006;120:8-15.
28. Petrovic P, Kalso E, Petersson KM, Ingvar M. Placebo and opioid analgesia – imaging a shared neuronal network. *Science*. 2002;295:1737-1740.
29. Bingel U, Schoell E, Herken W, Büchel C, May A. Habituation to painful stimulation involves the antinociceptive system. *Pain*. 2007;131:21-30.
30. Valet M, Sprenger T, Boecker H, et al. Distraction modulates connectivity of the cingulo-frontal cortex and the midbrain during pain—an fMRI analysis. *Pain*. 2004;109:399-408.
31. Seifert F, Bschorer K, De Col R, et al. Medial prefrontal cortex activity is predictive for hyperalgesia and pharmacological antihyperalgesia. *J Neurosci*. 2009;29:6167-6175.
32. Ploner M, Lee MC, Wiech K, Bingel U, Tracey I. Flexible cerebral connectivity patterns subserve contextual modulations of pain. *Cereb Cortex*. 2010;21:719-726.
33. Petrovic P, Kalso E, Petersson KM, Andersson J, Fransson P, Ingvar M. A prefrontal non-opioid mechanism in placebo analgesia. *Pain*. 2010;150:59-65.
34. Fernández-de-las-Peñas C, Galán-del-Río F, Fernández-Carnero J, Pesquera J, Arendt-Nielsen L, Svensson P. Bilateral widespread mechanical pain sensitivity in women with myofascial temporomandibular disorder: Evidence of impairment in central nociceptive processing. *J Pain*. 2009;10:1170-1178.
35. Giesecke J, Reed BD, Haefner HK, Giesecke T, Clauw DJ, Gracely RH. Quantitative sensory testing in vulvodynia patients and increased peripheral pressure pain sensitivity. *Obstet Gynecol*. 2004; 104:126-133.
36. Petzke F, Clauw DJ, Ambrose K, Khine A, Gracely RH. Increased pain sensitivity in fibromyalgia: Effects of stimulus type and mode of presentation. *Pain*. 2003;105:403-413.
37. Apkarian AV, Bushnell MC, Treede RD, Zubieta JK. Human brain mechanisms of pain perception and regulation in health and disease. *Eur J Pain*. 2005;9:463-484.
38. Damoiseaux JS, Greicius MD. Greater than the sum of its parts: A review of studies combining structural connectivity and resting-state functional connectivity. *Brain Struct Funct*. 2009;213:525-533.

SUPPORTING INFORMATION

Additional Supporting Information may be found in the online version of this article:

Fig S1.—Gracely Box Scale (GBS).
Fig S2.—Correlation between left anterior IC–rACC connectivity and pain intensity (VAS) in TMD patients.
Fig S3.—Group difference between left anterior IC–rACC functional connectivity: healthy controls and TMD patients.
Table S1.—Seed region central coordinates.
Table S2.—Depression/anxiety correlations with clinical pain measures.

Please note: Wiley-Blackwell is not responsible for the content or functionality of any supporting materials supplied by the authors. Any queries (other than missing material) should be directed to the corresponding author for the article.